

# Rearrangements and Cycloadditions

This chapter examines reactions that involve molecular rearrangements and cycloadditions. The use of these terms will not be restricted to concerted, pericyclic reactions, however. Often, stepwise processes that involve a net transformation equivalent to a pericyclic reaction are catalyzed by transition metals. The incorporation of chiral ligands into these metal catalysts introduces the possibility of asymmetric induction by inter-ligand chirality transfer. The chapter is divided into two main parts (rearrangements and cycloadditions), and subdivided by the standard classifications for pericyclic reactions (*e.g.*, [1,3], [2,3], [4+2], etc.). The latter classification is for convenience only, and does not imply adherence to the pericyclic selection rules. Indeed, the first reaction to be described is a net [1,3]-suprafacial hydrogen shift, which is symmetry forbidden if concerted.

## 6.1 Rearrangements

Many rearrangements are highly stereoselective reactions and have found considerable application in organic synthesis. Perhaps the most common class of sigmatropic rearrangements includes such [3,3]-rearrangements as the Cope and Claisen rearrangements, the latter with its many variants (reviews: [1-8]). However, the vast majority of [3,3]-rearrangements in which stereochemistry is an important element involve enantiomerically pure starting materials, which places this class of reactions outside the purview of this book.<sup>1</sup> Here, we will focus on two types of rearrangements: [1,3]-hydrogen shifts and [2,3]-Wittig rearrangements. The former is a transition metal catalyzed reaction sequence that has found tremendous importance in industry. The latter is a rearrangement that (like [3,3]-rearrangements) has many applications in stereoselective reactions of enantiomerically pure compounds. But since the [2,3]-Wittig rearrangement involves anionic intermediates, a number of possibilities for asymmetric synthesis also arise. The substrates for [2,3]- (and [3,3]-) rearrangements are often derived from chiral secondary alcohols, which are in turn available by several asymmetric synthesis methods. The discussion of the Wittig rearrangement therefore includes references to methods of asymmetric synthesis of the chiral precursors, which is also relevant to many applications of [3,3]-rearrangements.

### 6.1.1 [1,3]-Hydrogen shifts

It has long been recognized that certain transition metal complexes can catalyze the migration of carbon-carbon double bonds.<sup>2</sup> When the catalyst is a transition metal hydride, the mechanism involves initial reversible addition of the metal

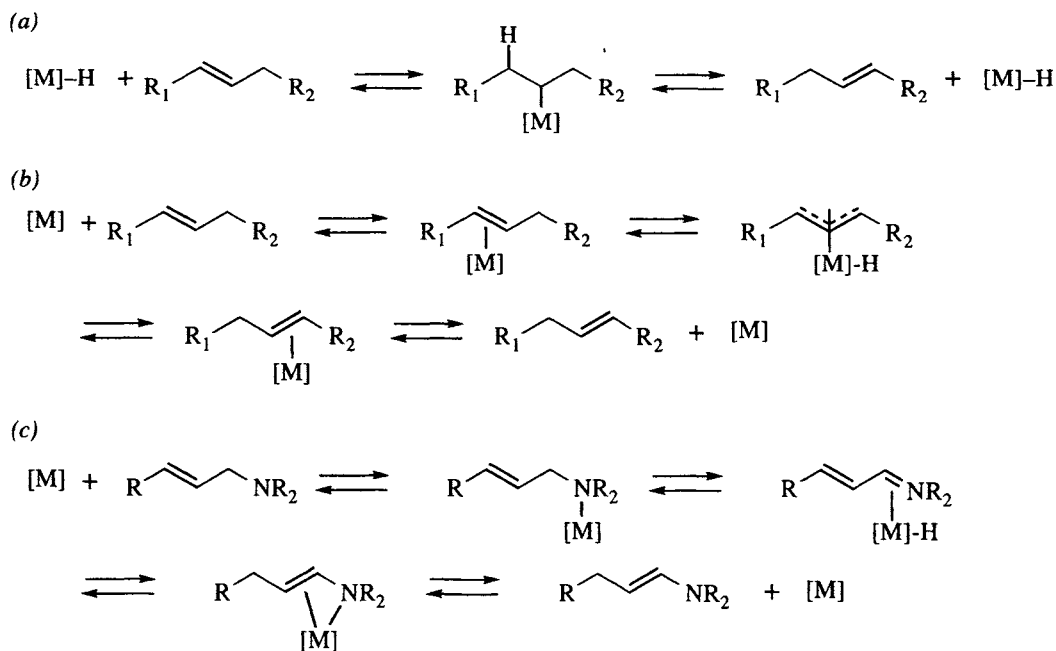
<sup>1</sup> For an example of the Ireland-Claisen rearrangement mediated by a chiral catalyst, see ref. [9]

<sup>2</sup> For a summary of early examples, see pp. 266-303 of ref. [10].

hydride across the double bond to produce a metal  $\sigma$ -alkyl. A double bond is regenerated by elimination of the metal hydride, and if a different hydrogen is eliminated, the net result to the olefin is migration (Scheme 6.1a) [10]. This mechanism is therefore not a strict 1,3-hydrogen shift, but only resembles one when starting material and product are compared. If the catalyst is not a metal hydride, the first step is  $\pi$ -complexation of the metal to the double bond, followed by migratory insertion of the metal, producing a  $\pi$ -allyl metal hydride, then reversal of the sequence at the other end of the allyl system (Scheme 6.1b) [10]. If the olefin has an allylic heteroatom, a third mechanism may intervene. With allylic amines for example (Scheme 6.1c) [11], initial coordination occurs at nitrogen, and migratory insertion yields a  $\pi$ -complexed iminium metal hydride. Rearrangement then yields a bidentate enamine-metal complex, and dissociation liberates the enamine.

All of these processes are under thermodynamic control, and the migration is only useful when there is an isomer that is in a thermodynamic well. For the rearrangements shown in Scheme 6.1a and b, this is the case when the rearrangement affords a more highly substituted alkene, or when the double bond moves into conjugation with a functional group such as a carbonyl. The net rearrangement can involve several individual “[1,3]-rearrangement” steps, such as migration around a ring. Such sequential shifts are blocked by a quaternary carbon. The rearrangement of an allylic amine to an enamine is also thermodynamically favored (Scheme 6.1c).

For the purposes of asymmetric synthesis, the initial alkene must be prochiral (*i.e.*, either 1,1-disubstituted or trisubstituted), so that the rearrangement produces a new stereogenic center. As shown in Figure 6.1, this is often contrathermodynamic, *but not in the case of compounds with allylic heteroatoms*.



**Scheme 6.1.** Transition metal catalyzed 1,3-hydrogen shifts. (a) Metal hydride catalyst. (b) Metal catalyst. (c) Metal catalyzed rearrangement of allylic amines to enamines.

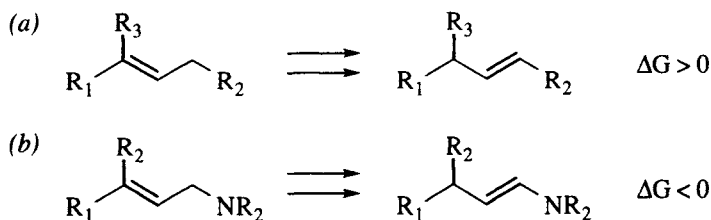
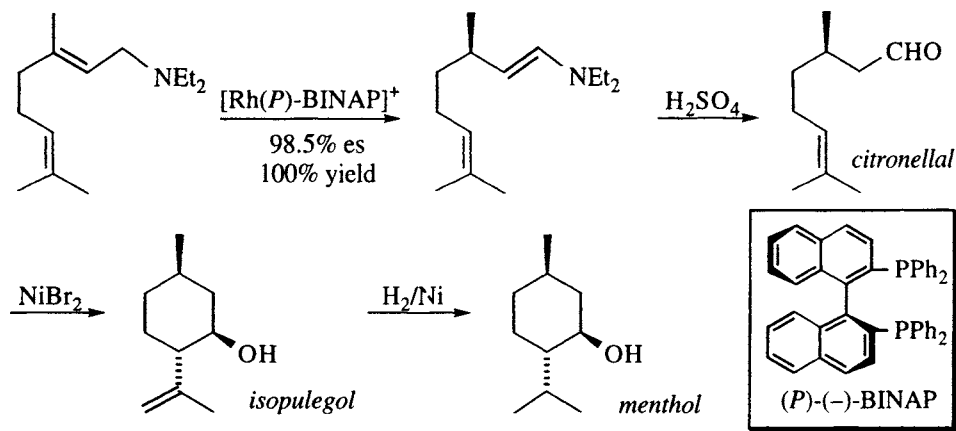


**Figure 6.1.** (a) Contrathermodynamic isomerization of a trisubstituted alkene to a disubstituted one. (b) Thermodynamically favored isomerization of an allylic amine to an enamine.

Following years of less successful attempts by other groups ( $\leq 53\%$  enantioselectivity; reviews: [12,13] and pp. 266-303 of ref. [10]), Otsuka reported in 1978 that allylic amines could be rearranged to enamines with a chiral  $\text{Co}^{\text{II}}$  catalyst with modest (66:34) enantioselectivity [14]. Further studies [11,15,16] revealed that a cationic  $\text{Rh}^{\text{I}}$  catalyst having arylphosphine ligands (the best is BINAP, 2,2'-bis(diphenylphosphino)-1,1'-binaphthyl) affords excellent selectivity (97-99% es) with very high catalyst turnover (300,000). This reaction has been scaled up, and is now known as the "Takasago process." It (Scheme 6.2) is used for the commercial manufacture of  $\sim 1500$  tons per year (nearly 40% of the world market) of citronellal and menthol [11,16], and has been described as "the most impressive achievement to date in the area of asymmetric catalysis" [17]. It is worth mentioning that, although citronellal is available from natural sources, the enantiomer ratio of the natural product is only 90:10.

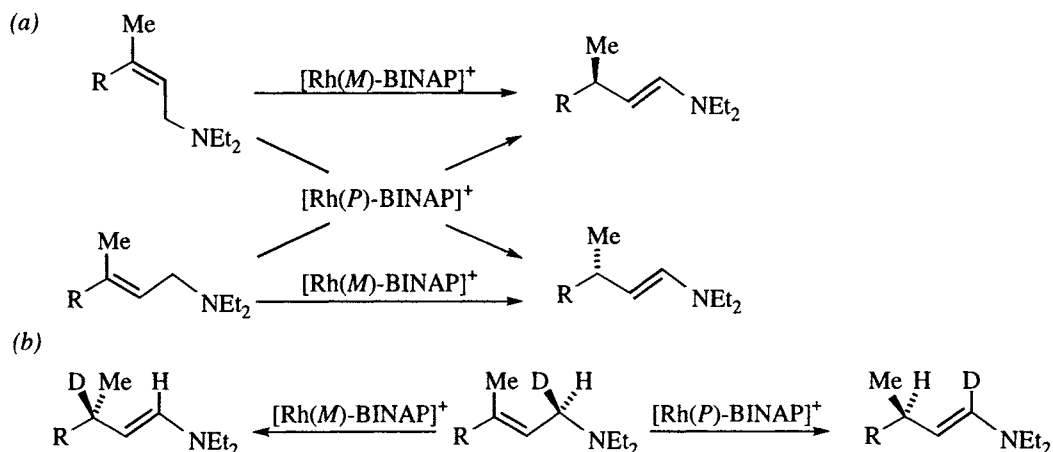


**Scheme 6.2.** The Takasago process for the commercial manufacture of citronellal, isopulegol, and menthol [16].<sup>3</sup>

Two aspects of the reaction are stereospecific. The first is that geometric isomers of the allylic amines afford enantiomeric enamines, as shown in Scheme 6.3a [19]. Note that the geometry of the enamine double bond is *not* dependent on the stereochemistry of the double bond of the allylic amine, however. The second

<sup>3</sup> In accord with the recommendation of Prelog and Helmchen, the *P,M* nomenclature system is used to describe the configuration of molecules containing chirality axes and planes [18]. Note that  $R = M$  and  $S = P$ . See the glossary, Section 1.6, for an explanation of these terms.

stereospecific feature is revealed by the deuterium labeling studies shown in Scheme 6.3b: the *R*-C<sub>1</sub>-*d* allylic amine, when subjected to enantiomeric rhodium catalysts, undergoes deuterium migration with *M*-BINAP, and hydrogen migration with *R*-BINAP [11]. An isotope effect was not observed, indicating that the carbon-hydrogen (or deuterium) bond breaking step is not rate determining. Furthermore, experiments (not shown) using a mixture of  $-CD_2NEt_2$  and  $-CH_2NEt_2$  amines revealed no crossover, indicating that the migration is intramolecular [11].



**Scheme 6.3.** Stereospecific aspects of rhodium catalyzed asymmetric [1,3]-hydrogen shifts.

There are two (limiting) possibilities that could explain the enantioselectivity: a group-selective metal insertion distinguishing the enantiotopic allylic protons, or a face-selective addition that distinguishes the enantiotopic double bond faces. Figure 6.2 illustrates the conformational analysis of the intermediates involved in the sequence (Scheme 6.1c). First of all, the lowest energy conformation around the

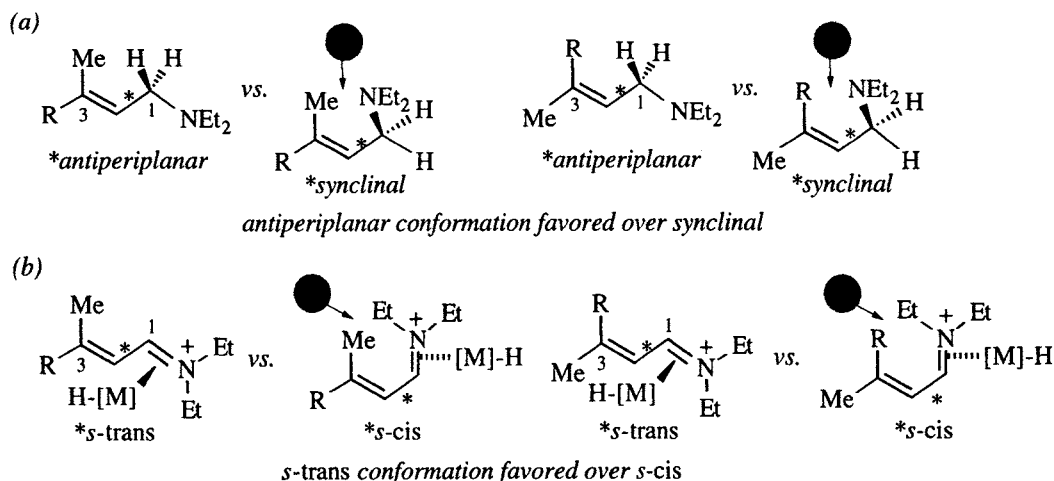


**Figure 6.2.** Severe conformational restrictions due to A<sup>1,3</sup> strain are placed on the intermediates in the asymmetric [1,3]-rearrangement of allylic amines. (a) The starting material (as well as the nitrogen-coordinated rhodium complex) favors the antiperiplanar conformation. (b) The  $\pi$ -bonded metal hydride intermediate is restricted to the *s*-trans conformation.

N–C<sub>1</sub>–C<sub>2</sub>–C<sub>3</sub> bond (\*) of the allylic amine is antiperiplanar due to A<sup>1,3</sup> strain in the synclinal conformation (Figure 6.2a). Coordination of the catalyst to the nitrogen (step 1 in Scheme 6.1c) will only increase the energetic bias in favor of the antiperiplanar conformation.<sup>4</sup> The second step of the reaction sequence is the migratory insertion of the metal into the C<sub>1</sub>–H bond to give a  $\pi$ -bonded  $\alpha,\beta$ -unsaturated iminium ion. Figure 6.2b shows that only the *s*-trans conformer of this species is accessible, because of severe A<sup>1,3</sup> interactions between the diethylamino substituents and the C<sub>3</sub> substituent in the *s*-cis conformation.

Examination of the conformers illustrated in Figure 6.2b reveals the origin of the *Re/Si* face selectivity in the transfer of hydrogen to C<sub>3</sub>. The illustrated conformers have the metal hydride bound to the *Re* face of the iminium ion. Since the *s*-cis conformation is not accessible, and since the rearrangement corresponding to the third step of Scheme 6.1c is suprafacial, the step that determines the configuration of the  $\pi$ -bonded iminium metal hydride also determines the absolute configuration at C<sub>3</sub> in the product. This step is the migratory insertion of the metal into the C<sub>1</sub>–H bond (*i.e.*, step 2 of Scheme 6.1c). Thus, the Takasago process is an example of a group-selective insertion of a metal into one of two enantiotopic carbon hydrogen bonds. The *M*-BINAP rhodium inserts into the C–H<sub>*Re*</sub> bond and the *P*-BINAP rhodium inserts into the C–H<sub>*Si*</sub> bond.

The interligand asymmetric induction from the binaphthyl moiety to C<sub>3</sub> of the allylic amine covers a considerable distance and deserves comment. As noted above, the enantioselectivity of the overall process is determined in the step where the metal inserts into one of the enantiotopic C<sub>1</sub>-protons. The solid state conformation of the *P*-BINAP ligand has been established by two X-ray crystal structures (of ruthenium complexes: [20,21]), and is illustrated in Figure 6.3a, with the other ligands removed for clarity. Note that the chirality sense of the binaphthyl moiety places the four *P*-phenyl substituents in *quasi*-axial and *quasi*-equatorial orientations. It is apparent that the 'upper right' and 'lower left' quadrants (which are equivalent due to symmetry) have the most free space for accomodating additional bound ligands. Attachment of the allylic amine in the antiperiplanar C<sub>1</sub>–C<sub>2</sub> conformation to the square-planar rhodium complex is illustrated in Figure 6.3b. (The two possible binding sites are equivalent due to symmetry.) The migratory insertion step must occur through a 4-membered ring transition structure, and the two possibilities are illustrated in Figures 6.3c and d. Note that insertion into the H<sub>*Re*</sub>–C bond forces the double bond moiety into close proximity with the *quasi*-equatorial phenyl on the left (Figure 6.3c), whereas metal insertion into the H<sub>*Si*</sub>–C bond moves the double bond into the vacant lower left quadrant. The latter is favored.

The catalytic cycle shown in Scheme 6.4 has been proposed to account for the kinetics and observable intermediates in the reaction [11]. Starting from the top, the allylic amine displaces a solvent to form the *N*-coordinated rhodium species.

<sup>4</sup> Low temperature <sup>1</sup>H and <sup>31</sup>P NMR studies indicated that only the nitrogen of allylic amines is bound to the metal. No evidence could be found for an *N*- $\pi$ -chelate that might stabilize the synclinal conformation [11].

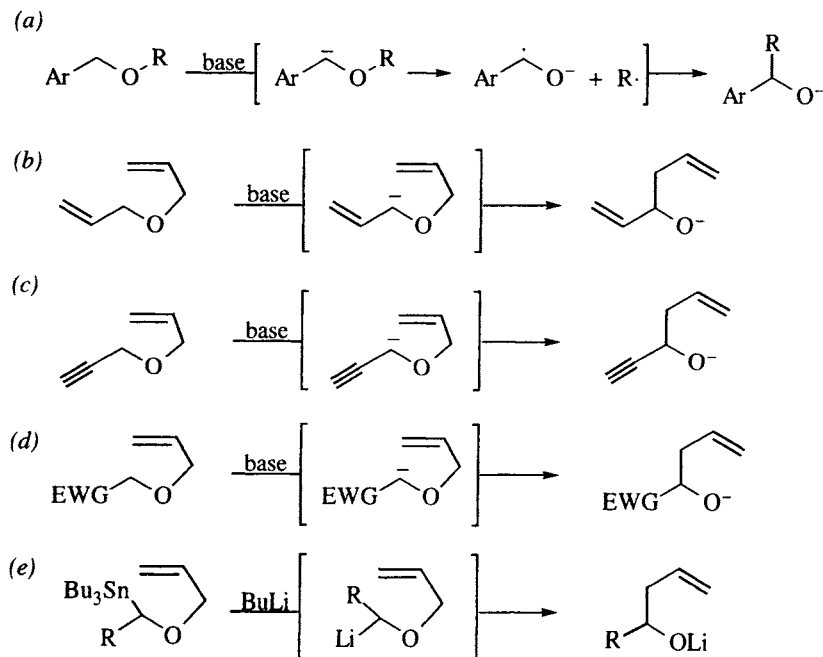


Investigation of the scope of the asymmetric rearrangement of allylic amines has led to the following generalizations [11]: (i) both C<sub>1</sub> and C<sub>2</sub> should have no alkyl substituents (substitution at either position would erase the preference for the antiperiplanar and *s*-trans conformations, *cf.* Figure 6.2); (ii) C<sub>3</sub> may be substituted with an aryl group (or also be only monosubstituted, but the latter circumstance has no stereochemical consequence); (iii) the nitrogen substituents must not be aryl (a less basic nitrogen fails to bind the rhodium and is not affected by the catalyst).

Isomerization of allylic alcohols occurs in reasonable yields but with poor enantioselectivity [22], although kinetic resolution of 4-hydroxycyclopentenone has been reported [23]. Reliable laboratory-scale procedures for the synthesis of BINAP and for the asymmetric rearrangement have been published [24,25], making this a good candidate for further applications in asymmetric synthesis.

### 6.1.2 [2,3]-Wittig rearrangements

What is now known as the [1,2]-Wittig rearrangement was apparently first observed in the 1920s by Schorigin [26,27], and by Schlenk and Bergmann [28], who reported that reductive metalation of benzyl alkyl ethers with lithium or sodium afforded rearranged products. In 1942, Wittig reported that benzyl ethers could be deprotonated with phenyl lithium, and similarly rearranged [29,30] (Scheme 6.5a). It is now agreed that the [1,2]-rearrangement involves successive deprotonation,

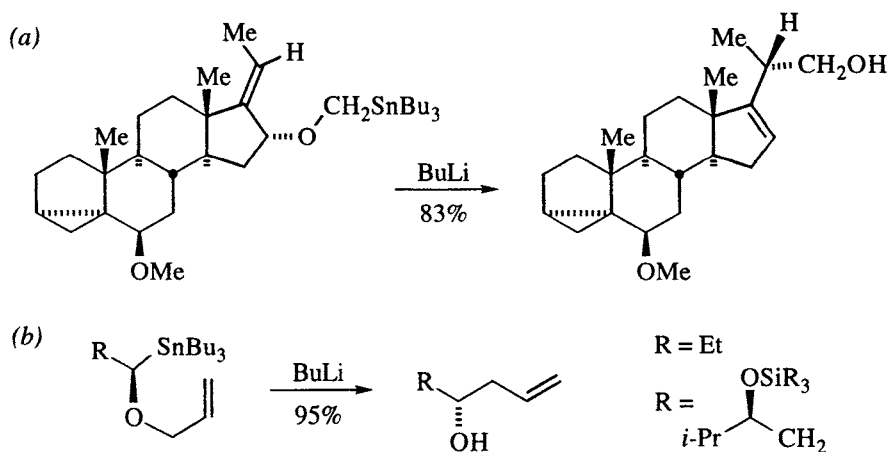


**Scheme 6.5** (a) The [1,2]-Wittig rearrangement [29,30]. (b) The [2,3]-Wittig rearrangement [31]. (c) The [2,3]-Wittig rearrangement of propargyl allyl ethers occurs by deprotonation at the propargylic position. (d) Similarly, electron withdrawing groups (EWG) can be used to influence the site of deprotonation. (e) The Still variant of the [2,3]-Wittig, which uses a tin-lithium transmetalation to control anion formation [32].

homolysis of the opposite carbon–oxygen bond, and recombination to an alkoxide [33,34].<sup>5</sup> The [2,3]-variant was first observed by Wittig (although not recognized as such) in 1949 [36] and by Hauser two years later (Scheme 6.5b, [31]), and was shown in subsequent studies to proceed by a concerted  $S_Ni$  mechanism [37,38]. When the [1,2]- and [2,3]-rearrangements can compete, the [2,3]-Wittig rearrangement predominates at low temperatures [39–41].<sup>6</sup>

With unsymmetrical ethers, the problem of the regiochemistry of metalation arises. Three approaches have successfully addressed this issue. One takes advantage of the fact that propargyl allyl ethers deprotonate exclusively at the propargylic position [48,49] (Scheme 6.5c). Second, an electron withdrawing group (EWG) that stabilizes the anion on one side of the ether can be used to control the site of deprotonation, although enolates may suffer competitive [3,3]-rearrangement [50,51], (Scheme 6.5d). Finally, the regiochemical issue can be eliminated by using tin–lithium exchange to generate the carbanion at a specific site ([32], Scheme 6.5e).

The migration across the allyl system is suprafacial [41], as illustrated by the example shown in Scheme 6.6a [52,53]. The configuration of the carbanionic carbon<sup>7</sup> inverts during the rearrangement, as predicted by theory in 1990 [55], and subsequently proven by three independent studies in 1992 [56–58], the simplest of which is illustrated in Scheme 6.6b. Thus, the [2,3]-Wittig rearrangement is a  $[\pi 2_s + \sigma 2_a + \sigma 2_a]$ -rearrangement, which is symmetry allowed for a concerted six electron process with two inversions [35].



**Scheme 6.6.** (a) Example illustrating the suprafacial nature of the migration across the allyl moiety [52]. (b) Examples illustrating inversion of configuration at the metalated carbon [57,58].

The approximate geometries of four calculated transition structures are shown in Figure 6.4. When the lithium is included in the calculation (Figure 6.4a), all nonhydrogen atoms except the middle carbon of the allyl system are approximately coplanar [55]. When the lithium is removed, the envelope conformation is main-

<sup>5</sup> Note that a concerted [1,2]-carbanion migration is symmetry forbidden [35].

<sup>6</sup> For reviews of the Wittig rearrangements, see ref. [42–47].

<sup>7</sup>  $\alpha$ -Alkoxyorganolithiums are configurationally stable below about  $-30^\circ$  (section 3.2.1, [54]).



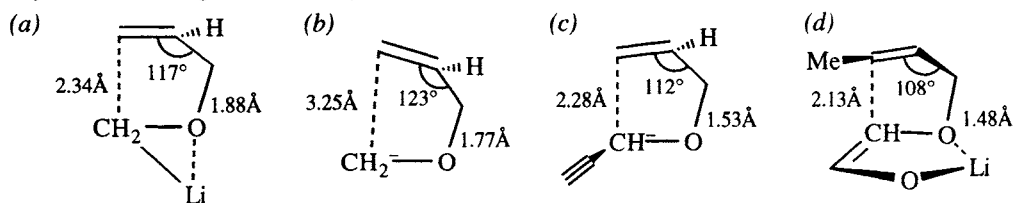


**Figure 6.4.** Ab initio transition structures for the [2,3]-Wittig rearrangement. (a) Structure including a lithium, in which the metal is antiperiplanar to both carbons of the allyl system and bridges the carbon and oxygen [55]. (b) Calculated transition structure for [2,3]-rearrangement of the naked  $\text{ROCH}_2^-$  anion [59]. (c) Calculated transition structure for the [2,3]-rearrangement of a propargyl anion. Orientation of the alkynyl moiety on the convex face is favored by 2.1 kcal/mole [59]. (d) For the rearrangement of a lithium enolate, the endo structure is favored [59]. (The author is grateful to Professors Y. Wu and K. N. Houk, who kindly supplied the indicated bond lengths and angles in a private communication.)

tained, but the bond lengths and angles change dramatically, as shown in Figure 6.4b [59]. For the naked anion, the transition structure is extremely early, with practically no bond making or breaking having occurred. When the lithium is present, the transition structure is somewhat later, which may be an artifact of the method, since the calculation requires that the lithium be unsolvated and in the gas phase. Since one cannot ignore the presence of the cation, we may assume that the real transition state geometry probably lies somewhere between these two structures. When the carbanion is stabilized by an alkynyl group (Figure 6.4c) or is an enolate (Figure 6.4d), the calculated transition structure is much more compressed [59]. Note for example, that the forming and breaking bonds are shorter than in the other two structures, and also note that the bond angle is smaller.

#### 6.1.2.1 Simple diastereoselectivity

The aspects of diastereoselectivity in the [2,3]-Wittig rearrangement that we will be concerned with involve the geometry of the double bond and the configuration of the allylic and ‘carbanionic’ carbons in the allyl ether. Figure 6.5a illustrates diastereomeric transition structures for [2,3]-rearrangements of  $\alpha$ -allyloxy organolithiums. If there is a substituent ( $\text{R}_1$ ) at the allylic position,  $\text{A}^{1,2}$  and  $\text{A}^{1,3}$  allylic strain will play a role. If both  $\text{R}_1$  and  $\text{R}_2$  are not hydrogen,  $\text{A}^{1,2}$  strain will disfavor the left conformer. If the alkene has the *Z* configuration,  $\text{A}^{1,3}$  strain is particularly severe in the structure on the right. With reference to Figure 6.4, note that  $\text{A}^{1,2}$  strain will be alleviated by a small allylic bond angle and that  $\text{A}^{1,3}$  strain will be enhanced by a small bond angle.

Similar transition structures having stereogenic carbanionic carbons are illustrated in Figure 6.5b. For electrostatic reasons, an electron rich substituent such as an alkyl, vinyl, or alkynyl group will preferably occupy the convex face of the envelope conformation, while an electropositive substituent favors the concave side [55,59].

If the carbanionic carbon is trigonal, such as with enolates, the preference is to occupy the concave face, as shown in Figure 6.5c. This effect is reminiscent of the endo effect in Diels-Alder reactions (Section 6.6), and is also consistent with

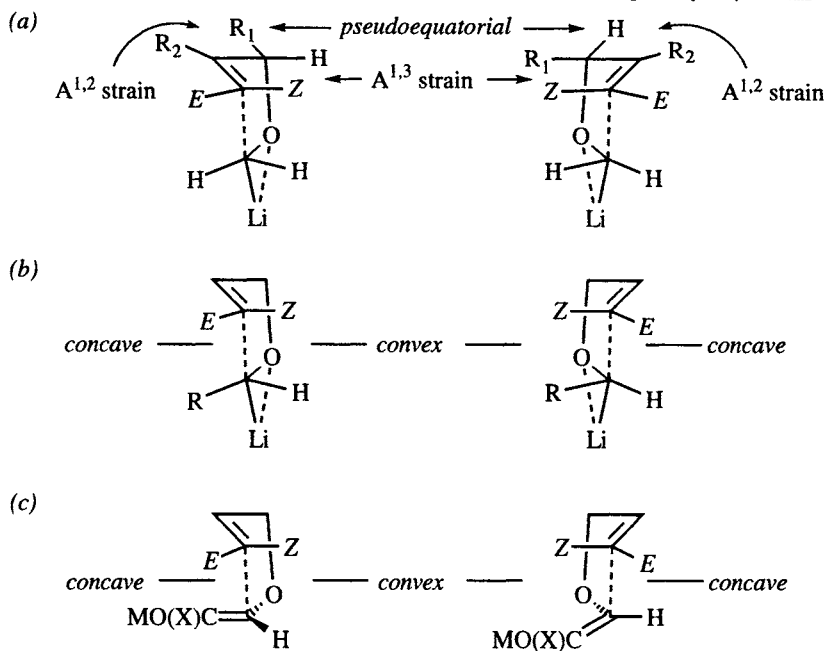


**Figure 6.5.** Factors influencing the relative configuration of the products in [2,3]-Wittig rearrangements: (a) Diastereomeric transition states illustrating the possibility of allylic strain. (b) The conformation having R on the convex face of the envelope is preferred for alkyl, vinyl, and alkynyl substituents. (c) For enolates, the concave orientation (synclinal double bonds) is preferred.

Seebach's topological rule suggesting a preference of synclinal donor/acceptor orientations in a Newman projection along the forming bond (*cf.* Figure 5.8, [60]). For *Z*(*O*)-enolates, additional stabilization can be had by metal chelation with the ether oxygen (*cf.* Figure 6.4d).

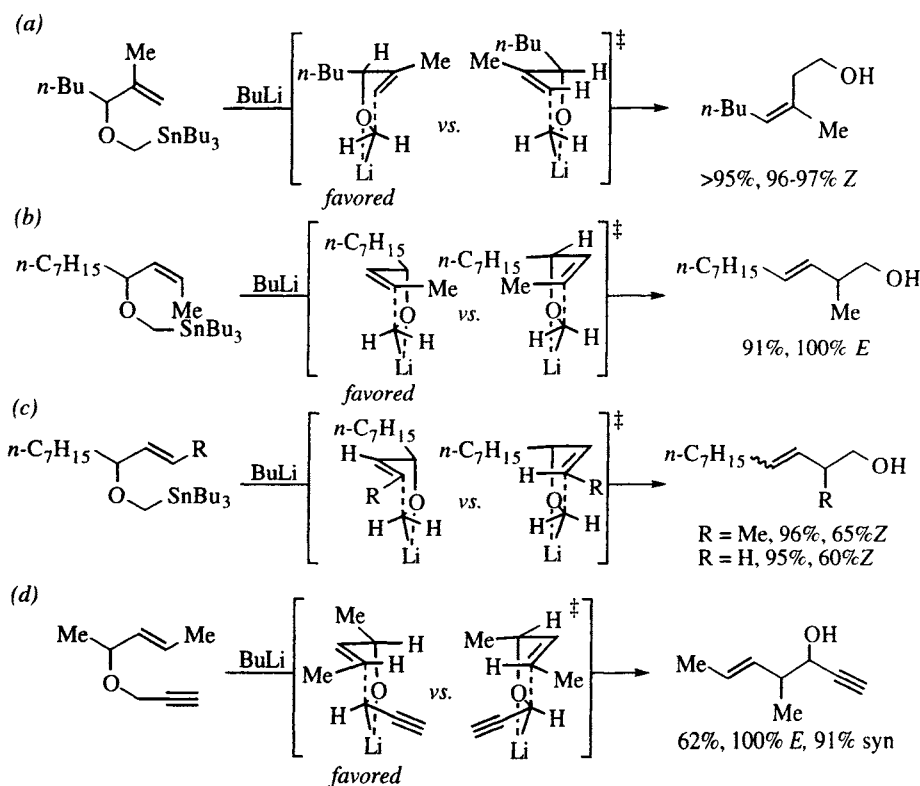
Each one of the effects illustrated in Figure 6.5 is attributable to a stereogenic element in the starting material (olefin geometry or absolute configuration at the allylic or carbanionic carbon), and is an example of single asymmetric induction. When more than one element is present, these effects can operate as matched or mismatched pairs of double asymmetric induction, and very high selectivities can be achieved when they operate in concert. Additionally, it is possible to introduce a stereogenic element elsewhere, such as a chiral auxiliary (X of Figure 6.5c). Conversely, when two elements are dissonant, lower selectivity may be expected.

The reader should recognize that these five-membered-ring transition states are considerably more flexible than, for example, a chair structure such as the Zimmerman-Traxler transition state in aldol additions (*cf.* Scheme 5.1).<sup>8</sup> This flexibility complicates the analysis of the various effects. A few examples serve to illustrate how these effects influence the configuration of the double bond and stereocenters in the product.

<sup>8</sup> Indeed, transition state models having slightly different envelope or half-chair conformations have been proposed (*cf.* ref.[44-46,61]).

**Effect of allylic and double bond substitution on product configuration.** Scheme 6.7 illustrates the influence of allylic strain between alkyl substituents on the double bond and allylic positions, uncomplicated by substitution at the carbanionic carbon. As shown in Scheme 6.7a, tin-lithium exchange affords an anion that rearranges (*cf.* Figure 6.5a,  $R_1 = n\text{-Bu}$ ,  $R_2 = \text{Me}$ ,  $E = Z = \text{H}$ ) to give a near quantitative yield of alkene with 96-97% diastereoselectivity [32]. In this example,  $A^{1,2}$  strain is relieved when the butyl group adopts the pseudoaxial orientation.

Scheme 6.7b illustrates the influence of  $A^{1,3}$  strain between two alkyl groups (*cf.* Figure 6.5a,  $R_1 = n\text{-heptyl}$ ,  $R_2 = \text{H}$ ,  $E = \text{H}$ ,  $Z = \text{Me}$ ), this time favoring the pseudoequatorial conformation for the allylic substituent, so as to avoid the *Z*-methyl. [2,3]-Wittig rearrangement is 100% stereoselective for the *E*-alkene [32]. In contrast, when the alkene is unsubstituted in the “*Z*-position”, the selectivity for a particular olefin geometry is severely diminished. Scheme 6.7c lists two such examples having *E* or unsubstituted alkene as educt, which are only 60-65% selective for the *Z*-product. It was noted (*cf.* Figure 6.4c, [59]) that propargylic anions rearrange *via* a transition structure that has significantly shorter bond lengths, and also a compressed allylic bond angle. The latter effect amplifies  $A^{1,3}$  strain, and *E* selectivity is restored when the carbanionic carbon is propargylic (Scheme 6.7d, [48]).



**Scheme 6.7.** The effects of allylic strain on the stereoselectivity of alkene formation [32]. (a)  $A^{1,2}$  strain and the selective formation of *Z*-alkenes. (b)  $A^{1,3}$  strain causes selective formation of *E*-alkenes. (c) If one or both of the ‘partners’ (*cf.* Figure 6.5a,  $R_1$ ,  $R_2$ , or *Z*) is hydrogen, the selectivity is diminished. (d)  $A^{1,3}$  strain produces 100% *E* selectivity when the carbanionic carbon is propargylic [48].

**Effect of anion substitution on relative configuration.** As seen in Scheme 6.7d, if both carbons involved in bond formation have heterotopic faces, two adjacent stereocenters are formed in the rearrangement. The topicity of these examples can be analyzed by reference to Figure 6.6, which defines the facial topicity for the components of the bond forming reaction, and also shows how these heterotopic faces are combined to form either syn or anti relative configurations in the product. Figure 6.6a and c show the topicities for *Z*-alkenes, while Figure 6.6b and d illustrate similar transition structures for *E*-alkenes. Note that the preceding discussion analyzed the combined effects of substitution on the double bond and at the allylic position. The structures in Figure 6.6 are unsubstituted at the allylic position, so that the factors affecting relative configuration can be analyzed independent of the effects of an allyl substituent.

Many examples of this type of reaction have been reported in the literature, but only with a few alkyl substituents on the metalated carbon are high selectivities consistently achieved. Table 6.1 lists several such examples, which can be rationalized by the indicated structures in Figure 6.6. Recall (Figure 6.5b and accompanying discussion) that theory predicts that electron rich alkyl substituents will prefer the convex face of the transition structures (*i.e.*, Figure 6.6a and d), for electrostatic reasons [55].

Entry 1 was the first example, reported in 1970 [40], of a highly stereoselective [2,3]-Wittig rearrangement, but comparison with entry 5 shows that only the *Z* isomer is selective. Entries 2-4 illustrate substituted propargyl *Z* allyl ethers,

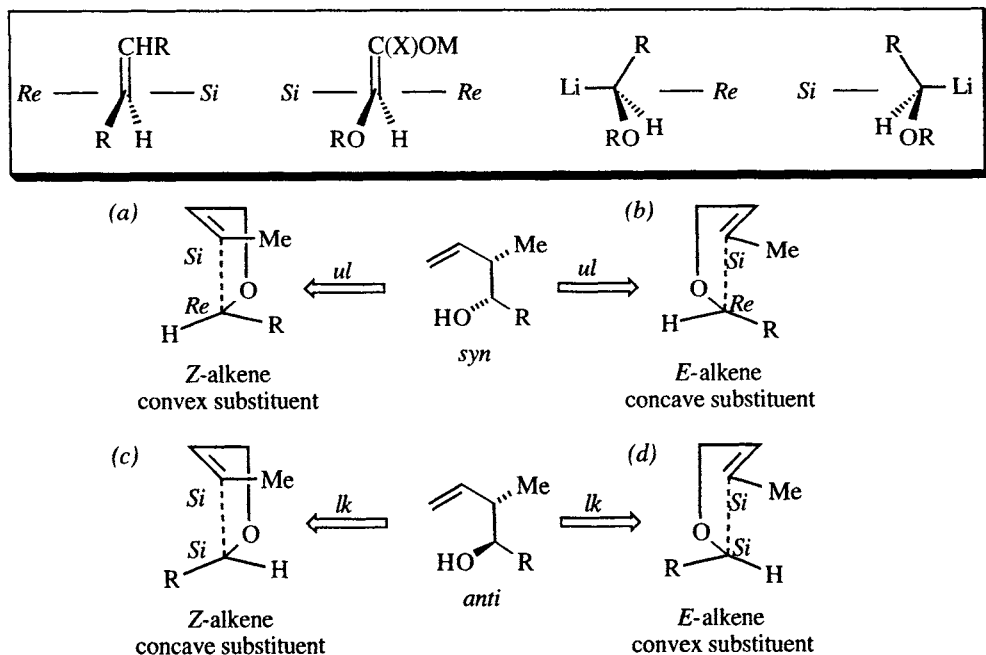
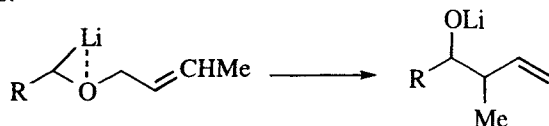


**Figure 6.6.** *Inset:* Heterotopic faces for determining relative topicity (note inversion at the stereogenic RLi). (a,b) *Syn* product is formed by two combinations of *ul* topicity. (c,d) *Anti* product is formed by two combinations of *lk* topicity. In transition states a-d, the metal is omitted. When R is an alkyl group, it would be bridged to the C–O bond, antiperiplanar to the allyl group (*cf.* Figure 6.4a, b). If R is a carbonyl, the metal will be attached to the enolate oxygen (*cf.* Figure 6.5c).

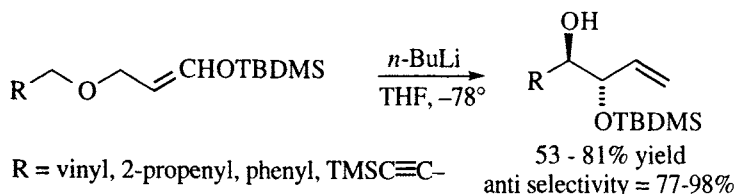
**Table 6.1.** Selective [2,3]-Wittig rearrangements of  $\alpha$ -phenyl,  $\alpha$ -propargyl, and  $\alpha$ -alkyl organolithiums, showing a high  $Z \rightarrow \text{syn}$  /  $E \rightarrow \text{anti}$  correlation. The 'Path' column refers to the transition structures in Figure 6.6.



Entry	R	E/Z	Path	Config.	% ds	% Yield	Ref.
1	Ph	Z	a	100% syn	100	—	[40]
2	HC≡C	98%Z	a	88% syn	90	56	[48]
3	MeC≡C	98%Z	a	98% syn	100	55	[48]
4	TMSC≡C	93%Z	a (& b)	98% syn	105 (!)	74	[48]
5	Ph	E	b & d	50:50	50	—	[40]
6	HC≡C	93%E	d	93% anti	100	72	J751, [48]
7	MeC≡C	93%E	d	92%anti	99	65	J751[48]
8	TMSC≡C	93%E	b	75% syn	73	72	[48]
9	Et	E	d	99% anti	99	95	[58]

which show a consistently high  $Z \rightarrow \text{syn}$  selectivity, consistent with the transition structure in Figure 6.6a being favored over Figure 6.6c [48]. Entry 4 (trimethylsilylalkyne) is particularly striking because the product has a higher syn/anti ratio than the  $Z/E$  ratio in the starting material! This is not experimental error, as shown by Entry 8, which is also highly syn selective even though the starting material is 93%  $E$ , and anti product was expected [48]. Entries 6 and 7 show a more predictable tendency for very high  $E \rightarrow \text{anti}$  stereoselectivity (Figure 6.6d favored over Figure 6.6c), underscoring the anomalous nature of Entry 8. Entry 9 demonstrates that carbanions that are not resonance stabilized are also highly selective. In this case, the organolithium was generated by transmetalation of an organostannane, and again high  $E \rightarrow \text{anti}$  stereoselectivity is observed [58].

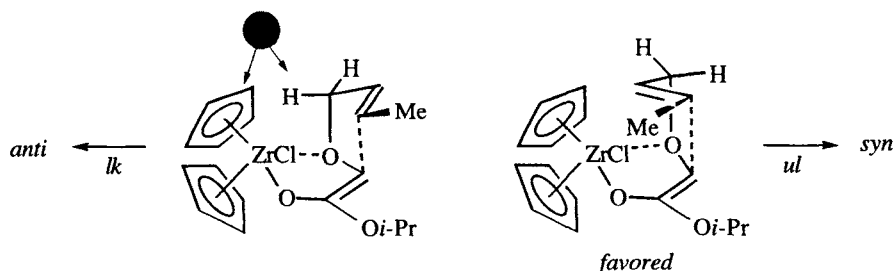
When the alkenyl component is an *O-tert*-butyldimethylsilyl (TBDMS) enol ether, another anomaly occurs: independent of enol ether geometry, the anti product is favored (Scheme 6.8) [62]. With trimethylsilylpropargyl ethers, the anti selectivity is 95-98%, making this reaction an excellent route for the preparation of anti 1,2-diols. In these cases, transition structures similar to Figure 6.6c and d are operative, the dominant influence being mutual repulsion between the carbanion substituent, R, and the *O*-silyl group.



**Scheme 6.8.** The [2,3]-Wittig rearrangement of silyl enol ethers is anti selective independent of carbanion substituent and double bond geometry [62].

For lithium enolate anions, the tendency is for the enolate to occupy the concave face of the transition structure (*cf.* Figure 6.4d and 6.5c) and therefore to prefer transition structures such as those illustrated in Figure 6.6b and c.<sup>9</sup> Table 6.2 lists several examples of simple acyclic diastereoselection, which show a tendency for *E* → *syn* and *Z* → *anti* selectivity, in contrast to the tendency observed for hydrocarbon substituted carbanions (Table 6.1). Entries 1 and 2 involve dianions of crotyloxy acetates, and show *E* → *syn* and *Z* → *anti* selectivity. A more complex example involving extension of a steroid side chain (similar to Scheme 6.6a), is 100% *anti* selective from an '*E*'-alkene, however [53].

The ester enolates illustrated in entries 3 and 4 are considerably more selective when the lithium cation is exchanged for dicyclopentadienyl zirconium [63]. It is suggested that the zirconium chelates the  $\alpha$ -alkoxy oxygen in these examples, and that the cyclopentadienyl ligands influence the topicity in the transition state [63]. Scheme 6.9 illustrates how the *lk* topicity may be disfavored by a steric interaction between a pseudoaxial allylic hydrogen and a cyclopentadienyl ligand. The *Z*-alkene isomer (entry 4) is also *syn*-selective, although less so than the *E* isomer, and the yield is not encouraging. The rationale illustrated in Scheme 6.9 [63] implies that deprotonation of the ester affords the *Z*(*O*)-enolate, in contrast to the expected (Section 3.1.1) tendency of esters to afford *E*(*O*)-enolates. In his review of enolate formation [64], Wilcox notes that *Z*(*O*)-enolate formation by deprotonation of  $\alpha$ -alkoxy esters would be expected if chelation were the dominant influence, but that the results reported in the literature show no consistent trend.<sup>10</sup>



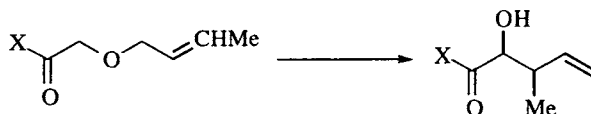
**Scheme 6.9.** Rationale for the *ul* selectivity of dicyclopentadienylzirconium ester enolates in [2,3]-Wittig rearrangements.

Pyrrolidinyll amides undoubtedly form *Z*(*O*)-enolates, and the [2,3]-Wittig rearrangement of the *E*-alkene (entry 5, [69] is highly selective. The *Z*-alkene was not tested, and propargylic amide enolates do not rearrange [70]. Entry 5 also shows the highest yield in the Table. As will be seen, amides of *C*<sub>2</sub>-symmetric amines can be excellent chiral auxiliaries in this process.

<sup>9</sup> Note also that enolates may suffer competitive [3,3]-sigmatropic rearrangement [44,50,51].

<sup>10</sup> Based on the relative configuration of the products of Ireland-Claisen rearrangements, two groups have concluded that *Z*(*O*)-enolate formation predominates [65,66]. On the other hand, two other groups quenched  $\alpha$ -alkoxy ester enolates with trialkylsilyl chlorides and found mixtures of enol ether (ketene acetal) isomers [67,68].

**Table 6.2.** [2,3]-Wittig rearrangements of  $\alpha$ -allyloxy enolates. The 'Path' column refers to the transition structures in Figure 6.6. All examples used LDA as base; entries 3 and 4 also have  $\text{Cp}_2\text{ZrCl}_2$  as additive (Cp =  $\eta^5$ -cyclopentadienyl).



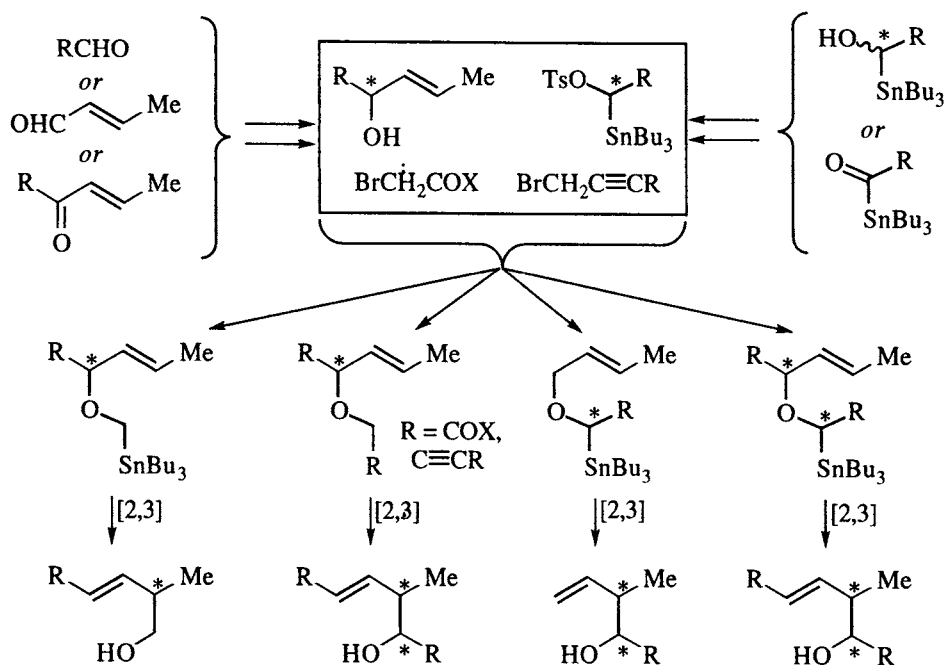
Entry	X	E/Z	Path	Config.	% ds	% Yield	Ref.
1	OH	93% <i>E</i>	b	65% syn <sup>11</sup>	70	60	[71]
2	OH	95% <i>Z</i>	c	75% anti <sup>9</sup>	79	73	[71]
3	Oi-Pr, as $\text{Cp}_2\text{ZrCl}_2$ enolate	<i>E</i>	b	98% syn	98	47	[63]
4	Oi-Pr, as $\text{Cp}_2\text{ZrCl}_2$ enolate	<i>Z</i>	a	88% syn	88	15	[63]
5	pyrroli- dinyI	<i>E</i>	b	96% syn	96	97	[69]

#### 6.1.2.2 Chirality transfer in enantiopure educts

As seen in the previous section, substitution at the double bond, the allylic position, and the carbanionic carbon influence the configuration of the new double bond and the *relative configuration* of the stereocenter(s) in the product of a [2,3]-Wittig rearrangement. In this section, it will be seen that the *absolute configuration* of stereocenters at the allylic and carbanionic carbons determine the *absolute configuration* of the stereocenter(s) in the product (Scheme 6.10). In fact, several examples already cited involve chiral educts being transformed into chiral products (*cf.* Scheme 6.6b, Scheme 6.7b and c, Table 6.1, entry 9), although this point was not the focus of the discussion. It should come as no surprise that a transition structure that is sufficiently organized to afford good selectivity in the formation of one double bond isomer or one relative configuration, can also afford good enantioselectivity in the formation of one or two new stereocenters.

Scheme 6.10 illustrates generic schemes for the asymmetric synthesis of homoallylic alcohols using a [2,3]-Wittig reaction as a key step. In these sequences, the absolute configuration and enantiomeric purity of the starting materials are determined by their method of preparation (or commercial source), and the following examples will show that the chirality sense of the starting material controls the absolute configuration of the product via the principles of simple diastereoselectivity outlined in the preceding sections. The absolute configuration of a

<sup>11</sup> It should be noted that the original reference (J754) uses the ambiguous erythro/threo nomenclature without drawing a reference structure. Later, in a review by the same authors [44], the same nomenclature is used but apparently to indicate the opposite relative configurations. Additionally, the review [44] states a different selectivity for the *E*-alkene than is given in the original article (J754). Table 6.2 lists the selectivities from the original article with the relative configurations as drawn in the review.

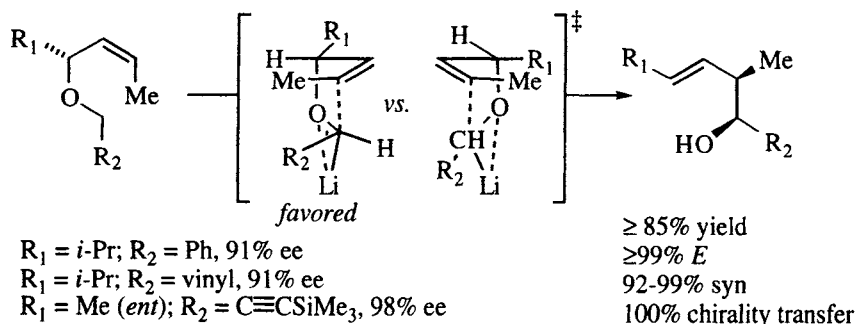


**Scheme 6.10.** *Top:* Some of the possible paths for the preparation of chiral building blocks for the assembly of substrates for a [2,3]-Wittig rearrangement. *Bottom:* Intramolecular asymmetric induction in [2,3]-Wittig rearrangements.

stereocenter at the allylic (or propargylic) position may be set by asymmetric reduction of an allylic or propargylic ketone (Chapter 7) or asymmetric addition to an aldehyde (Chapter 4). The absolute configuration at the tin-bearing carbon can be set by asymmetric reduction of acyl stannanes [72-74], kinetic resolution using a lipase [75], or oxidation of  $\alpha$ -stannylborates [76]. In certain cases, the carbanion configuration can be controlled by enantioselective deprotonation.

Qualitative evidence that the [2,3]-Wittig rearrangement of nonracemic substrates might have high enantioselectivities was reported in the early 1970s (*e.g.*, see ref. [41,77]), but it was some years before this aspect of the reaction was quantitated. The evidence that eventually appeared is completely consistent with the tenets of simple diastereoselectivity outlined in the preceding section. For example in 1984, Midland [78] and Nakai [79] showed that nonracemic ethers with stereocenters at the allylic position *and* having the *Z* configuration at the double bond are highly selective for the product having the *E*-configured double bond and syn relative configuration at the two new stereocenters. In addition, the chirality transfer was quantitative, as illustrated in Scheme 6.11. Substituents at the allylic position and the *Z*-olefinic site are susceptible to severe  $A^{1,3}$  strain in one of the conformers of the transition state (*cf.* Figure 6.5a, Scheme 6.7b), and this effect determines the absolute configuration at one of the two new stereocenters. Additionally, the two faces of the carbanionic carbon in these examples are heterotopic; the topicity is determined by the greater preference of the carbanionic substituent to occupy the convex face of the envelope transition structure (*cf.* Figure 6.6a). When  $R_1$  is isopropyl, the *E*-alkene isomers show only 60-62% selectivity for the anti isomer [78].

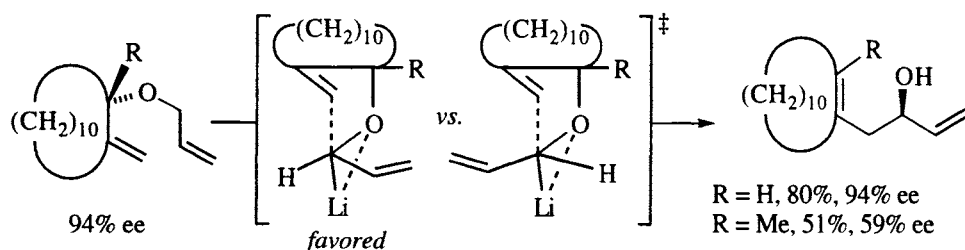




**Scheme 6.11.** Asymmetric induction and chirality transfer in [2,3]-Wittig rearrangements of allylic benzyl [78], allyl [78], and trimethylsilylpropargyl [79] ethers.

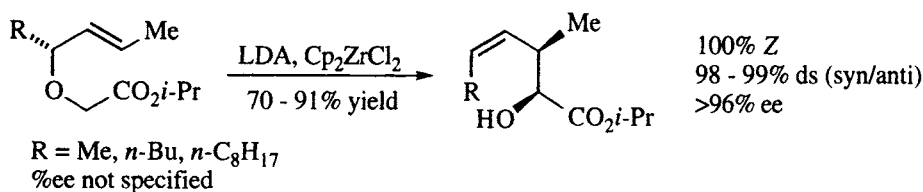
In these cases, the isopropyl probably favors a pseudoequatorial conformation and there is only a slight preference for the phenyl or vinyl carbanion substituent to occupy the convex face of the transition structure.

Marshall reported two examples that differed only in the degree of substitution at the allylic position. In one case, with a quaternary allylic carbon, the enantiomeric purity of the product was only 59% ee (Scheme 6.12) [80]. Apparently there is less preference for the carbanionic substituent to occupy the convex face in preference to the concave face of the transition structure. When the angular methyl is replaced by hydrogen, the chirality transfer is 100%.



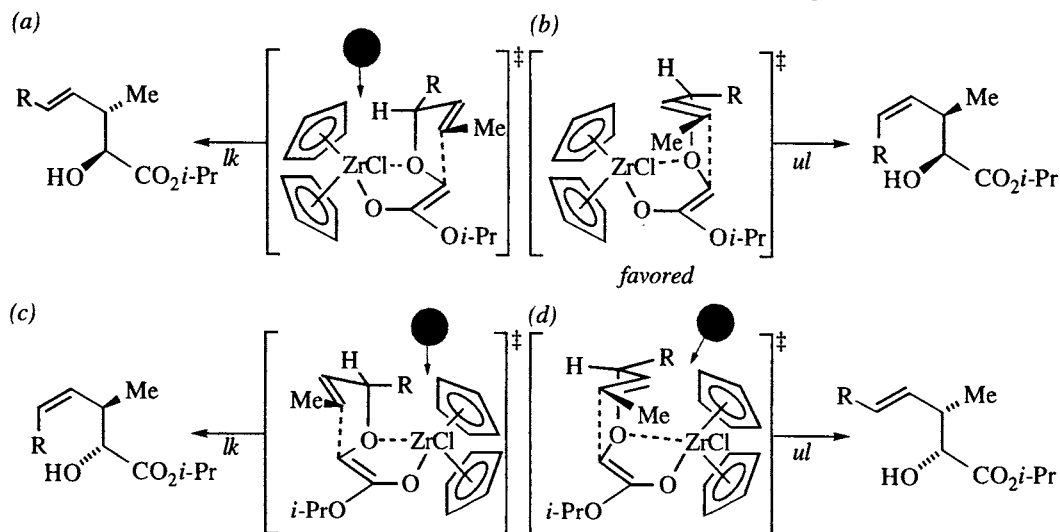
**Scheme 6.12.** A low enantioselectivity may ensue in some instances, for example when a transannular interaction destabilizes the favored carbanion configuration [80].

In 1986 [63], Katsuki showed that the dicyclopentadienylzirconium ester enolates shown in Scheme 6.13 afforded products where three stereochemical elements in the product were controlled with a high degree of selectivity: the double bond geometry, the relative configuration, and the absolute configuration. Only one double bond isomer was observed, the syn/anti diastereoselectivity was 98-99%, and the enantioselectivity was >98%.



**Scheme 6.13.** Asymmetric induction in [2,3]-Wittig rearrangements of chiral  $\alpha$ -alkoxy esters [63].

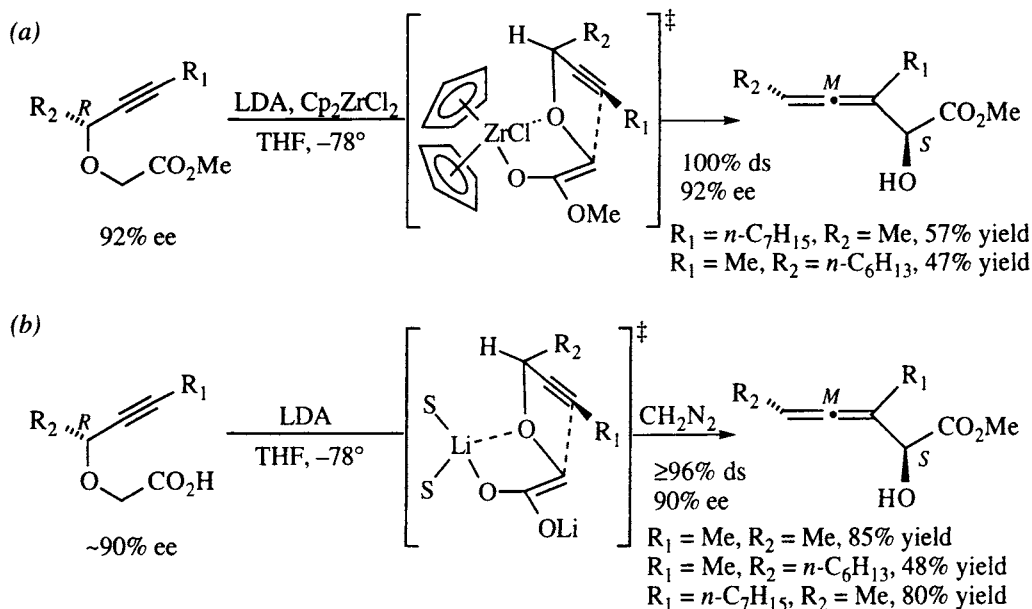
With three stereogenic elements in the product, there are a total of eight possible stereoisomers. However, if it is assumed that the possible transition structures are similar to those shown in Scheme 6.9, there are only four possibilities for the [2,3]-rearrangement, as shown in Scheme 6.14. (Recall from Figure 6.4d that enolate transition structures have shorter bond lengths and smaller allylic bond angles than the other transition structures.) The two having *lk* topology, Scheme 6.14a and c, are disfavored by having the pseudoaxial allylic substituent in close proximity to the cyclopentadiene ligand. Of the two possible *ul* transition structures, the R group is on the less crowded convex face of the bicyclic structure in Scheme 6.14b, but on the concave face in d, where it encounters the cyclopentadiene ligand.



**Scheme 6.14.** Possible transition structures for the [2,3]-Wittig rearrangement of the *R*-allylic ester enolates shown in Scheme 6.13. For amide enolates, see Scheme 6.22.

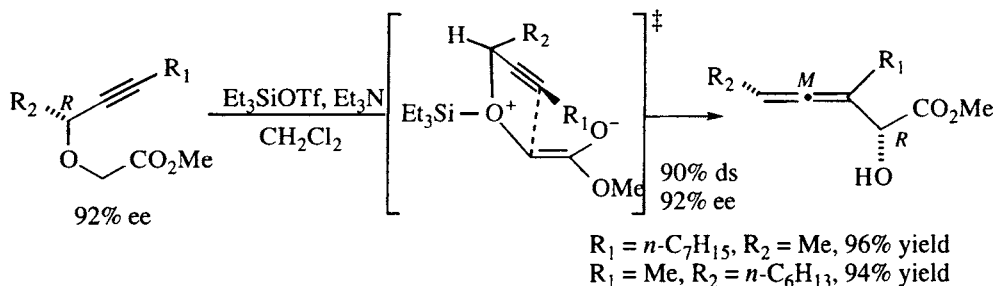
Using a similar protocol, Marshall showed that the propargyloxy esters shown in Scheme 6.15a undergo [2,3]-Wittig rearrangements with 100% chirality transfer [81,82]. Marshall also showed that the corresponding lithium carboxylate dianions rearrange with 100% chirality transfer, and with excellent diastereoselectivity; often the yields are higher, as shown by the examples in Scheme 6.15b [81-83]. Similar to the rationale for the selective rearrangement of the  $\alpha$ -allyloxy ester enolates in Scheme 6.13, the rationale for the asymmetric induction in the present case has the propargylic substituent on the convex face of the transition state assembly (cf. Scheme 6.14b).

Following the lead provided by Nakai, who showed that racemic allyloxy esters can be rearranged using trimethylsilyl triflate [84], Marshall examined similar conditions for the rearrangement of nonracemic propargyloxy esters, and reported the results tabulated in Scheme 6.16 [82]. These two reactants are identical to the two reported in Scheme 6.15a that were rearranged under strongly basic conditions. In the silyl triflate mediated rearrangement, the yields are much higher, although the selectivity is somewhat lower. Additionally, the relative configuration of the allene and the C-2 stereocenter are different. Nevertheless, the chirality transfer is



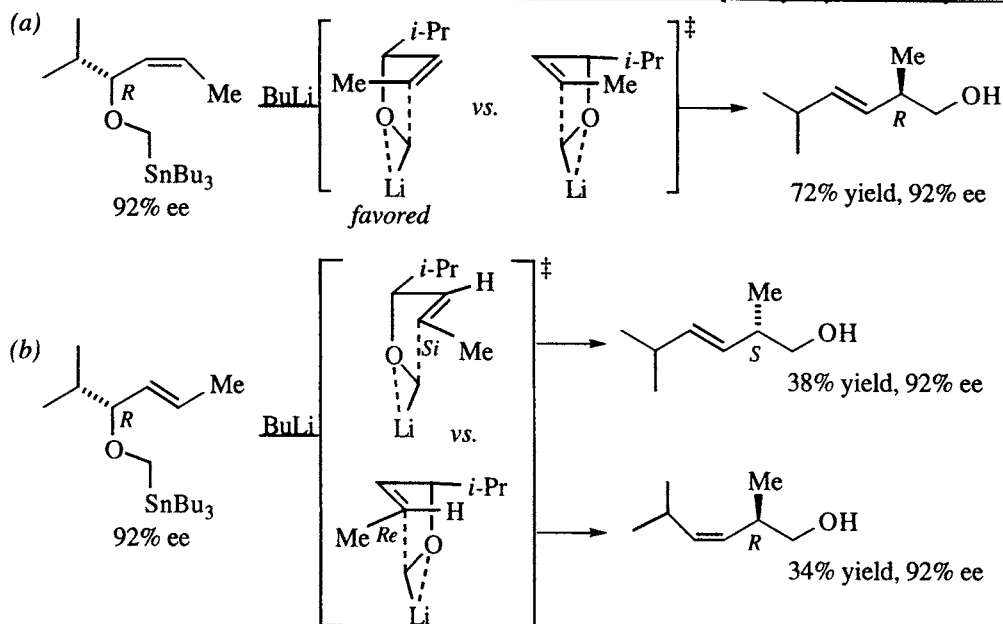
**Scheme 6.15.** [2,3]-Wittig rearrangements of chiral propargyloxy acetates: (a) Zirconium ester enolates [81,82]. (b) Lithium endiolates, S = solvent [81-83].

100% (*i.e.*, both the major and minor isomer have the same enantiomeric purity as the starting propargyl ether). An advantage of this procedure over the base-mediated protocol is that terminal alkynes ( $R_1 = \text{H}$ ) survive the silicon-mediated process [82]. Nakai suggested an 'oxygen ylide' as the intermediate in these silicon-mediated [2,3]-rearrangements, with the silicon and the enolate moieties trans to each other in the 5-membered ring transition structure [84], as shown for the propargyl ether in Scheme 6.16 [82].



**Scheme 6.16.** Silicon-mediated [2,3]-Wittig rearrangement of chiral propargyloxy acetates [82]. The minor diastereomer is the C-2 *S* hydroxyl.

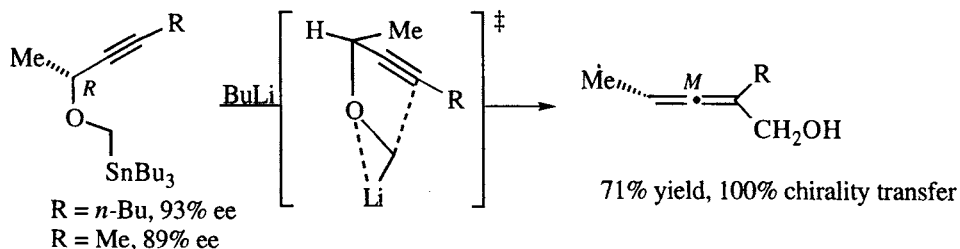
Chirality transfer in the rearrangement of allyloxymethyl stannanes is complete, even in cases where the rearrangement itself is not selective for one product, as shown by the examples in Scheme 6.17 [85]. Recall from Scheme 6.7b and c that in the Still-Wittig rearrangement, one product double bond configuration is formed selectively only when the educt has the *Z* configuration. This is due to severe  $A^{1,3}$  strain in one of the two transition structures (*e.g.*, between the isopropyl and the methyl in Scheme 6.17a). In 1985, Midland reported that rearrangement of the *Z*-



**Scheme 6.17.** [2,3]-Still-Wittig rearrangements of allyl ethers [85].

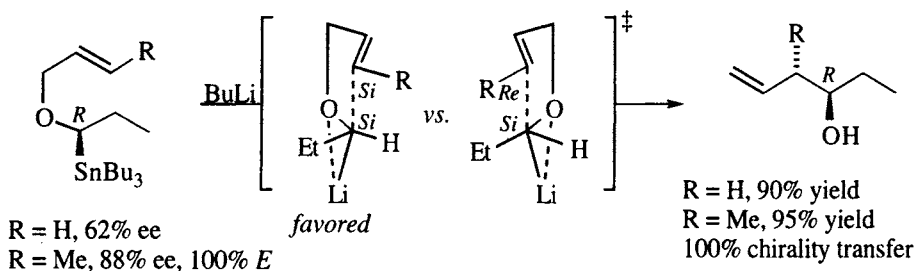
olefin illustrated in Scheme 6.17a is 100% selective for the *E*-double bond geometry, and that the enantiomeric purity of the product matches the enantiomeric purity of the starting material. As expected (*cf.* Scheme 6.7c), the isomeric *E*-educt affords a 53:47 mixture of *E* and *Z* products, as shown in Scheme 6.17b. However, chirality transfer for the formation of each of these products is 100%, even though the absolute configurations of the newly created stereocenter in the two products are opposite! This result may be explained by examining the two transition structures illustrated. The conformation that presents the *Si* face of the olefin to the metalated carbon (Scheme 6.17b, top) is destabilized by  $A^{1,2}$  strain (between the isopropyl and the neighboring vinyl proton) while the conformer that presents the *Re* face is destabilized by  $A^{1,3}$  strain (between the isopropyl and the other vinylic hydrogen). These two effects are approximately equal in this relatively 'loose' transition structure (*cf.* Figure 6.4a and b), so the product ratio is nearly equal.

The rearrangement of propargyloxy stannanes is highly selective, as shown by Marshall in 1989 [83]. The two examples illustrated in Scheme 6.18 show 100% chirality transfer. In this case, there is no conformational ambiguity, since neither of the carbons involved in bond formation are heterotopic.



**Scheme 6.18.** [2,3]-Still-Wittig rearrangements of propargyl ethers [83].

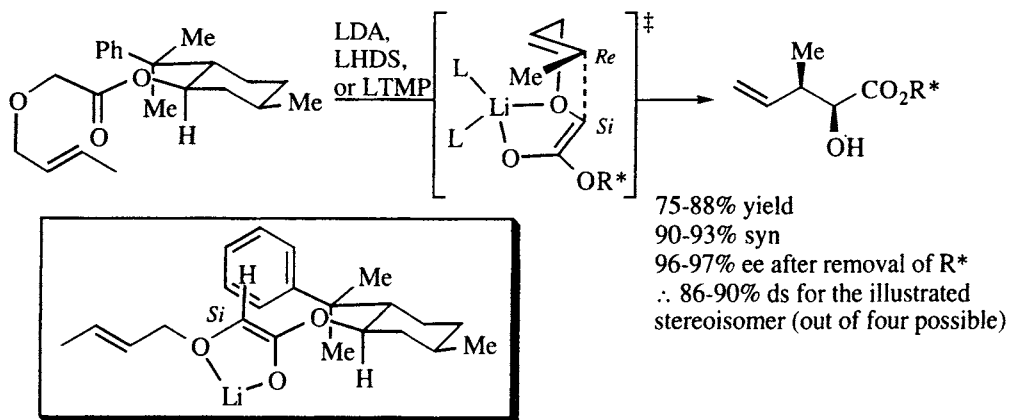
Chirality transfer is also quantitative when the metalated carbon is stereogenic, as shown by the examples in Scheme 6.19 [58]. When R is hydrogen, the two faces of the terminal allylic carbon are homotopic and it does not matter which of the illustrated transition structures is involved. The only important point is that the metal-bearing carbon undergoes inversion of configuration (see also Scheme 6.6b). When R is methyl, the metal-bearing carbon still undergoes inversion, but the configuration at the second stereocenter is determined by consideration of the two illustrated transition structures. Here, the *ul* topology is favored (the reaction is 99% diastereoselective for the anti relative configuration) because of the preference for the ethyl group to occupy the convex face of the transition structure (see Table 6.1, entry 9).



**Scheme 6.19.** [2,3]-Still-Wittig rearrangements of allyl ethers having stereogenic metalated carbons [58].

### 6.1.2.3 Chiral auxiliaries and chiral bases

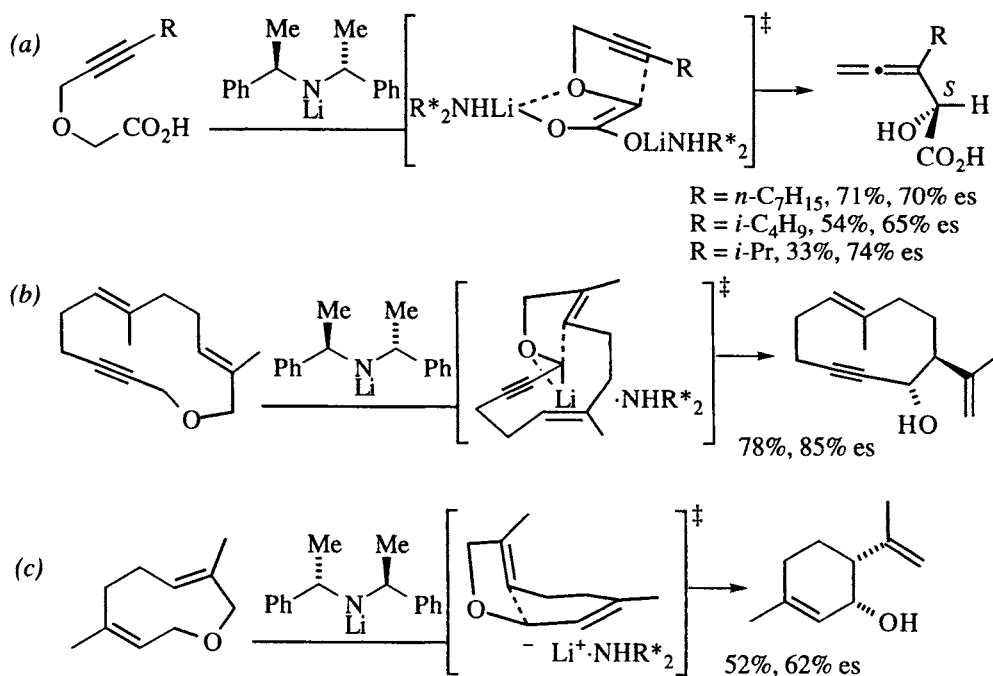
The examples of [2,3]-Wittig rearrangements of allyloxy enolates listed in Table 6.2 show good to excellent simple diastereoselectivity. Chiral auxiliaries, in the form of esters of chiral alcohols and amides of  $C_2$ -symmetric chiral amines have been evaluated in these rearrangements. For example, Nakai showed that the lithium enolates of 8-phenylmenthol esters afford good simple diastereoselectivity with good asymmetric induction as well (Scheme 6.20, [86]. As before, the rationale invokes an  $\alpha$ -alkoxyenolate that chelates the lithium metal. The inset of Scheme 6.20 illustrates the most stable conformation of the chelated enolate, and shows the



**Scheme 6.20.** 8-Phenylmenthol as a chiral auxiliary in the [2,3]-Wittig rearrangement [86].  
*Inset:* Rationale for the *Si*-face selectivity of the enolate.

rationale for preferential attack on the *Si* face of the enolate. The preferred topicity of an enolate is often *ul* (cf. Figure 5.4d, Figure 6.5c, Scheme 6.9, Scheme 6.13), which produces the syn rearrangement product, as shown in the illustrated transition structure. There is a slight dependence of the selectivity on the specific lithium amide base used, so it is likely that the amine (conjugate acid of the base) is still associated with the lithium enolate (cf. Section 3.1.1).

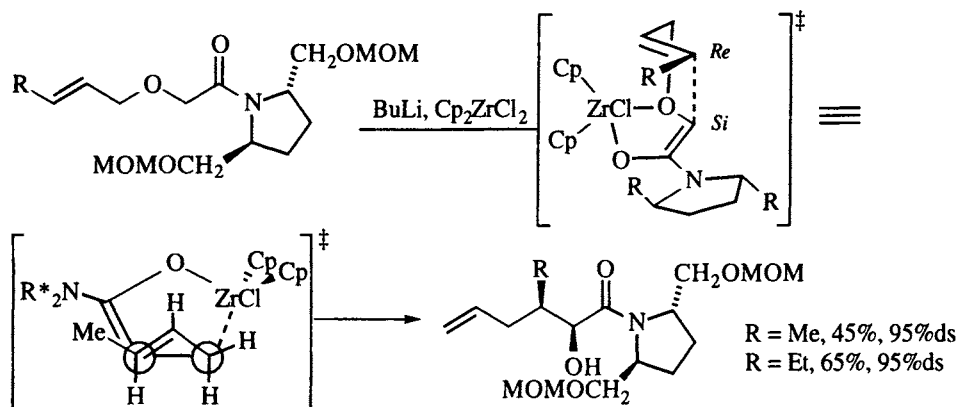
Other examples that underscore the close association of the amine with the lithium ion are examples of interligand asymmetric induction,<sup>12</sup> reported by Marshall and illustrated in Scheme 6.21. In Scheme 6.21a [70], Overberger's base is used to doubly deprotonate a propargyloxy acetic acid; presumably, the enolate is chelated by the  $\alpha$  oxygen, as shown in the illustrated transition structure. Higher enantioselectivity is achieved with the 13-membered propargyl ether shown in Scheme 6.21b [87,88]. This example exhibits the highest degree of asymmetric induction for [2,3]-Wittig rearrangements using the Overberger base. Even other cyclic ethers afford only low selectivity, such as the example shown in Scheme 6.21c [89]. Nevertheless, the principle of interligand asymmetric induction is established by these examples; it then remains to improve on the observed selectivities. A rationale to explain the absolute configuration of the latter two examples may involve an enantioselective deprotonation or a mixed aggregate.



**Scheme 6.21.** Asymmetric [2,3]-Wittig rearrangements using a chiral lithium amide base [70,87-89]. The transition structure leading to the major enantiomer is illustrated.

<sup>12</sup> Interligand asymmetric induction is when one chiral ligand on a metal influences the absolute configuration of a new stereogenic unit on a second ligand of the metal (Section 1.3).

As indicated by Entry 5 in Table 6.2, the lithium enolates of pyrrolidine amides show excellent simple diastereoselectivity, and rearrange in excellent yields [69]. These amides also show a slight dependence of selectivity on the structure of the amide base used [69]. Monosubstituted pyrrolidine amides were poor auxiliaries for this reaction ( $\leq 76\%$  ds) [69], but  $C_2$ -symmetric pyrrolidines are highly selective, as shown in Scheme 6.22 [90]. The *Si* facial selectivity of the lithium enolate and the illustrated zirconium enolate were comparable, but only the zirconium enolate also showed a high preference for the *ul* topicity illustrated. The two views of the transition structure rationalize both the topicity and the absolute configuration of the product. The enolate *Si* face is favored because the closer of the two pyrrolidine stereocenters blocks the *Re* face. The *ul* topicity is favored because when the enolate moiety is on the concave face of the cyclopentane envelope, a severe interaction between a pseudoaxial hydrogen and a cyclopentadiene is avoided (*cf.* Scheme 6.14 a for another illustration).



**Scheme 6.22.** [2,3]-Wittig rearrangement of amide zirconium enolates using Katsuki's pyrrolidine auxiliary [90].

Any reaction that forms a bond between two prochiral atoms in a stereoselective manner is a valuable synthetic method. Some of the natural products that have been made in nonracemic form using the [2,3]-Wittig rearrangement as the key step are illustrated in Figure 6.7. The stereocenters formed in the Wittig rearrangement are indicated (\*).

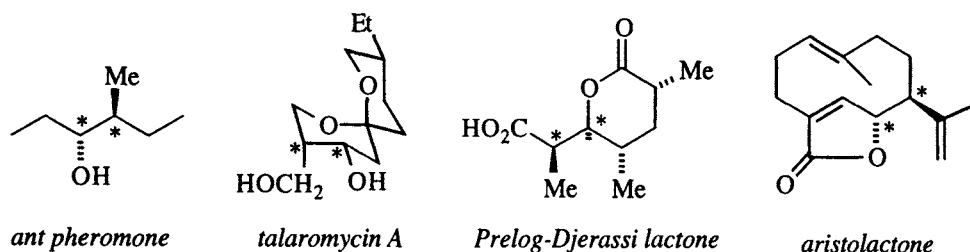


**Figure 6.7.** Natural products using the [2,3]-Wittig rearrangement as the key step: (a) ant pheromone [58]; (b) talaromycin A (J768); (c) Prelog-Djerassi lactone (J771); (d) aristolactone [87,88].

## 6.2 Cycloadditions

Cycloaddition reactions have considerable value in organic synthesis for a number of reasons, not the least of which are that two bonds are formed in one operation and that the reactions often exhibit high stereoselectivities. Even if this huge field were limited only to examples that fall into the category of asymmetric synthesis, it would take several volumes to completely do it justice. In this section, only selected [2+1]- and [4+2]-cycloadditions (and equivalent transformations) are covered, and the discussion is not limited to concerted processes.

### 6.2.1 [2+1]-Cyclopropanations and related processes<sup>13</sup>

Although the addition of carbene to a double bond to make a cyclopropane is well known, it is not particularly useful synthetically because of the tendency for extensive side reactions and lack of selectivity for thermally or photochemically generated carbenes. Similar processes involving carbenoids (species that are not free carbenes) are much more useful from the preparative standpoint [91,92]. For example, metal catalyzed decomposition of diazoalkanes usually results in addition to double bonds without the interference of side reactions such as C–H insertions. Consider the possible retrosynthetic approaches to a 1,2-disubstituted cyclopropane shown in Figure 6.8. Disconnection *a* entails the addition of a methylene across a double bond, a conversion that is often stereospecific (*e.g.*, the Simmons-Smith reaction [93]). Disconnections *b* and *c* are more problematic, since the issue of *cis/trans* product isomers (simple diastereoselection) arises.

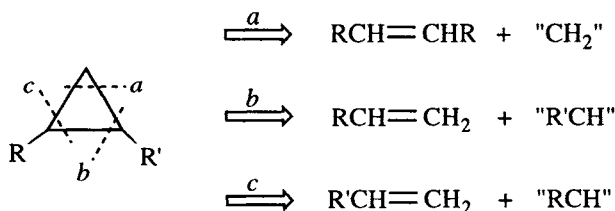


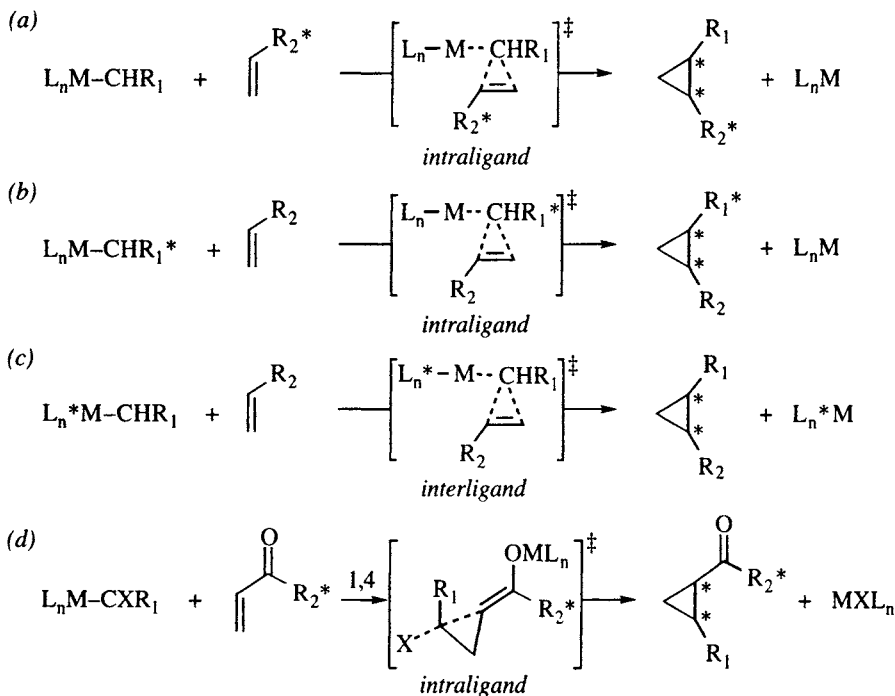
**Figure 6.8.** Retrosynthesis of 1,2-disubstituted cyclopropanes.

Two strategies have been taken to apply cyclopropanations to asymmetric synthesis: auxiliary based methods whereby a covalently attached adjuvant renders either the olefin or the cyclopropanating reagent chiral, and processes that utilize a chiral ligand on a metal catalyst. Scheme 6.23 illustrates these approaches as applied to the more complex case of disconnections *b* and *c* of Figure 6.8. Scheme 6.23a and b show chiral auxiliaries ( $\text{R}^*$ ) in the olefin and carbenoid moieties, respectively, while Scheme 6.23c shows a chiral ligand on the metal. Since the transition states of both processes still involve the metal, asymmetric syntheses using these reactions may be said to occur by intraligand or interligand asymmetric induction. Still another approach to asymmetric cyclopropanations involves reaction

<sup>13</sup> Not covered in this section are cyclopropanations that involve initial 1,3-dipolar cycloadditions of diazoalkanes to give pyrazolines, followed ring contraction and nitrogen extrusion.

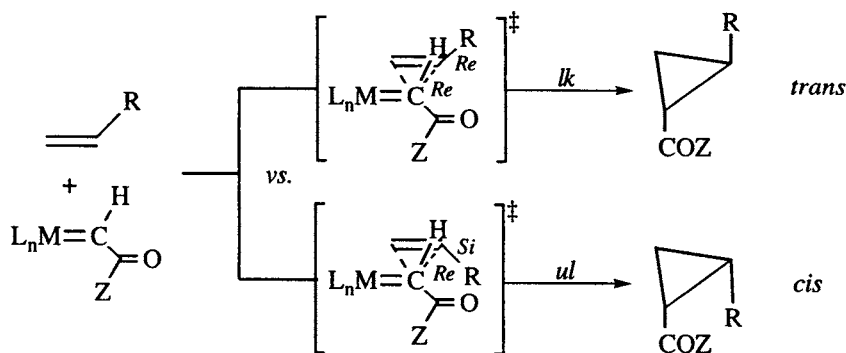


sequences, such as a tandem 1,4 addition–intramolecular alkylation, that do not involve carbenes but which accomplish a similar transformation (also by intraligand asymmetric induction, Scheme 6.23d). Double asymmetric induction may be achieved by ‘crossing’ two methods, for example by using a chiral catalyst to promote reaction with a carbenoid and olefin that are also chiral. As will be seen, double asymmetric induction is often used in cyclopropanations of carbenes as a means of enhancing selectivity.



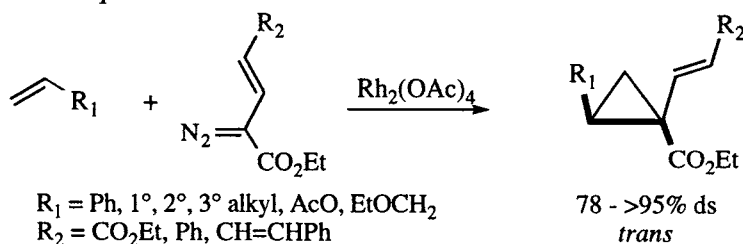
**Scheme 6.23.** General strategies for asymmetric induction in cyclopropanations.

The issue of simple stereoselectivity in cyclopropanations of the types shown in Figure 6.8, disconnections *b* and *c*, is not a trivial one, and relatively few additions of ketocarbenoids (by far the most common type of carbenoid studied) show high selectivity. The difficulty can be seen by inspection of the transition states of Scheme 6.24. The transition state leading to the *trans* isomer (*lk* topicity) is usually favored, but unless the COZ group is quite large, the *trans*-selectivities are not great. Recently, for example, Doyle showed that if *Z* = OEt (*i.e.*, ethyl diazoacetate), the  $\text{Rh}_2(\text{OAc})_4$  catalyzed cyclopropanation of alkenes having *R* = *n*-alkyl, Ph, and *i*-Pr is only about 60–70% *trans*-selective. With *R* = *tert*-butyl, the selectivity is 81%. If the olefin is in a ring, the selectivity is not much better [94]. If hindered esters (*Z* = OCMe- $\text{Pr}_2$ ) or amides (*Z* =  $\text{Ni-Pr}_2$ ) are used, the *trans*-selectivity for the  $\text{Rh}_2(\text{OAc})_4$  catalyzed cyclopropanation of styrene can be improved to 71% and 98%, respectively [95]. BHT esters (*Z* = O-2,6-*t*-Bu-4-Me- $\text{C}_6\text{H}_2$ ) also give good *trans*-selectivity (71–97%) with a variety of alkenes [96]. With  $\text{Rh}_2(\text{NHCOMe})_4$  as catalyst, these selectivities can be increased further due to the decreased reactivity of the rhodium carbenoid, which results in a more selective reaction [95,96].



**Scheme 6.24.** Transition states and relative topicities for cycloaddition of ketocardenoids and monosubstituted alkenes.

H. Davies has found that vinyl carbenoids tend to show high selectivities in  $\text{Rh}_2(\text{OAc})_4$  catalyzed cycloadditions, as shown by the examples in Scheme 6.25 [97]. It is also important to note that the stereoselectivity of the cyclopropanations shown in Schemes 6.24 and 6.25 are not due only to steric effects. For example, changing  $\text{R}_1$  in Scheme 6.25 from *n*-butyl to *tert*-butyl lowers the selectivity from 85% to 78% ( $\text{R}_2 = \text{CO}_2\text{Et}$ ), while changing  $\text{R}_2$  from phenyl to  $\text{CO}_2\text{Et}$  ( $\text{R}_1 = \text{Ph}$ ), lowers the selectivity from >95% to 89% [97]. Presumably there is a contribution to the relative stabilities of the transition states by both electronic and steric effects, but they have not been quantified.



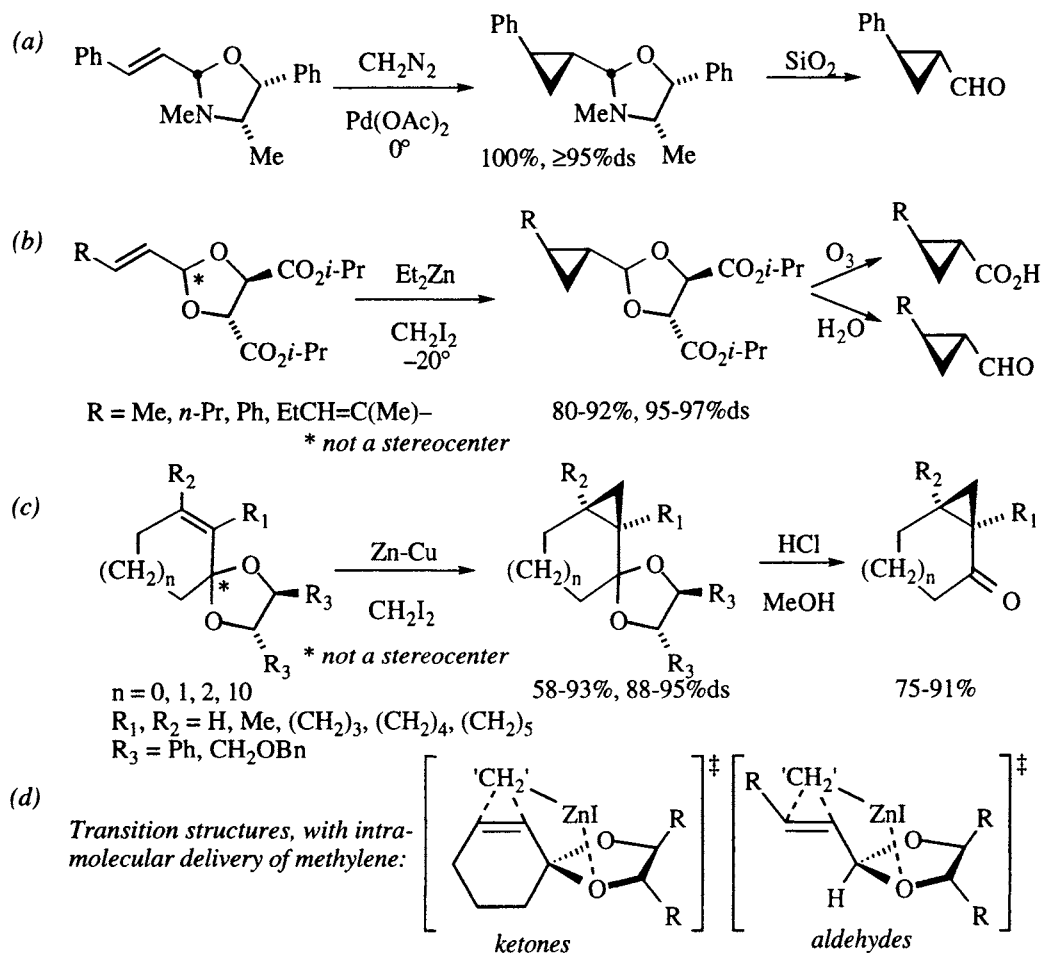
**Scheme 6.25.** Diastereoselective cyclopropanations of vinyl carbenoids [97]. For disubstituted carbenes, *cis/trans* nomenclature is used to describe relative configuration, referring to  $\text{R}_1$  relative to the carbonyl moiety, as shown in bold.

The following discussion is organized along the lines of the examples in Scheme 6.23. First, auxiliary-based methods are discussed, followed by methods using chiral catalysts, including examples of double asymmetric induction employing chiral catalysts on chiral substrates and substrates having chiral auxiliaries attached, and finally stepwise cyclopropanation sequences. Within each section, the addition of “ $\text{CH}_2$ ” is covered first (*i.e.*, disconnection *a* in Figure 6.8), followed by examples of the addition of “ $\text{RCH}$ ” (*i.e.*, disconnections *b* and *c* of Figure 6.8).

#### 6.2.1.1 Chiral auxiliaries for carbenoid cyclopropanations

Cyclopropanations of functionalized alkenes using the Simmons-Smith reaction [93], or a similar cyclopropanation, have been developed by modifying carbonyl and hydroxyl groups with chiral auxiliaries. A single example was reported by Carrié in 1982 (Scheme 6.26a, [98]), whereby the oxazolidine derived from con-

densation of (–)-ephedrine and cinnamaldehyde was cyclopropanated with diazomethane using palladium acetate as catalyst. The yield was quantitative and the selectivity was  $\geq 95\%$ , but no further examples were provided. More systematic studies were undertaken by the groups of Yamamoto [99,100] and Mash [101–104]. Both of these groups used  $C_2$ -symmetric acetals as auxiliaries, as shown in Scheme 6.26b–c. Yamamoto studied the tartrate-derived acetals shown in Scheme 6.26b while Mash examined a series of related acetals, including the two shown in Scheme 6.26c. Both groups showed that the acetal could be hydrolyzed in the normal manner to the corresponding carbonyl compound, but Yamamoto also showed that the acetal could be cleaved to the carboxylic acid using ozone.

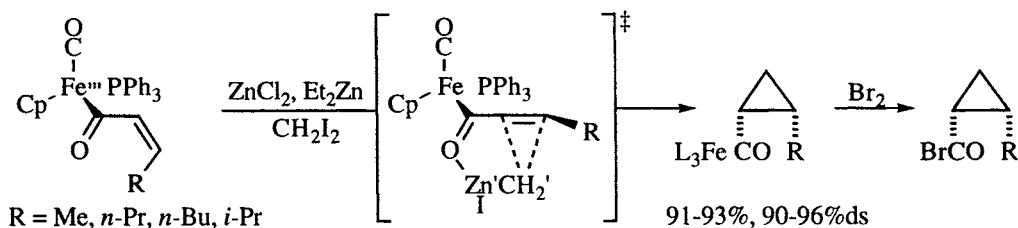


**Scheme 6.26.** Auxiliary-based asymmetric cyclopropanations (addition of “CH<sub>2</sub>”) of  $\alpha,\beta$ -unsaturated aldehydes and ketones. (a) [98]; (b) [99,100]; (c) [101–104]; (d) Proposed transition structures [104]. Only one zinc and the transfer methylene are shown; other atoms associated with the Simmons-Smith reagent are deleted for clarity.

Note that in both the aldehyde and ketone acetals, the acetal carbon is not stereogenic, due to the  $C_2$  symmetry of the starting diol. For the ketone acetals, there is no conformational ambiguity, and the mechanistic rationale shown in Scheme 6.26d was proposed to account for the selectivity of the reaction [104].

Thus, coordination of the zinc to one of the diastereotopic oxygens and oriented anti to the adjacent dioxolane substituent places the 'transfer methylene' on the face of the olefin toward the viewer, consistent with the observed absolute configuration. Note that coordination to the other oxygen and orienting anti to the adjacent substituent would place the 'transfer methylene' distal to the double bond. A similar explanation can be offered to rationalize the results of the aldehyde acetal additions, assuming that the olefin adopts the indicated conformation in the transition state.<sup>14</sup>

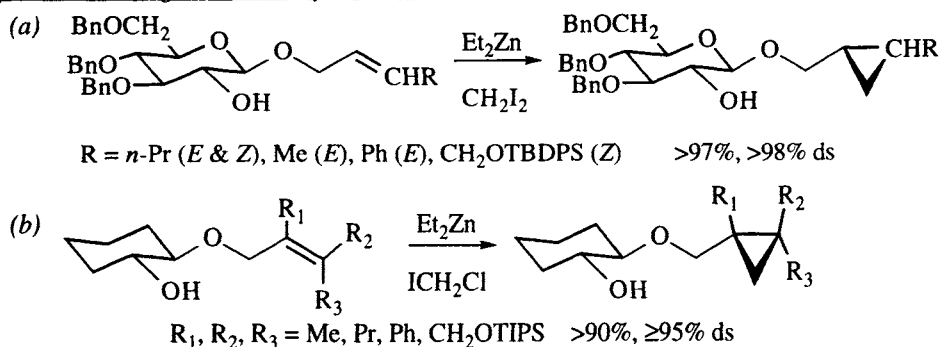
S. Davies has used an iron complex as an auxiliary for the asymmetric cyclopropanation of  $\alpha,\beta$ -unsaturated carbonyls [105]. The iron acyl is most stable in the *s*-cis conformation, as illustrated in Scheme 6.27, in order to avoid severe interactions between the iron ligands and R. Coordination of the Simmons-Smith reagent to the carbonyl oxygen, anti to the iron, forces the alkene moiety out of conjugation and approximately orthogonal to the carbonyl. Because of the bulky triphenyl phosphine in the rear, this rotation can only be towards the front. Transfer of the methylene via the illustrated transition state accounts for the observed diastereoselectivity. Oxidation with bromine removes the iron acyl and derivatization with  $\alpha$ -methylbenzyl amine allowed evaluation of the stereoselectivity.



**Scheme 6.27.** S. Davies's asymmetric cyclopropanation of Z-iron acyls [105].

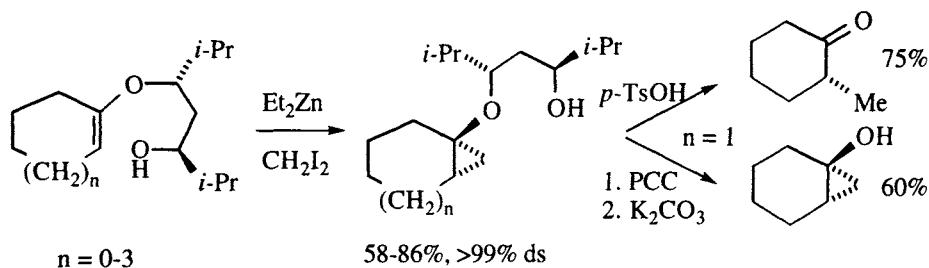
Charette has shown that allylic alcohols can be cyclopropanated by attaching a chiral auxiliary in the form of a glucose derivative [106] or *trans*-1,2-cyclohexane diol [107], as shown in Scheme 6.28. The yields are outstanding, as are the diastereoselectivities. The topicity can be rationalized by chelation of one of the zinc atoms of the Simmons-Smith reagent by the hydroxyl and the ether oxygen and intramolecular delivery of the methylene to the olefin in the conformation shown. Note however, that the conditions that are optimum for the glucose auxiliary afford very low selectivity in the cyclohexane diol system [107], which may mean that the mechanism is not so simple. Two procedures allow (destructive) removal of the auxiliary from the cyclopropane methanol. In one, the free hydroxyl of the glucose is triflated, the ring fragmented, and the resultant acylium ion hydrolyzed [106,108]. In another, the hydroxyl is converted to an iodide; halogen-lithium exchange then effects elimination of the alkoxide [107]. To get the opposite absolute configuration at the cyclopropane, a derivative of L-rhamnose may be used in place of the D-glucose [106], or the enantiomeric cyclohexane diol can be used.

<sup>14</sup> Although this explanation is self-consistent with that of the ketone acetals, a related 6-membered C<sub>2</sub>-symmetric aldehyde acetal affords cyclopropanation products with the opposite topicity sense [100]. Also, the structure of the Simmons-Smith reagent is unknown, and aggregates may be involved. Thus, this explanation must still be regarded as tentative.



**Scheme 6.28.** Asymmetric cyclopropanation of allylic alcohols: (a) Using a glucose-derived auxiliary [106]; (b) A cyclohexane diol auxiliary [107].

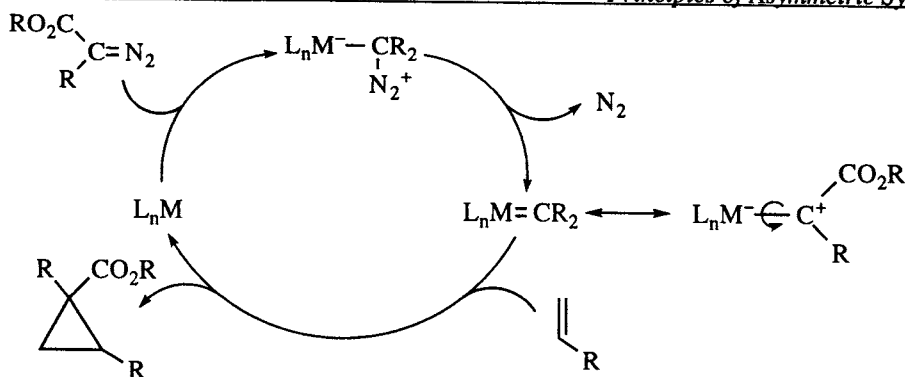
A process for the asymmetric cyclopropanation of the enol ethers of cyclic and acyclic ketones has been developed by Tai [109-111]. In this process, a  $C_2$ -symmetric acetal is isomerized to a hydroxy enol ether which serves as substrate for the Simmons-Smith cyclopropanation, as shown in Scheme 6.29. The stereoselectivity is nearly perfect, but a mechanistic hypothesis has not been proposed. The auxiliary may be removed either by hydrolysis, to give the methyl ketone, or by oxidation of the alcohol and  $\beta$ -elimination [111].



**Scheme 6.29.** Asymmetric cyclopropanation of ketone enol ethers [109-111].

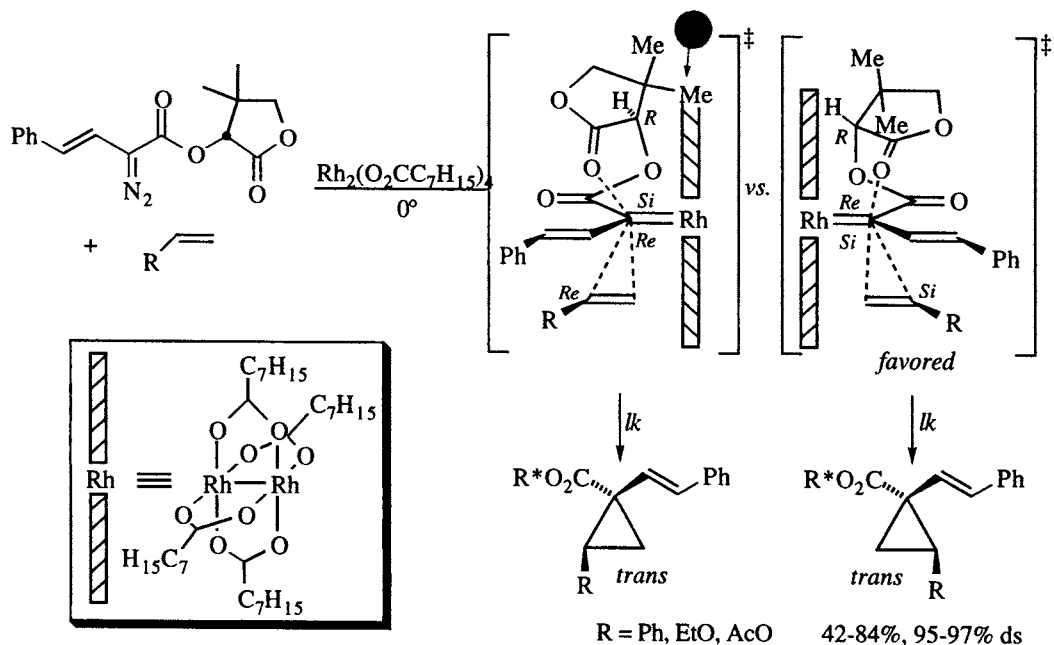
Cyclopropanation reactions involving diazoalkanes and catalyzed by transition metals involve metal carbenes as intermediates. Scheme 6.30 illustrates the proposed catalytic cycle for such processes [112]. The catalyst,  $L_nM$ , is coordinatively unsaturated and therefore electrophilic. Loss of nitrogen from the zwitterion at the top affords the metal carbene shown at the right. Two canonical forms for the metal carbenoid are shown. For rhodium carbenes, it is thought that they tend to resemble metal stabilized carbocations, with a low barrier to rotation [112,113]. For control of the absolute configuration at the carbenoid carbon in the cyclopropanation, an auxiliary (usually the alcohol of the ester) must somehow shield one face of the trigonal carbenoid carbon in order to influence the absolute configuration at that center. Also, recall (Scheme 6.24) that the simple diastereoselectivity (relative configuration) in these processes is not high unless very bulky esters are used.

In light of the above analysis, it is perhaps not surprising that asymmetric cyclopropanations of styrene using bornyl, menthyl, and 2-phenylcyclohexyl esters of diazoacetic acid afforded both poor cis/trans selectivity and low enantioselectivity with cuprous chloride [114] or rhodium acetate [115] catalysts. On the other hand,



**Scheme 6.30.** Catalytic cycle for the transition metal-catalyzed cyclopropanation of olefins by diazoalkanes (after [112] and [113]).

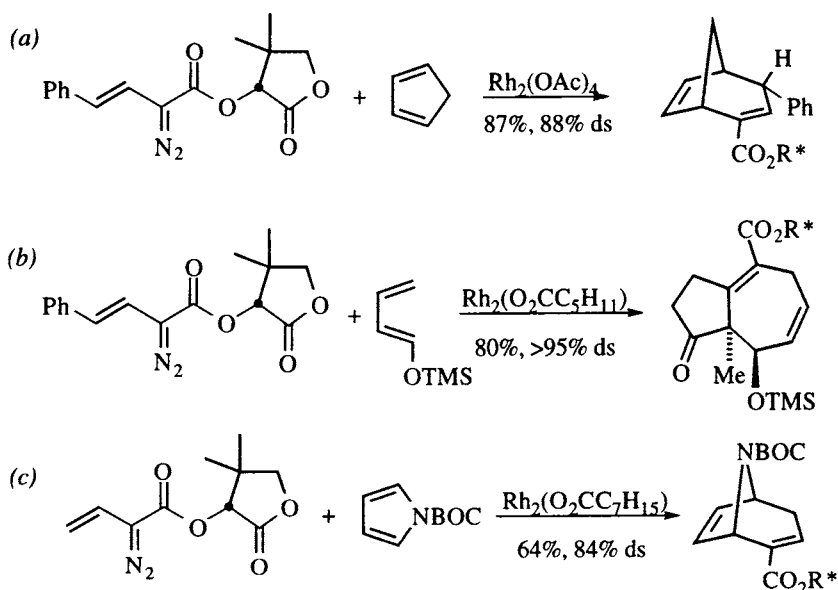
vinyl carbenoids (Scheme 6.25) show good simple diastereoselection [97], and H. Davies has shown that pantolactone is an excellent chiral auxiliary, as shown in Scheme 6.31 [116-118]. The mechanistic hypothesis involves intramolecular interaction of the pantolactone carbonyl with the electrophilic carbenoid carbon, which shields the *Re* face of the carbene. Note that the conformer in which the carbene's *Si* face is shielded suffers severe steric interactions between the catalyst 'wall' and the pantolactone moiety. Approach of the alkene toward the *Si* face of the carbene, coupled with diastereoselectivity favoring *lk* relative topicity, affords a mixture containing only the two *trans* diastereomers. The examples in Scheme 6.25



**Scheme 6.31.** Diastereoselective cyclopropanation of olefins with vinyl carbenes [116]. Note that only two of the four possible stereoisomers were found in the product mixture. The *trans* nomenclature refers to the relative configuration of R and CO<sub>2</sub>R\*, consistent with that of Scheme 6.24.

showed a lower *cis/trans* selectivity. In the examples shown in Scheme 6.31, however, only the two *trans* diastereomers are found. Thus, a weakness of the transition state models shown in Scheme 6.31 is that, although the absolute configuration is rationalized, it is not obvious why the *cis/trans* selectivity (*lk* topicity) should be 100%. This underscores the statement in the previous section which noted the presence of unquantified electronic effects contributing to the stereoselectivity of the rhodium catalyzed cyclopropanation using vinyl carbenes.

The *cis* relationship between the vinyl group and the R group of the olefin raises an interesting possibility: if the R group is also a vinyl substituent, the product of the cyclopropanation is a *cis*-divinylcyclopropane, precursor to a Cope rearrangement [119]. Although the Cope rearrangement destroys the stereocenters created in the cyclopropanation, it creates others, as shown by the examples in Scheme 6.32.

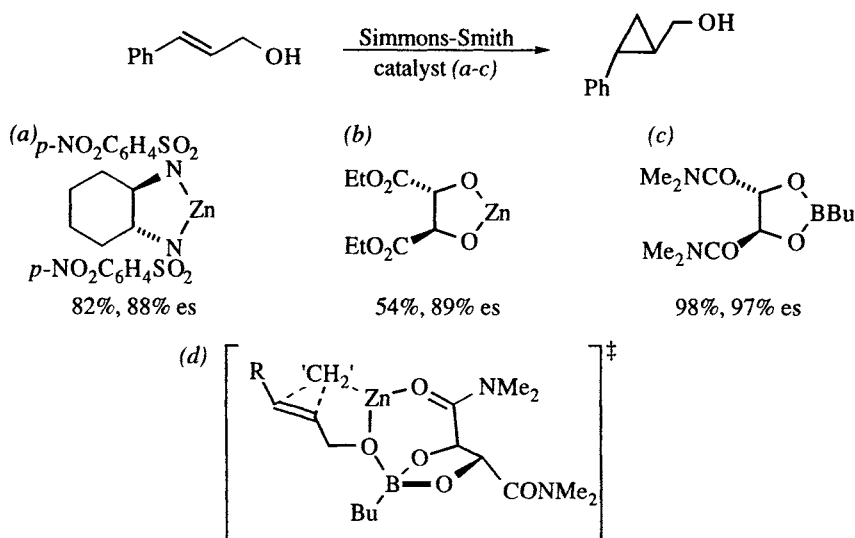


**Scheme 6.32.** Synthetic applications of vinylcarbene cyclopropanations coupled with a Cope rearrangement. (a,b) [116]; (c) [118].

#### 6.2.1.2 Chiral catalysts for carbenoid cyclopropanations

The first examples of the enantioselective Simmons-Smith cyclopropanations mediated by a chiral catalyst are very recent. Scheme 6.33 shows three catalysts for the cyclopropanation of *trans*-cinnamyl alcohol. The most selective appears to be Charette's dioxaborolane (Scheme 6.33c, [120-122], which also affords the highest yield of product, although this procedure is only suitable for small scale.<sup>15</sup> With other olefins, such as *cis* and *trans* disubstituted alkenes and  $\beta,\beta$ -trisubstituted alkenes, the yields are nearly as good and the enantioselectivities are 96-97%. An important finding in this study [120] was that, in addition to the Lewis acid (boron) that binds the alcohol, a second atom to chelate the zinc is also necessary. In the

<sup>15</sup> Charette has noted an explosion hazard on scale-up of the original procedure [121], and has published an alternative procedure [122].



**Scheme 6.33.** Asymmetric catalysts for the Simmons-Smith cyclopropanation of *trans*-cinnamyl alcohol: (a) [123]. (b) [124]. (c) [120,122]. (d) Transition state model for catalyst c [120]. Only one zinc and the transfer methylene are shown; other atoms associated with the Simmons-Smith reagent are deleted for clarity.

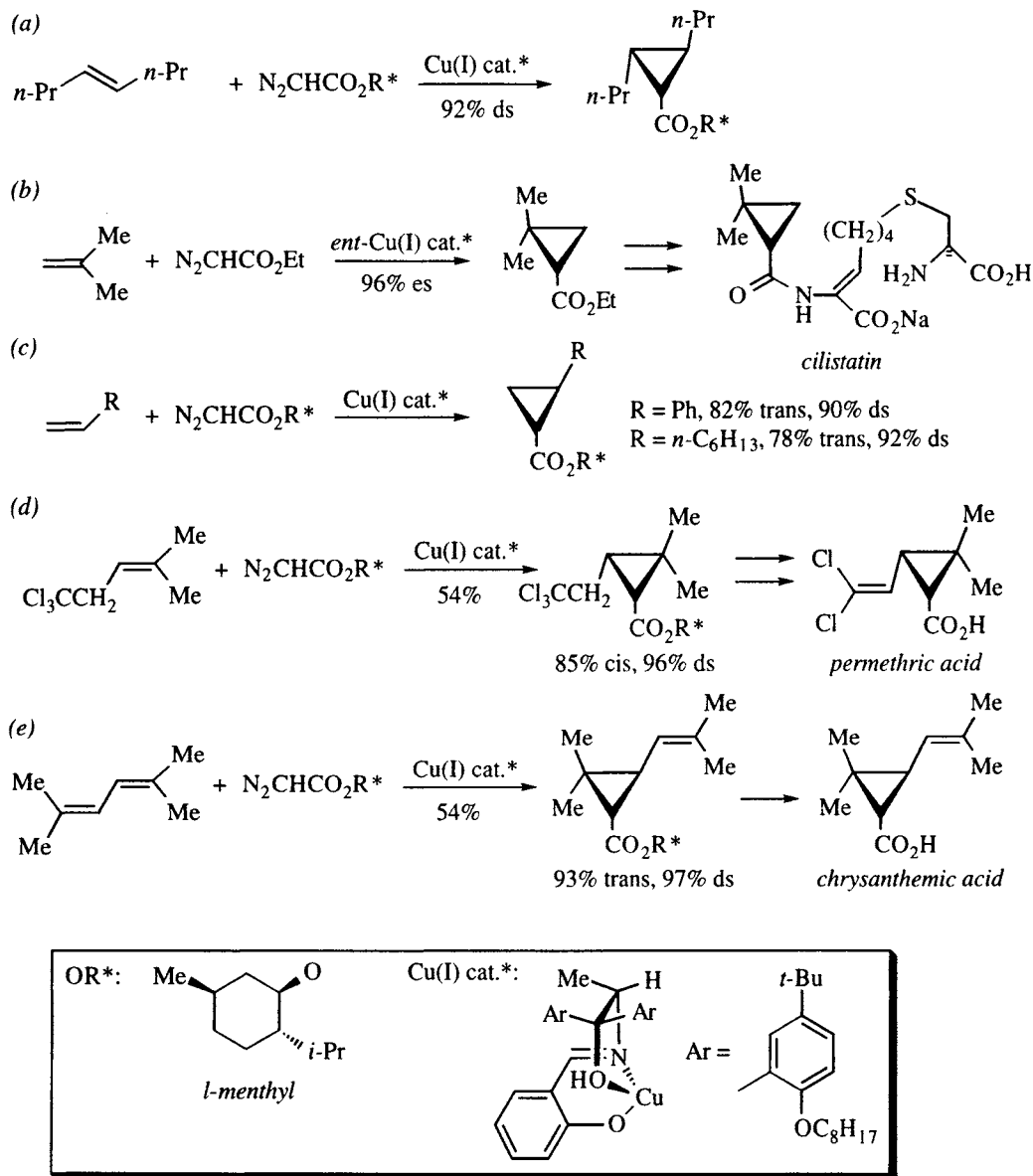
Charett catalyst, this atom is the amide carbonyl oxygen (Scheme 6.33d). Evidence for this feature is that when the amide substituents are replaced by phenyl groups, the cyclopropane product is racemic.

In 1966, Nozaki, et al., reported the first example of an asymmetric cyclopropanation using a chiral copper (II) catalyst [125]. Although the enantioselectivities were low (<10% ee), the contribution is important because it was the first example of an asymmetric synthesis using a chiral, homogeneous transition metal catalyst. Subsequently, Aratani optimized the ligand design and reported a number of asymmetric cyclopropanations, as shown in Scheme 6.34 [126-128]. For symmetrical *trans*-olefins, relative configuration is not an issue, and better selectivity is achieved with *l*-menthyl (from (–) menthol) diazoacetate than with the ethyl ester (double asymmetric induction, [127]). Cyclopropanation of isobutene is used on a factory scale for the commercial manufacture of the drug cilistatin (Scheme 6.34b) [128]. With monosubstituted olefins, relative as well as absolute configuration are an issue, but *trans* is favored, and double asymmetric induction again increases the stereoselectivity (Scheme 6.34c, [127]). Trisubstituted, unconjugated alkenes favor the *cis* relative configuration, as shown by the example in Scheme 6.34d, used in the synthesis of the *cis* isomer of the insecticide permethic acid [127]. Dienes, on the other hand, favor the *trans*-isomer, as shown by the synthesis of chrysanthemic acid shown in Scheme 6.34e [126,128].

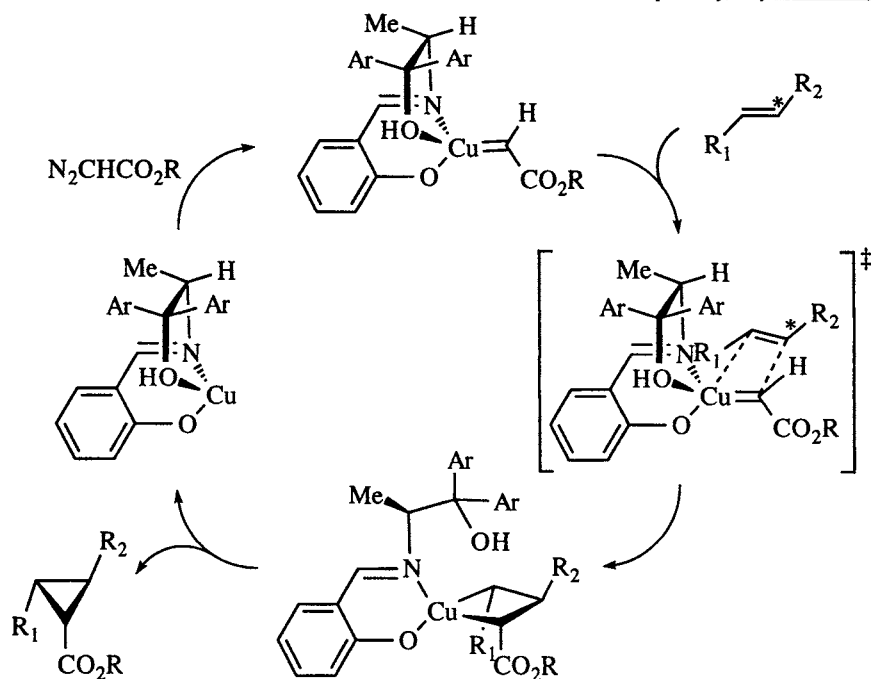
The mechanism that has been proposed to explain the relative and absolute configurations of these examples is illustrated in Scheme 6.35 [128]. The catalyst, shown on the left of the scheme, is coordinatively unsaturated. Reaction with the diazoalkane affords the copper carbene shown at the top. The olefin approaches from the less hindered back side (note that the absolute configuration of the carbene carbon is set at this point), such that the indicated carbon (\*, which is the one most



able to stabilize a cationic charge) is oriented toward the carbene carbon. This is consistent with the metal atom acting as a Lewis acid. A metallacyclobutane is thought to be a discrete intermediate (bottom), and as it is formed, the hydroxyl is released from the copper. Steric repulsion by the large aryl substituents of the chiral ligand tends to force  $R_1$  downward, cis to the ester function. Similarly, steric repulsion tends to favor  $R_2$  in a position trans to the ester. Collapse of the metallacyclobutane releases the cyclopropane and regenerates the catalyst.

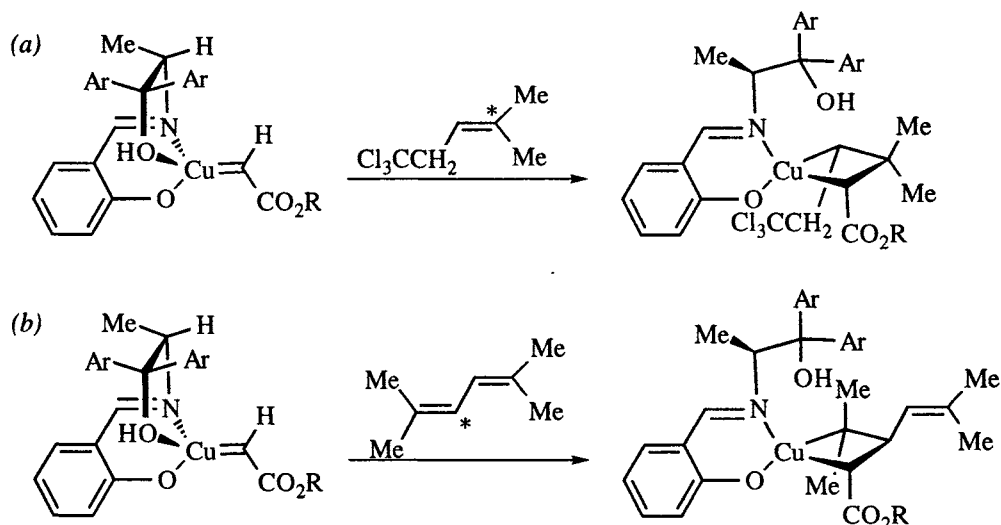


**Scheme 6.34.** Aratani's copper-catalyzed asymmetric cyclopropanation of olefins. (a) *trans*-1,2-disubstituted [127]. (b) 1,1-disubstituted [128]. (c) monosubstituted, *trans* favored [127]. (d) trisubstituted, *cis* favored [127]. (e) dienes, *trans* favored [126,128]. Inset: chiral auxiliary and coordinatively unsaturated chiral catalyst.



**Scheme 6.35.** Proposed catalytic cycle for asymmetric cyclopropanation using Aratani's copper catalyst [128].

This speculative rationale may be used to explain the apparent reversal of both relative and absolute configuration preference exhibited by the examples in Scheme 6.34d and e. In Scheme 6.34d,  $R_1$  is  $\text{Cl}_3\text{CCH}_2-$ ; attack of the copper occurs at the secondary carbon and the carbene carbon attaches to the tertiary site (\*), as shown in Scheme 6.36a. The controlling elements are the tertiary carbon of the olefin attaching to the carbene carbon, while the bulky  $\text{Cl}_3\text{CCH}_2-$  is oriented away from the nitrogen ligand. In the example in Scheme 6.34e, the more stable carbocation is



**Scheme 6.36.** Rationale for the relative and absolute configuration of the examples from (a) Scheme 6.34d, and (b) Scheme 6.34e [128].

allylic, so the trisubstituted olefin ‘turns around’ (Scheme 6.36b). Here, the controlling element is the *trans* orientation of the ester with respect to the isobutenyl group [128].

Several other groups have used  $C_2$ -symmetric ligands with copper and ruthenium as cyclopropanation catalysts. These ligands, shown in Figure 6.9, are generally more selective than the Aratani ligands. The first to be introduced was the semicorrin of Pfaltz (Figure 6.9a), and most of the others bear a close structural resemblance in that they all have pyrroline, oxazoline or bipyridine ligands chelating the metal. Copper(I) is the oxidation state of the active catalyst for all complexes containing copper, and the mechanism of the cyclopropanation using these catalysts is probably similar to that illustrated above (Schemes 6.35 and 6.36): electrophilic attack by copper, metallacyclobutane formation, etc. Table 6.3 lists selected examples for each ligand. It was generally found that bulky esters (*e.g.*, *tert*-butyl, BHT, menthyl) are more selective than less bulky ethyl esters (not listed). Entries 2 and 3 illustrate the effects of double asymmetric induction using the two enantiomers of menthol. Ligands c and f were also tested with both enantiomers of menthol, but there were no differences in selectivity. These examples show very high selectivity for *trans*-cyclopropanes; only one is *cis*-selective, but not by much (entry 18), which is >99% enantioselective for the *cis* product but only 62% enantioselective for the *trans*.

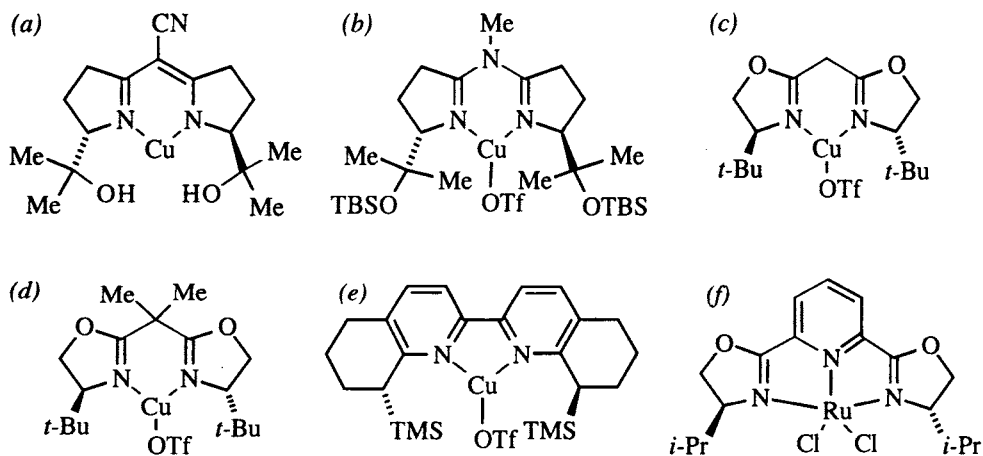


**Figure 6.9.**  $C_2$ -symmetric catalysts for cyclopropanation: (a) Pfaltz, 1988 [129]; (b) Pfaltz, 1992 [130]; (c) Masamune, 1990 [131] (see also [132]); (d) Evans, 1991 [133]; (e) Katsuki, 1993 [134]; (f) Nishiyama, 1994 [135].

Because of fluctuations in atom priority using the CIP sequencing rules (*i.e.*, in spite of their obvious differences, the CIP descriptor for the stereocenters in all ligands except e is *S*), we define the chirality sense of these ligands using the *P/M* nomenclature [136], applied to the R–C–N–M bond (see the inset in Figure 6.10). Thus, the ligands in Figure 6.9a and b have the *MM* configuration, while those in Figure 6.9c, d, and f have the *PP* configuration. Ligand 6.9e has an extra carbon and is not strictly definable by this system, but its symmetry features are similar to ligands 6.9a and b, so it is considered along with them.

**Table 6.3.** Asymmetric cyclopropanations. The "cat." column refers to the catalysts in Figure 6.9. For the structure of *l*-menthyl, see Scheme 6.34.

Entry	cat.	N <sub>2</sub> CO <sub>2</sub> R	alkene	% Yield	% trans	% es	Ref.
1	a	<i>t</i> -Bu	PhCH=CH <sub>2</sub>	60	81	96	[129]
2	a	<i>l</i> -menth	PhCH=CH <sub>2</sub>	65-75	85	95	[129]
3	a	<i>d</i> -menth	PhCH=CH <sub>2</sub>	60-70	82	98	[129]
4	a	<i>d</i> -menth	CH <sub>2</sub> =CHCH=CH <sub>2</sub>	60	63	98	[129]
5	a	<i>d</i> -menth	Me <sub>2</sub> C=CHCH=CH <sub>2</sub>	77	63	98	[129]
6	a	<i>d</i> -menth	<i>n</i> -C <sub>5</sub> H <sub>11</sub> CH=CH <sub>2</sub>	30	89	96	[129]
7	b	<i>t</i> -Bu	PhCH=CH <sub>2</sub>	75	81	97	[130]
8	b	<i>d</i> -menth	PhCH=CH <sub>2</sub>	75	84	99	[130]
9	c	<i>t</i> -Bu	PhCH=CH <sub>2</sub>	73	80	97	[131] <sup>a</sup>
10	c	<i>l</i> -menth	PhCH=CH <sub>2</sub>	72	86	99	[131] <sup>a</sup>
11	d	BHT	PhCH=CH <sub>2</sub>	85	94	>99	[131] <sup>a</sup>
12	d	BHT	PhCH <sub>2</sub> CH=CH <sub>2</sub>	-	-	93	[133]
13	d	BHT	Ph <sub>2</sub> C=CH <sub>2</sub>	70	-	>99	[133]
14	d	BHT	Me <sub>2</sub> C=CH <sub>2</sub>	91	-	>99	[133]
15	e	<i>t</i> -Bu	PhCH=CH <sub>2</sub>	75	86	96	[134]
16	e	<i>t</i> -Bu	<i>n</i> -C <sub>6</sub> H <sub>13</sub> CH=CH <sub>2</sub>	65	85	95	[134]
17	e	<i>t</i> -Bu	PhCH=CHCH=CH <sub>2</sub>	90	70	91	[134]
18	e	<i>t</i> -Bu	<i>E</i> -PhCH=CHMe	54	40	62	[134]
					60(cis)	>99	
19	e	<i>t</i> -Bu	<i>Z</i> -PhCH=CHMe	94	>99	86	[134]
20	f	<i>t</i> -Bu	PhCH=CH <sub>2</sub>	81	97	97	[135]
21	f	<i>l</i> -menth	PhCH=CH <sub>2</sub>	87	95	97	[135]
22	f	<i>l</i> -menth	<i>n</i> -C <sub>5</sub> H <sub>11</sub> CH=CH <sub>2</sub>	40	94	>99	[135]
23	f	<i>l</i> -menth	Ph <sub>2</sub> C=CH <sub>2</sub>	55	-	82	[135]
24	f	<i>l</i> -menth	Me <sub>2</sub> C=CHCH=CH <sub>2</sub>	86	79	99	[135]

<sup>a</sup> The absolute configuration reported in this paper is correct (1*R*, 2*R*), but it is drawn incorrectly.

In all cases, the *MM* ligand affords the 1*S*,2*S*-trans product and the *PP* ligand affords the 1*R*,2*R* product. The sense of diastereoselectivity and enantioselectivity can be explained using the cartoons in Figure 6.10 (this scheme is a model, not a mechanism). Because of the C<sub>2</sub>-symmetry of the ligands, the configuration of the carbene is the same whether the ester moiety is drawn up or down. Note that the vertical orientation of the carbene and the horizontal orientation of the ligand divide the reagent into four quadrants. Only in the *S,S*-trans product (from the *MM* complex) are steric interactions between the olefinic substituent and both the carbene ester and the ligand substituent avoided (*i.e.*, the olefin substituent is in the lower right quadrant). All other orientations produce repulsive interactions between the olefin and either the ester moiety or the ligand substituent. For ligands having the *PP* configuration, the preferred product is the *R,R*-trans-cyclopropane.

Weaknesses of the model in Figure 6.10 include the fact that there may be other ligands on the metal that are not taken into consideration here, and that it assumes a similar geometry of the carbene relative to the chelating ligand for all the com-

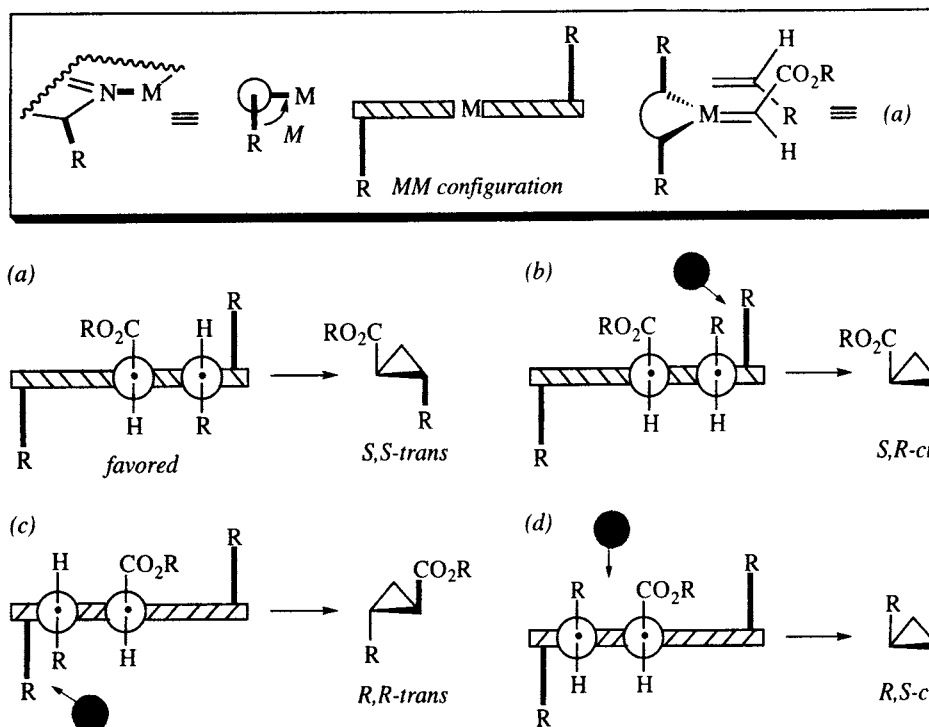
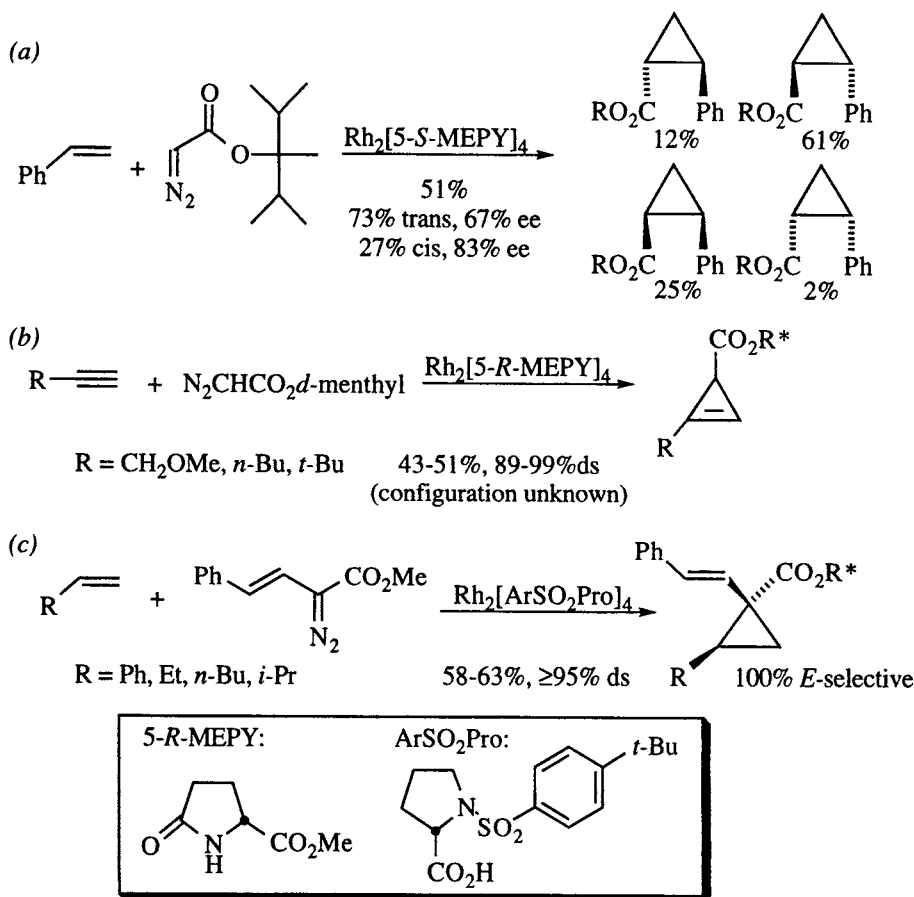


**Figure 6.10.** Inset: Definition of *M* configuration of metal complexes, and generalized side view of an *MM*-metal carbene complex with the olefin approaching from the rear (equivalent to the Newman projection shown in a). (a) Favored approach, leading to the *S,S*-trans product. (b) Disfavored approach, leading to *S,R*-cis product. (c) Disfavored approach leading to the *R,R* trans product. (d) Disfavored approach leading to the *R,S*-cis product. After ref. [112].

plexes. On the other hand, the formation of metallacyclobutanes in copper-catalyzed cyclopropanations appears to be an accepted hypothesis [112,133], and the consistency of these representations with an accumulating body of fact make them useful predictive models, and a good starting point for developing more detailed mechanistic hypotheses.

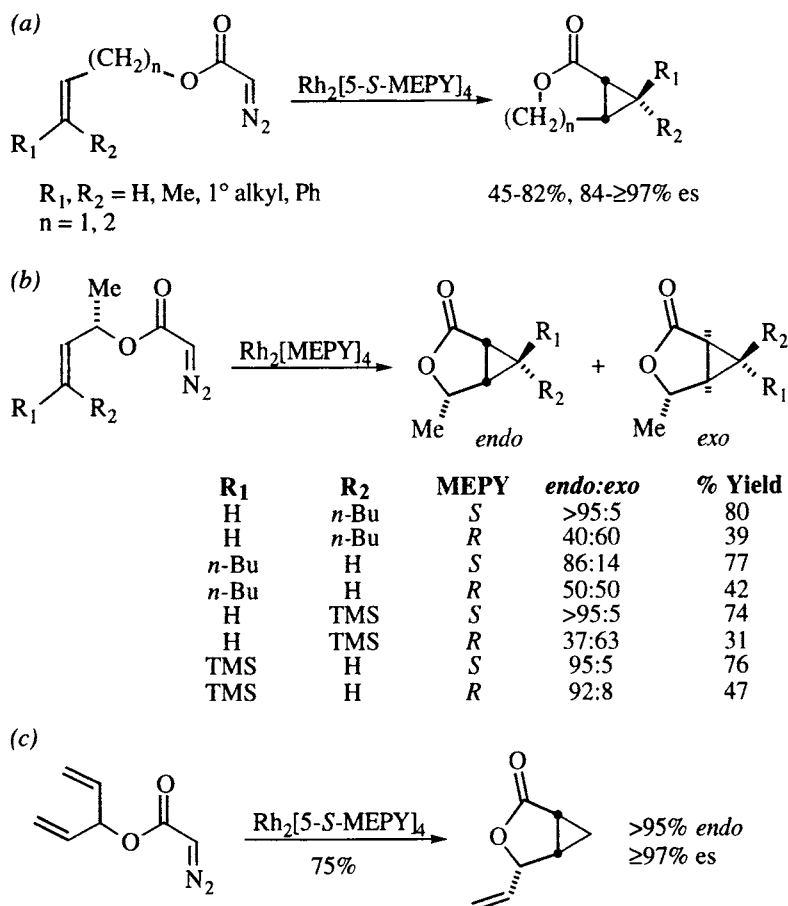
It was noted in the previous section that rhodium acetate catalyzed cyclopropanations of chiral diazo acetates afforded poor diastereoselectivity. Using achiral diazo acetates and methyl 2-oxopyrrolidinone-carboxylate (MEPY) as a chiral ligand on rhodium, reasonable trans selectivity and moderate enantioselectivity can be achieved, as shown by the example in Scheme 6.37a [137]. More recently, the groups of Doyle, H. Davies, and Whitesell have examined chiral esters with the  $\text{Rh}_2[\text{MEPY}]_4$  catalyst in the hopes of improving selectivity through double asymmetric induction, but the results still leave room for improvement [115]. Intermolecular cyclopropanation of alkynes produces only two stereoisomeric products, and Doyle and Müller have found that double asymmetric induction pushes the selectivities over 90% (although the absolute configuration was not determined), as shown in Scheme 6.37b [138]. Although these menthyl esters afford higher selectivities, they offer lower yields than ethyl diazoacetates (70-85% yields) due to competitive C-H insertion reactions. H. Davies has reported that the rhodium prolinato-catalyzed addition of vinyl carbenes to alkenes is 100% selective for the



**Scheme 6.37.** (a) Asymmetric cyclopropanation of styrene [137]. (b) Cyclopropanation of alkynes [137]. For menthyl structure, see Scheme 6.34. (c) Asymmetric cyclopropanation of alkenes with vinyl carbenes [139]. *Inset:* Ligand structures.

*E*-diastereomers, which are formed in an  $\geq 95:5$  ratio for several alkenes, as shown in Scheme 6.37c [139]. Surprisingly, Davies also noted that the stereoselectivity *decreased* when esters of larger alcohols were used.

Conformational considerations restrict the number of possible transition state geometries in intramolecular cyclopropanations, which are quite selective, as shown by the examples from Doyle, Martin, and Müller illustrated in Scheme 6.38a [140,141]. Intramolecular cyclopropanation of diazo esters of chiral allylic alcohols are subject to double asymmetric induction, as shown by the series of examples in Scheme 6.38b. For all of these substrates, the *exo* product is slightly preferred when cyclopropanation is mediated by an achiral catalyst [142], but this selectivity is reversed dramatically when the *S* ester is allowed to react with the 5-*S*-MEPY catalyst. This pronounced *endo* selectivity persists for both the *E* and the *Z*-alkenes, although it is higher for the *Z* alkenes. Note also that when the chirality sense of the substrate and the catalyst are mismatched (*S* substrate and *R* catalyst), the *endo* selectivities are low, unless  $\text{R}_1/\text{R}_2$  are trimethylsilyl. For the matched case of double asymmetric induction, the same features that cause the *endo* selectivity can be used



**Scheme 6.38.** (a) Enantioselectivity in intramolecular cyclopropanations [140,141]. (b) Double asymmetric induction in intramolecular cyclopropanations [142]. (c) Group-selective asymmetric cyclopropanation [142].

to effect the enantioselective (group selective) cyclopropanation of the divinyl alcohol illustrated in Scheme 6.38c. The group selectivity is significantly diminished, however, if there are substituents on the double bonds [142].

The mechanism by which selectivity is induced in rhodium mediated asymmetric cyclopropanations is not clear. What is known is that the pyrrolidinone of the MEPY catalyst is bonded to the rhodiums through the carboxamide, with the nitrogens *cis* to each other, as shown in Figure 6.11 [113]. This arrangement places the two carbomethoxy groups *cis* to each other on both sides of the catalyst. With

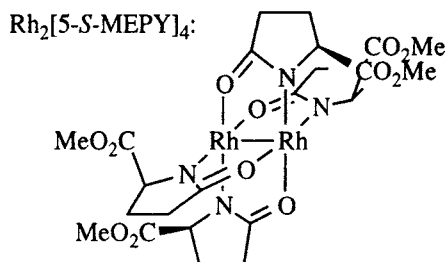
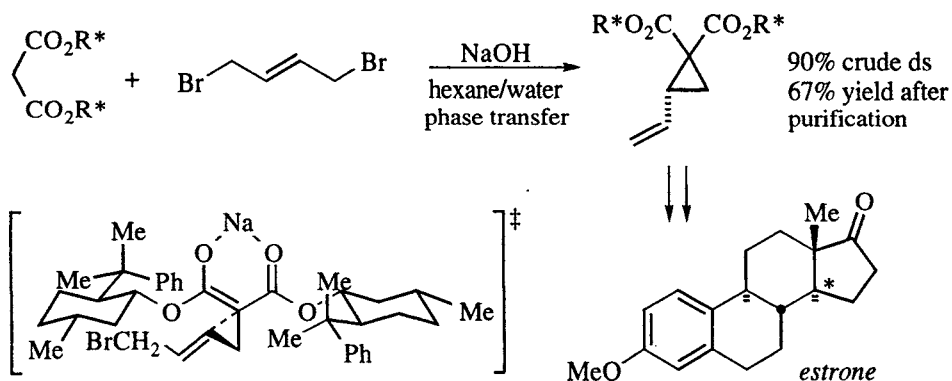


**Figure 6.11.** Depiction of the structure of Doyle's  $\text{Rh}_2[5\text{-S-MEPY}]_4$  catalyst, showing the *cis* arrangement of the nitrogens [113].

the carbene bound to the rhodium on the 'right side' for example, the two carbomethoxy groups will hinder approach of the olefin from the upper right quadrant and selectivity is determined by the effects of the carbomethoxy groups on the stabilities of the various possible conformations of the transition state. These effects are quite complex and have not been fully quantified, although efforts have been made [113].

### 6.2.1.3 Stepwise cyclopropanations

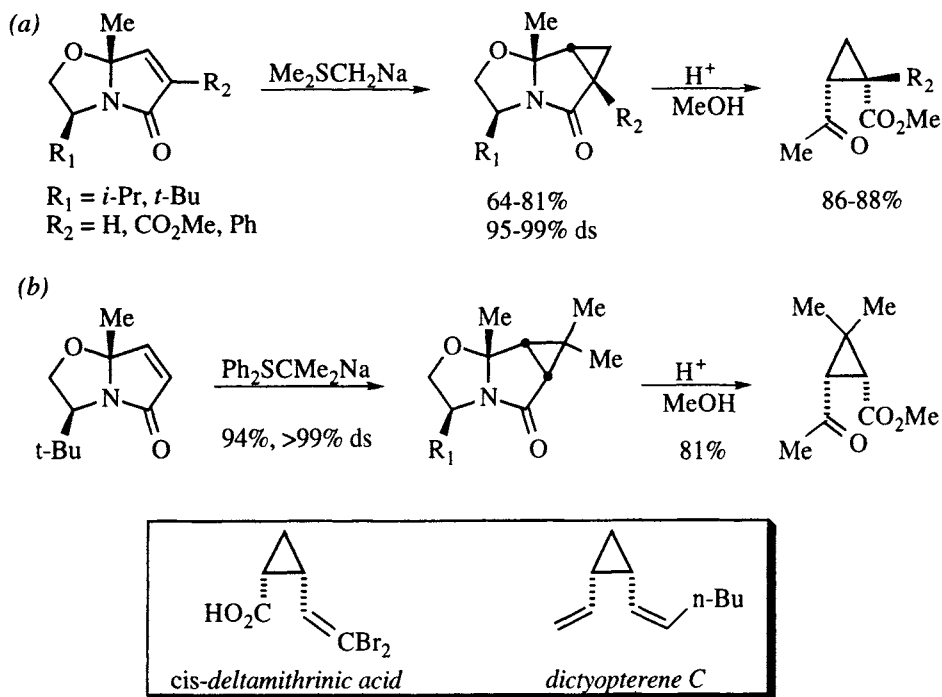
Chiral malonate esters have been used successfully in asymmetric cyclopropanations, as shown by the example in Scheme 6.39, part of a total synthesis of steroids such as estrone [143,144]. The key step in this sequence is an intramolecular  $S_N2'$  alkylation of the monosubstituted malonate. The rationale for the diastereoselectivity is shown in the illustrated transition structure. Note that the enolate has  $C_2$  symmetry, so it doesn't matter which face of the enolate is considered. The illustrated conformation has the ester residues syn to the enolate oxygens to relieve  $A^{1,3}$  strain, with the enolate oxygens and the carbinol methines eclipsed. The allyl halide moiety is oriented away from the dimethylphenyl substituent, exposing the alkene *Re* face to the enolate. The crude selectivity is about 90% as determined by conversion to the dimethyl ester and comparison of optical rotations [143], but a single diastereomer may be isolated in 67% yield by preparative HPLC [144]. This reaction deserves special note because it was conducted on a reasonably large scale: 67.5 grams of diester (127 mmol) [144].



**Scheme 6.39.** Asymmetric cyclopropanation of malonate enolates for steroid synthesis [143,144].

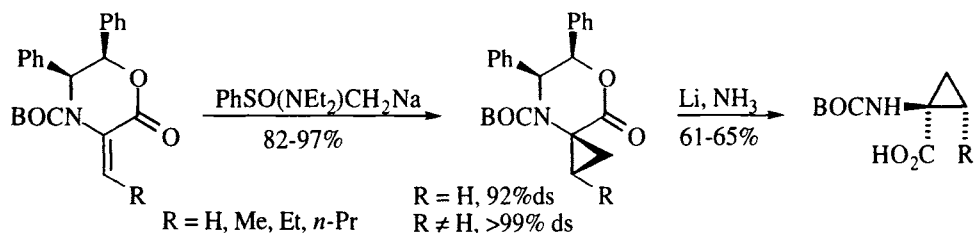
A more common strategy for stepwise asymmetric cyclopropanation is the use of chiral electrophiles. Meyers has used bicyclic lactams (*cf.* Scheme 3.19, 3.20) [145,146] as electrophilic auxiliaries in sulfur ylide cyclopropanations [147]. These auxiliaries, for reasons that are not entirely clear, are preferentially attacked from the  $\alpha$ -face. After separation of the diastereomers, the amino alcohol auxiliary may be removed by refluxing in acidic methanol or reductively [145]. This methodology has been used in asymmetric syntheses of *cis*-deltamethrinic acid and dictyopterene C, illustrated in the inset of Scheme 6.40 [145].





**Scheme 6.40.** Meyers's asymmetric cyclopropanations using the bicyclic lactam auxiliary.  
 (a) Methylene transfer. (b) Isopropylidene transfer. *Inset:* Synthesis targets [145].

For the synthesis of cyclopropyl amino acids, Williams has used an oxazinone auxiliary (*cf.* Scheme 3.12) as an electrophilic component in a sulfur ylide cyclopropanation using Johnson's sulfoximines, as illustrated in Scheme 6.41 [148]. Surprisingly, the sulfur ylide approaches from the  $\beta$  face; the authors speculate that there may be some sort of  $\pi$ -stacking between the phenyls on the oxazinone ring and the phenyl in the sulfoximine to account for this [149]. With Corey's [147] dimethylsulfonium methylide, the diastereoselectivity was only about 75%, but with Johnson's sulfoximines (used in racemic form), only one diastereomer could be detected for most substrates studied (with the exception of  $R = \text{H}$ , [149]). Dissolving metal reduction afforded moderate yields of the cyclopropyl amino acids.



**Scheme 6.41.** Williams asymmetric synthesis of cyclopropyl amino acids [149].

### 6.2.2 [4+2]-Diels-Alder cycloadditions

Many reactions may compete for the descriptor "the most important process in organic chemistry," but none can challenge the Diels-Alder reaction when it comes

to synthetic utility in the formation of six-membered rings.<sup>16</sup> The enormous body of work that includes synthetic applications and mechanistic investigations of this venerable reaction cannot be adequately summarized in anything less than a monograph. Even the literature limited to the asymmetric Diels-Alder reaction is formidable,<sup>17</sup> and the following review is therefore selective. The discussion is limited to examples that serve to illustrate some of the methods that have been developed for the synthesis of enantiopure cyclohexenes,<sup>18</sup> and for which transition state models have been proposed. It is hoped that this sampling will afford the reader a taste for the breadth of the process, as well as a basic knowledge of the types of transition state assemblies that favor stereoselective cycloadditions. The historical development of the asymmetric Diels-Alder reaction begins with auxiliary-based methods for (covalently) modifying the cycloaddition reactants, and has now progressed through chiral (stoichiometric) catalysts, to true catalysts [162] that are efficient in both enantioselectivity and turnover. Thus, the development of the Diels-Alder reaction is a microcosm of the field of asymmetric synthesis itself. The following discussion is organized according to the strategy employed: auxiliaries for dienophile modification, diene auxiliaries, and chiral catalysts.

#### 6.2.2.1 *Dienophile auxiliaries*

In general, cycloadditions catalyzed by Lewis acids proceed at significantly lower temperatures and with higher selectivities than their uncatalyzed counterparts. Factors that contribute to the increased selectivity of the catalyzed reactions include lower temperatures and more organized transition states. For enthalpy-controlled reactions, lowering temperatures increases selectivity (recall Section 1.4, equation 1.5). Coordination of a Lewis acid to the enone carbonyl not only activates the enone by electron withdrawal, it also restricts conformational motion and thereby reduces the number of competing transition states. Figure 6.12 illustrates several chiral auxiliaries for dienophile modification that have been used in the Diels-Alder reaction.

Principles of conformational analysis may be invoked to rationalize the face-selectivity of these compounds. Note, however, that there are two broad types of auxiliary: those that contain a second carbonyl and those that do not. The former may function by chelating the metal of the Lewis acid catalyst, while the latter can only act as monodentate ligands to the metal of the Lewis acid. Figure 6.13a illustrates the probable transition state conformations of ester dienophiles when bound as monodentate ligands to the Lewis acid catalyst, M (auxiliaries 6.12a-f). The C(=O)–O bond prefers the *Z* (or *cis*) conformation for a variety of reasons [163], but the preference is large: probably >4 kcal/mole. Because of this constraint, the C–O bond may be considered to be similar to a double bond (hence the *E/Z* or *cis/trans* designation). A subtle consequence of this constraint is the effect it has on

<sup>16</sup> Monographs reviewing the Diels-Alder reaction: [150,151]. For recent reviews with extensive references to other reviews and pertinent literature, see refs. [152-154].

<sup>17</sup> Reviews of the asymmetric Diels-Alder reaction: [155-157].

<sup>18</sup> For a monograph covering [4+2] cycloadditions that form heterocycles, see ref. [158]. For recent reviews, see ref. [159-161].

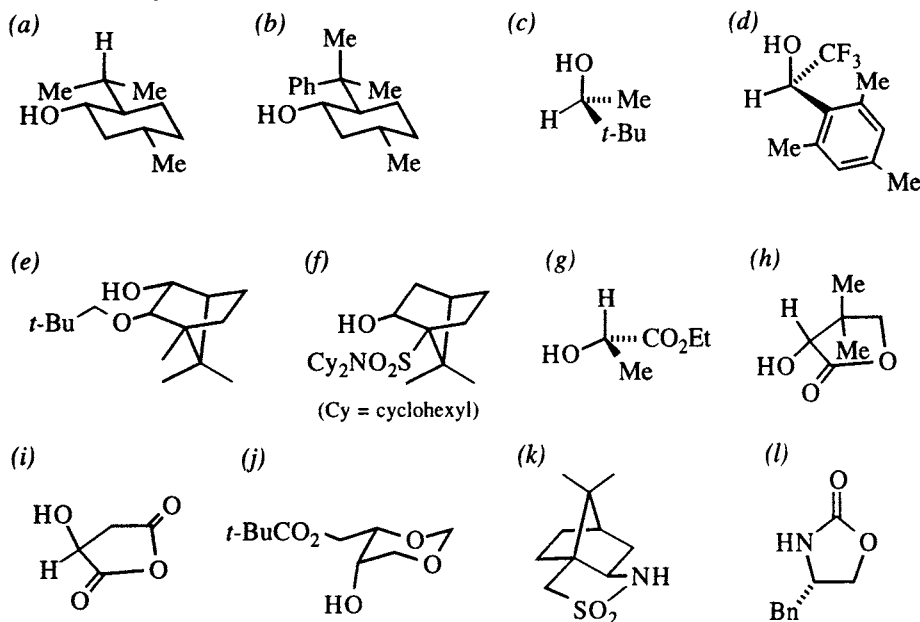


**Figure 6.12.** Dienophile chiral auxiliaries for the asymmetric Diels-Alder reaction. (a) [164]. (b) [165-167]. (c) [164,168]. (d) [169]. (e) [170], see also refs. [171,172]. (f) [173]. (g) [6]. (h) [174,175]. (i) [175]. (j) [176]. (k) [177]. (l) [178].

the conformation of the O–C bond (leading to the stereocenter of the chiral auxiliary). Because of  $A^{1,3}$  strain, the C–H bond of the carbinol carbon eclipses the carbonyl in the lowest energy conformation, which places the other two substituents (Large and Small in Figure 6.13) above and below the plane of the enone. When bound to a Lewis acid, the most stable conformation about the  $C_1$ – $C_2$  bond of the

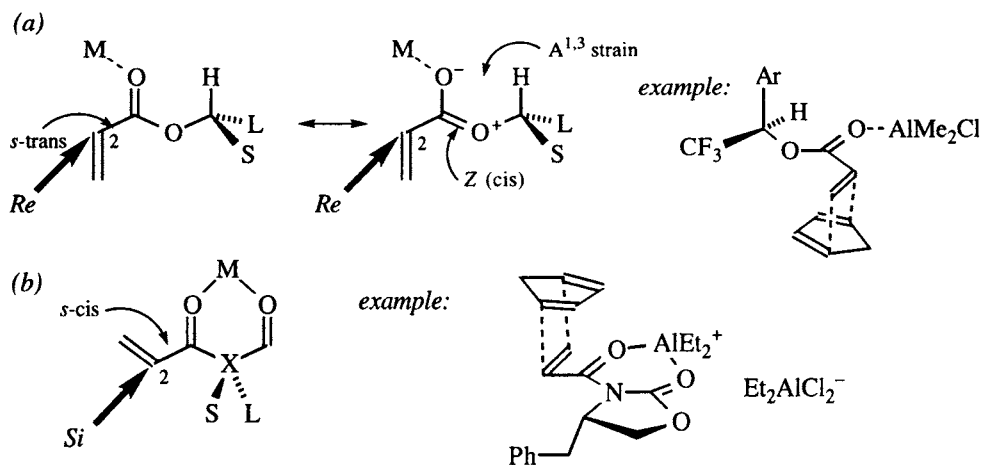


**Figure 6.13.** Probable transition state conformations of: (a) A monodentate dienophile complex such as Corey's mesityl trifluoroethanol auxiliary (Figure 6.12d, [169]). (b) A bidentate dienophile such as Evans's oxazolidinone (Figure 6.12l, [178]). S and L refer to the small and large substituents of the auxiliary.

acrylate is *s*-trans, as shown [179].<sup>19</sup> Approach of the diene from the direction of the C<sub>2</sub> *Re* face is favored since this is the face having the least steric interactions with the auxiliary (S vs. L). Note also that for an endo transition state, the diene should be oriented *toward* the ester auxiliary. The specific example shown is Corey's mesityl trifluoroethanol auxiliary (Figure 6.12d, [169]).

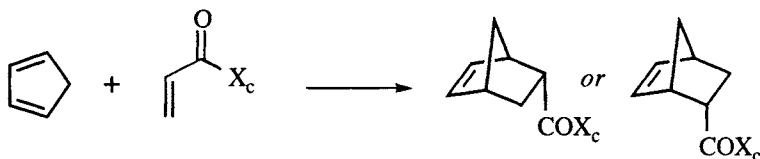
Figure 6.12g-l illustrates auxiliaries that may chelate the metal of the Lewis acid catalyst. In these cases, the metal is coordinated anti to the olefin and the preferred conformation of the C<sub>1</sub>–C<sub>2</sub> bond is *s*-cis, as shown in Figure 6.13b. Again, the preferred approach of the diene is from the direction of the viewer, but because of the different conformation of the enone, it is now the C<sub>2</sub> *Si* face. The example is Evans's oxazolidinone [178]. In this example, the Lewis acid is Et<sub>2</sub>AlCl, but more than one molar equivalent is required for optimum results [178]. Castellino has shown by NMR that Et<sub>2</sub>AlCl initially binds in a monodentate fashion, but excess acid creates a bidentate dione·AlEt<sub>2</sub><sup>+</sup> complex having a Cl<sub>2</sub>AlEt<sub>2</sub><sup>–</sup> gegenion [180].

**Acrylates.** Cyclopentadiene is often used to evaluate selectivity in asymmetric Diels-Alder reactions. Table 6.4 lists the selectivities found for acrylate cycloadditions using the auxiliaries shown in Figure 6.13 under conditions that are optimized for each auxiliary. Note that there are four possible norbornene stereoisomers, two endo and two exo. In accord with Alder's endo rule, the endo is heavily favored in all these examples. Although several authors report selectivities in these reactions in terms of selectivity for one endo adduct over the other, the selectivities indicated in the table reflect the *total* diastereoselectivity of the major adduct over the other three, if this information could be deduced from the information provided in the paper.

Because of the different conditions (Lewis acid, temperature, solvent) used for each of these auxiliaries, it is difficult to determine the "most selective" auxiliary. Indeed, considerations such as ease of separability and reaction scale are important factors in selecting an auxiliary for any given application. Our concern is the factors governing selectivity. An analysis of auxiliary 6.12e and two close relatives illustrate how structural changes can affect the selectivity of the cycloaddition and how conformational principles can explain the effects. Scheme 6.42 shows three acrylate/cyclopentadiene cycloadditions with three very similar auxiliaries, run with the same catalyst at similar temperatures, but which exhibit markedly different stereoselectivities. All of these auxiliaries were designed to place the acrylate and a shielding neopentyl group on a rigid scaffolding (camphor skeleton) such that the enone and a *tert*-butyl group lie (more or less) parallel, and they are thought to react via a nonchelated conformation analogous to Figure 6.13a. Scheme 6.42a duplicates the data listed in Table 6.4, entry 5 [170]. This auxiliary, developed by Oppolzer, shows outstanding selectivity at –20°, but its close counterpart, shown in Scheme 6.42b, exhibits significantly lower (although still useful) selectivity [170]. The only difference is the relationship of the bridgehead methyl to the neopentyl. In the absence of the bridgehead methyl, the *tert*-butyl can rotate away from the acrylate, leaving the *Si* face more accessible. The auxiliary in Scheme 6.42c was

<sup>19</sup> In the absence of a Lewis acid catalyst, both *s*-cis and *s*-trans conformers are present.

**Table 6.4.** Asymmetric Diels-Alder reactions of cyclopentadiene and acrylates. The  $X_c$  column refers to the auxiliaries in Figure 6.12; the probable transition state (TS) conformations of the dienophile are illustrated in Figure 6.13; the % ds refers to the formation of one of the four possible products (two endo and two exo isomers).

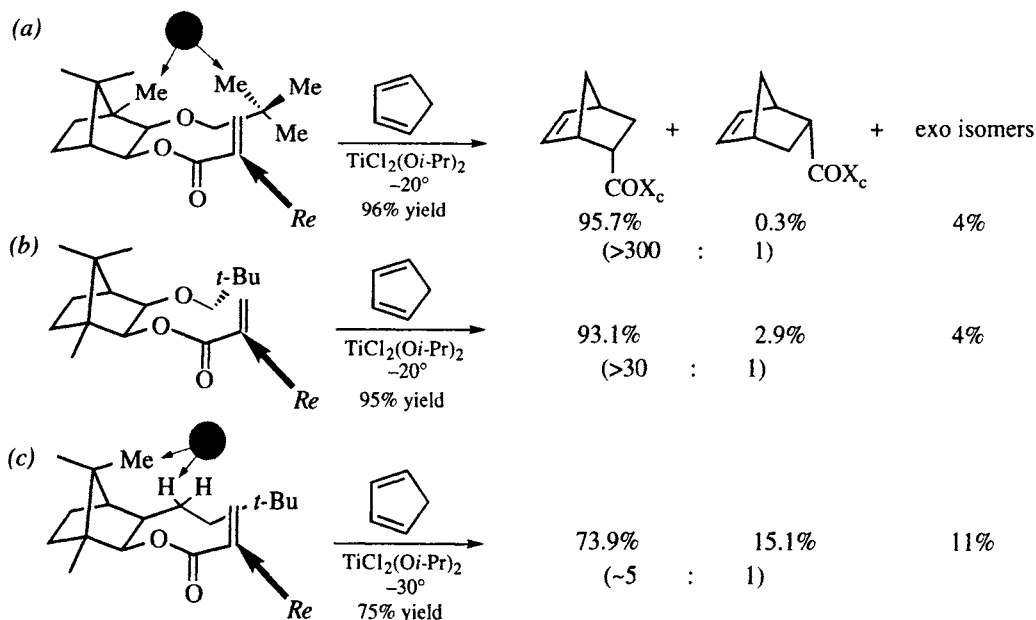


configuration depends on chirality sense of  $X_c$

Entry	$X_c$	Lewis Acid	Probable TS	Temp.	% yield	% ds	Ref.
1	a	$\text{BF}_3 \cdot \text{OEt}_2$	non-chelated	$-70^\circ$	80	91	[164]
2	b	$\text{SnCl}_4$	non-chelated	$0^\circ$	95	75	[165,166]
3	c	$\text{BF}_3 \cdot \text{OEt}_2$	non-chelated	$-70^\circ$	75	87	[164,168]
4	d	$\text{Me}_2\text{AlCl}$	non-chelated	$-78^\circ$	96	97	[169]
5	e	$\text{TiCl}_2(\text{O}i\text{-Pr})_2$	non-chelated	$-20^\circ$	96	96	[170]
6	f	$\text{TiCl}_2(\text{O}i\text{-Pr})_2$	non-chelated	$-20^\circ$	97	89	[173]
7	g	$\text{TiCl}_4$	chelated <sup>a</sup>	$-63^\circ$	88	91	[6]
8	h	$\text{TiCl}_4$	chelated <sup>a</sup>	$-64^\circ$	81	95	[174,175]
9	i	$\text{TiCl}_4$	chelated <sup>a</sup>	$-78^\circ$	86	97	[175]
10	j	$\text{Et}_2\text{AlCl}$	chelated <sup>b</sup>	$-70^\circ$	88	99	[176]
11	k	$\text{Et}_2\text{AlCl}$	chelated	$-130^\circ$	96	95	[177]
12	l	$\text{Et}_2\text{AlCl}$	chelated	$-100^\circ$	94	78	[178]

<sup>a</sup> In this case, the  $\text{TiCl}_4$  is thought to shield one face of the enone [181].

<sup>b</sup> Chelation is postulated to occur at a ring oxygen.



**Scheme 6.42.** Camphor-derived auxiliaries for asymmetric Diels-Alder cycloadditions. (a,b) [170]. (c) [171]. The auxiliary illustrated in (a) is the enantiomer of that reported in ref. [170].

prepared to further probe the effects of conformation on selectivity [171]. In this case, an oxygen has been replaced by a methylene. The most likely rationale for the further lowering of selectivity (compare Scheme 6.42b and c) is that the protons of the methylene experience unfavorable van der Waals repulsion with the indicated methyl in the conformation which most shields the acrylate *Si* face. Population of other (unspecified) conformations results in both lower endo selectivity, and lower *Re* facial selectivity within the endo manifold. It is interesting to recall the discussion in Chapter 1 on selectivity (*cf.* Figure 1.3 and the accompanying discussion) which emphasized the small energetic differences that can result in large effects on selectivity. In Scheme 6.42, the selectivities for the three examples correspond to differences in energies of activation ( $\Delta\Delta G^\ddagger$ ) of 2.9, 1.7, and 0.8 kcal/mole for examples 6.42a-c, respectively, for the two endo isomers. In each case, an increment of approximately 1 kcal/mole (about the same as the energy difference between *gauche* and *anti* butane) has a profound effect on the observed selectivity.

The presence of a potential chelating functional group in an auxiliary does not necessarily mean that chelation occurs. For example, in his optimization studies of *S*-ethyl lactate as a chiral auxiliary (Figure 6.12g), Helmchen noted a marked dependence on the identity and amount of the Lewis acid added [6]. For example, excess  $\text{TiCl}_4$  or  $\text{SnCl}_4$  induced cyclopentadiene addition to the  $\text{C}_2$  *Si* face of the acrylate, whereas excess  $\text{BF}_3\cdot\text{OEt}_2$  or  $\text{AlCl}_3$  catalyzed addition to the  $\text{C}_2$  *Re* face [6]. Moreover, a dependence of selectivity on the stoichiometry (acrylate/acid) was also noted [174]. Figure 6.14 shows three (among many) conformations that could be important in the transition state. Figure 6.14a illustrates a chelating conformation that was found in the X-ray crystal structure of a  $\text{TiCl}_4$  complex (Figure 6.14d, [181]), while Figure 6.14b and c show possible monodentate conformers: Figure 6.14b shows monodentate coordination to one Lewis acid, while Figure 6.14c shows monodentate coordination to two Lewis acids. The differing face-selectivity of the Lewis acids mentioned above was attributed to a chelated transition structure in the case of  $\text{TiCl}_4$  and  $\text{SnCl}_4$  (*i.e.*, Figure 6.14a), and reactive intermediates such as shown in Figure 6.14b and c were postulated for  $\text{BF}_3\cdot\text{OEt}_2$  and  $\text{AlCl}_3$  catalysts [174].

Without any further information, it is not obvious what facial selectivity might be expected from any of these conformations. However, the crystal structure (Figure 6.14d) of the  $\text{TiCl}_4$  complex of *O*-acryloyl ethyl lactate reveals the probable origin of the observed stereoselectivity [181]. Interestingly, the coordination of the two carbonyl oxygens to titanium shows appreciable  $\pi$ -character, which produces a geometry in which a chlorine on the titanium shields the  $\text{C}_2$  *Re* face of the acrylate [181]. Additional notable features of the crystal structure include a small ( $\sim 40^\circ$ )  $\text{H}-\text{C}-\text{O}-\text{C}(=\text{O})$  torsion angle (*cf.* Figure 6.13a) and an even smaller  $\text{O}-\text{C}(=\text{O})-\text{C}-\text{Me}$  angle ( $20^\circ$ ). Comparing the conformations of Figure 6.14a-c suggests that an entropic price must be paid in order to populate conformation 6.14a. But the small torsion angle observed between the ethoxy and the methyl suggest that this price might be avoided if these functional groups were constrained in a ring. Scheme 6.43 shows a comparison of the data of Table 6.4, entries 7-9. Substitution of pantolactone (Figure 6.12h) for ethyl lactate as the auxiliary under

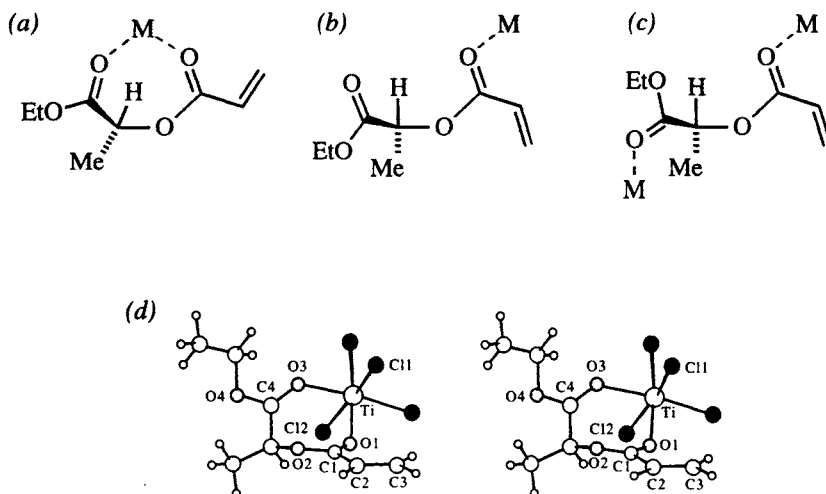
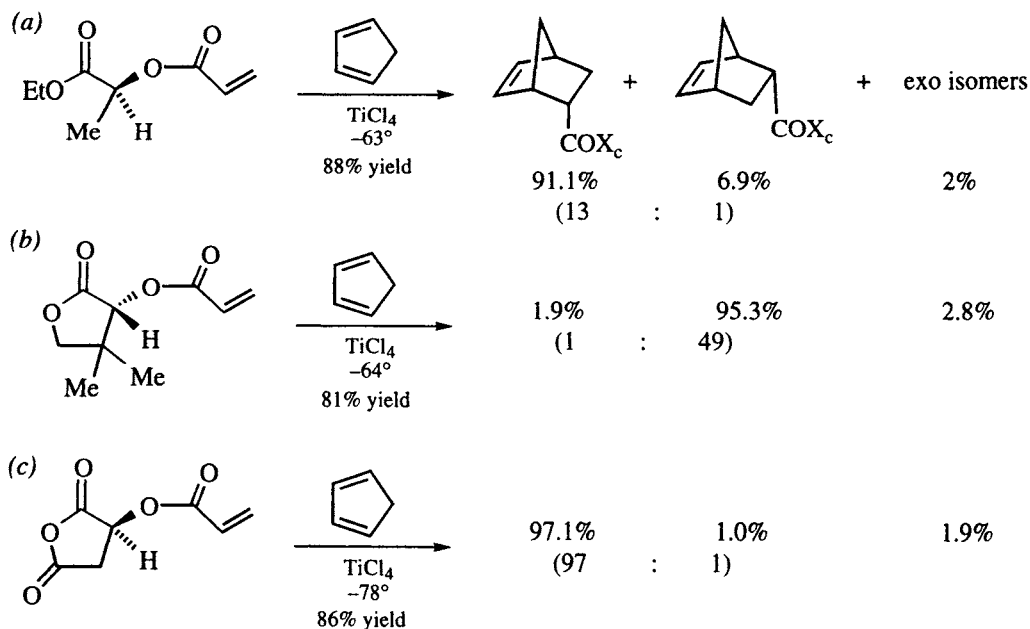


**Figure 6.14.** (a-c) Possible conformations of *O*-acryloyl lactates coordinated to one or more Lewis acids (after ref. [174]). (d) Stereoview of the crystal structure of *O*-acryloyl ethyl lactate · TiCl<sub>4</sub> complex (reprinted with permission from ref. [181]).

otherwise identical conditions (Scheme 6.43b) yields an increase in selectivity from 91% to 95%, corresponding to an increase in relative rates from 13:1 to 49:1 for formation of the two endo isomers. This corresponds to free energies of activation ( $\Delta\Delta G^\ddagger$ ) of 1.1 and 1.6 kcal/mole, respectively. Note also that the *gem* dimethyls of the pantolactone are not important contributors to the selectivity, as shown by

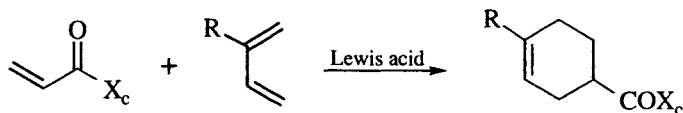


**Scheme 6.43.** Acrylate ester cycloadditions using chelating auxiliaries: (a) [6]; (b) [174,175]; (c) [175].

comparison of the selectivities in Scheme 6.43b and c, respectively. The latter auxiliary (Figure 6.12i, Table 6.4, entry 9) exhibits still higher selectivity, but at lower temperature. The relative rate corresponds to  $\Delta\Delta G^\ddagger = 1.8$  kcal/mole, which would give a relative rate of about 70:1 at  $-63^\circ$ , not significantly different from auxiliary 6.12h at that temperature (Scheme 6.43b and Table 6.4, entry 8). The steric shielding for all three auxiliaries is thought to be a chlorine on titanium.

Several of these auxiliaries were also tested with acyclic dienes. Table 6.5 lists the stereoselectivities found. Here again, Lewis acid catalysis was found to be advantageous in each case. The cycloadditions in entries 1 and 2 are thought to proceed by monodentate coordination to the catalyst (Figure 6.13a), while entries 3-6 proceed through a chelated intermediate. For the auxiliaries in Figure 6.12h, k, and l, high selectivities are also observed with *E*-crotonates and *E*-2-bromoacrylates, as would be expected by examination of the position of an *E*- $\beta$ -substituent in the chelated transition structures of Figure 6.13b.

**Table 6.5.** Examples of asymmetric cycloadditions of acrylates with acyclic dienes. The  $X_c$  column refers to Figure 6.12.



Entry	$X_c$	Lewis Acid	Diene	% yield	% ds	Ref.
1	b	TiCl <sub>4</sub>	butadiene	70	93	[167]
2	e	TiCl <sub>4</sub>	butadiene	98	98	[172]
3	h	TiCl <sub>4</sub>	butadiene	73 <sup>a</sup>	93	[174]
4	k	EtAlCl <sub>2</sub>	butadiene	93	97	[177]
5	h	TiCl <sub>4</sub>	2-methylbutadiene	76 <sup>a</sup>	97	[174]
6	l	Et <sub>2</sub> AlCl	2-methylbutadiene	85	95	[178]

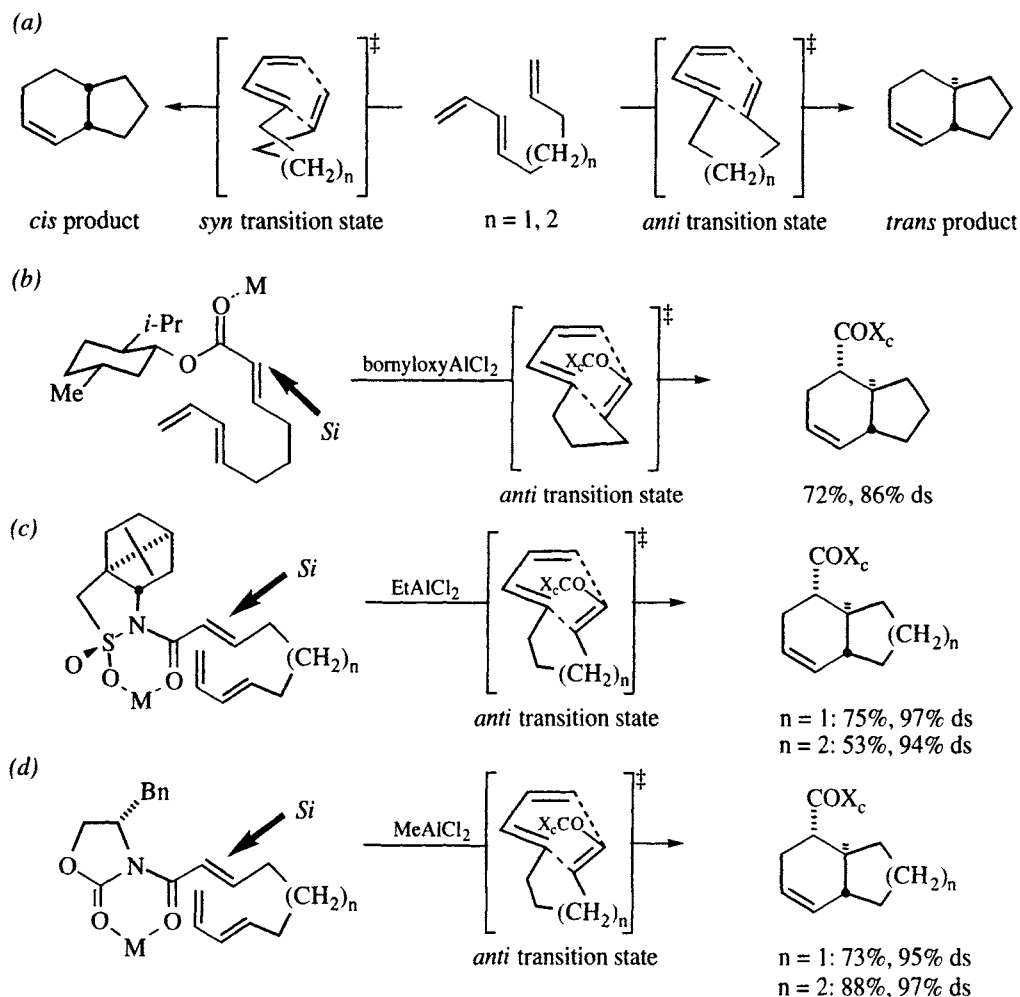
<sup>a</sup> Yield of a single diastereomer after 3 recrystallizations.

**Intramolecular Cycloadditions.** Diels-Alder reactions<sup>20</sup> having diene and dienophile connected by three or four atom carbon chains are selective (for trans-fused bicyclic adducts) only when the dienophile is trans and when Lewis acid catalysis is employed. The competing transition states are illustrated in Scheme 6.44a [182]. The auxiliaries illustrated in Figure 6.12a, k, and l have been used to modify the dienophile fragment for asymmetric intramolecular Diels-Alder reactions for trienes having these attributes. The examples shown in Scheme 6.44b-d reveal that the facial selectivity dictated by chelating and non-chelating auxiliaries as rationalized in Figure 6.13 determine the chirality sense of the trans-fused product.<sup>21</sup> Thus, the absolute configuration of the product obtained using the menthyl auxiliary (Scheme 6.44b) is consistent with an *s*-trans C<sub>1</sub>-C<sub>2</sub> conformation (cf. Figure 6.13a) and an anti transition state. The camphor sultam (Scheme 6.44c)

<sup>20</sup> For reviews of the intramolecular Diels-Alder reaction, see ref. [151,153,182,183].

<sup>21</sup> For ease of comparison, the chirality sense of the camphor sultam is inverted from that reported in the literature [184] so that the favored approach at C<sub>2</sub> is toward the *Si* face for all three examples.

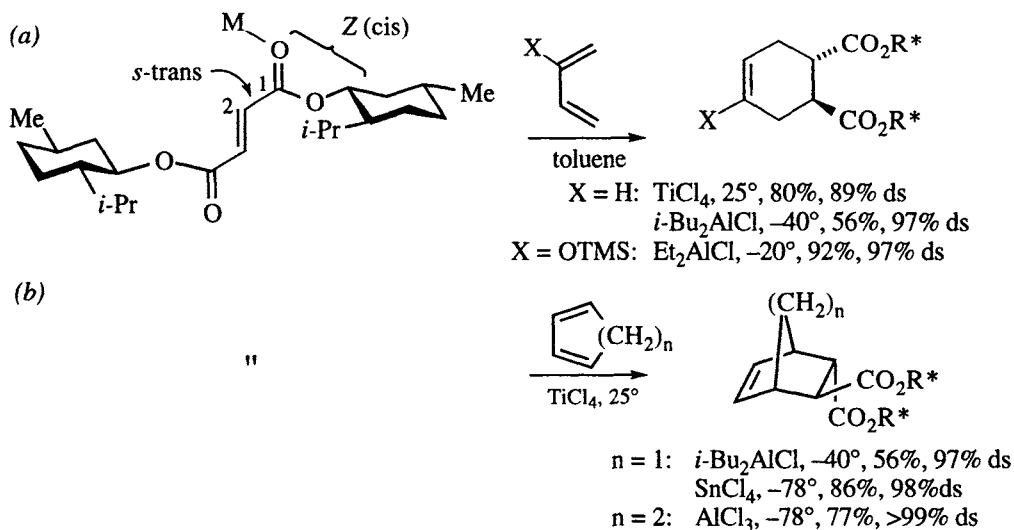




**Scheme 6.44.** (a) Syn and anti transition states for the intramolecular Diels-Alder reaction [182]. (b) The contribution of the chiral Lewis acid to the stereoselectivity was negligible [185]. (c) [184]; the illustrated examples are enantiomeric to those reported. (d) [178].

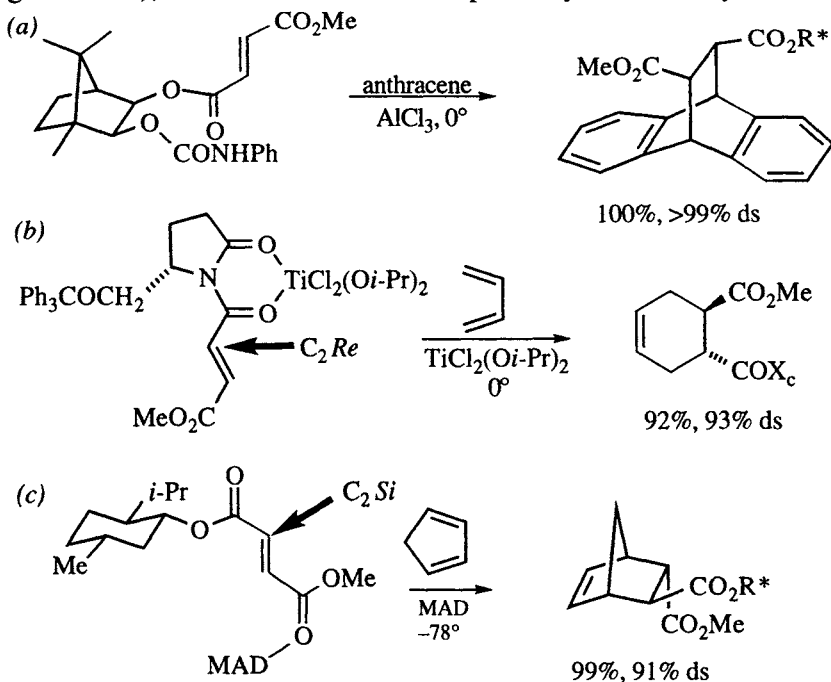
and oxazolidinone imide (Scheme 6.44d) appear to react through an *s*-cis C<sub>1</sub>–C<sub>2</sub> conformation (*cf.* Figure 6.13b) in the anti transition state.

**Fumarates.** Asymmetric cycloaddition to fumarates has been accomplished by modification of either one or both ends of the diacid. In fact, addition of butadiene to dimethyl fumarate, reported by Walborsky in 1961, was the first highly selective (89% ds) asymmetric Diels-Alder reaction ever recorded [186,187]. Scheme 6.45 shows examples of cycloadditions of several dienes to dimethyl fumarate [186–189]. Scheme 6.45a illustrates the presumed reactive conformation of dimethyl fumarate. This conformation features (*cf.* Figure 6.13a) an *s*-trans conformation at C<sub>1</sub>–C<sub>2</sub>, *cis* orientation of the ester ligand relative to the carbonyl oxygen, and orientation of the menthyl moiety to relieve A<sup>1,3</sup> strain. In this conformation, preferred approach of the diene is from the (rear) C<sub>2</sub> *Si* face. In addition to menthol (Figure 6.12a) 1-mesityl trifluoroethanol (Figure 6.12d) has been used as a *bis*-auxiliary [169].



**Scheme 6.45.** Asymmetric cycloadditions to doubly modified fumarates. (a)  $X = H$ : ref. [186-188].  $X = OTMS$ : ref. [188]. (b)  $n = 1$ : ref. [188,189].  $n = 2$ : ref. [189].

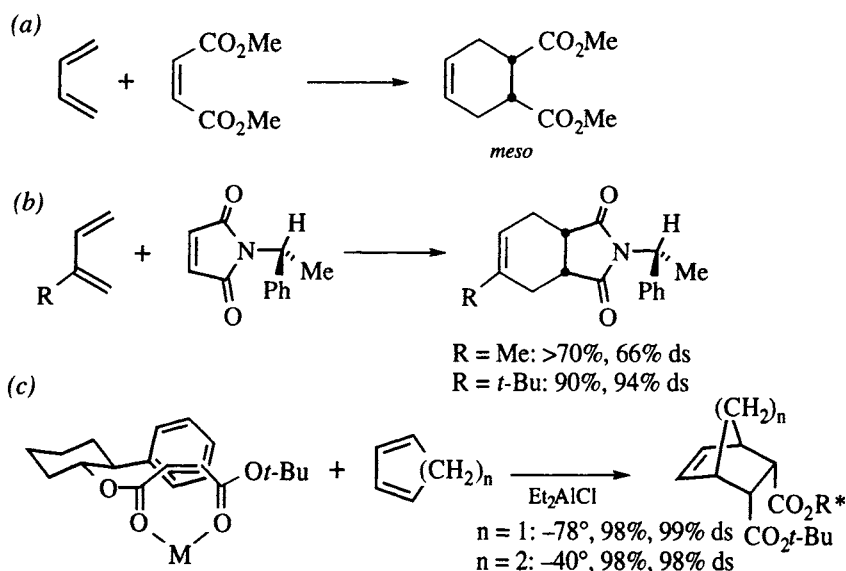
Another approach to fumarate modification is to attach the chiral auxiliary to only one of the two carboxylate groups. One auxiliary for this purpose was introduced by Helmchen, as illustrated in Scheme 6.46a [190]. The only diene reported for this auxiliary was anthracene, probably because unsymmetrical dienes would introduce additional stereoisomers into the product mixture. In this case, the conformation of the ester is similar to that presented in previous examples (cf., Scheme 6.45a, Figure 6.13a), but the conformation is probably additionally constrained by



**Scheme 6.46.** Asymmetric Diels-Alder reactions to fumarates having only one auxiliary. (a) ref. [190]. (b) ref. [191]. (c) ref. [192].

coordination of the metal to the phenylurethane carbonyl. Again, the favored approach is from the C<sub>2</sub> (or C<sub>3</sub>) Si (rear) face. Later, Koga studied the pyrrolidinone auxiliary shown in Scheme 6.46b [191] and Yamamoto examined methyl menthyl fumarate in Scheme 6.46c [192]. Koga's auxiliary showed excellent selectivity with a titanium catalyst in cycloadditions with butadiene. Yamamoto found that methylaluminum bis(2,6-di-*tert*-butyl-4-methylphenoxide (MAD) is 91% selective for the illustrated isomer [192]. The face-selectivity of the Koga auxiliary can be rationalized by titanium chelation of the two carbonyls as shown in Figure 6.13b. For the Yamamoto auxiliary, it is thought that the MAD binds to the methyl ester in favor of the menthyl ester, but that the face-selectivity is determined by the menthyl auxiliary (*cf.* Figure 6.13a). In addition to the face-selectivity, the reaction is also selective for the isomer having the menthyl in the *exo* position, due to the diene orienting away from the MAD and menthyl moieties, and toward the methoxy, as illustrated.

**Maleates.** Cycloaddition of a symmetrical diene such as butadiene or cyclopentadiene to maleic acid or a symmetrical derivative affords achiral (*meso*) adducts (Scheme 6.46a). To break the symmetry, either the diene or the dienophile must be unsymmetrical. For example, cycloaddition of an unsymmetric diene would give a chiral adduct, and Scheme 6.47b shows one such approach. Maleimide having an  $\alpha$ -methylbenzyl auxiliary on nitrogen is highly selective when there is a large substituent at the diene 2-position [193]. A second tactic is the same as the fumarate approach in Scheme 6.46: attach an auxiliary to only one carboxyl group. After considerable experimentation, Yamamoto showed that 2-phenylcyclohexanol is an excellent auxiliary for *tert*-butyl maleate, as shown in Scheme 6.47c [194]. In this case, the catalyst is thought to chelate the two carbonyls with the phenyl group interacting with the double bond in a  $\pi$ -stacking arrangement.



**Scheme 6.47.** (a) Cycloadditions of symmetrical dienes to maleates gives achiral products. (b) Asymmetric cycloadditions to chiral maleimide [193]. (c) Asymmetric cycloadditions to chiral maleic ester [194].

Figure 6.15 shows some natural products synthesized using the asymmetric Diels-Alder reaction. It is interesting to note that none of these compounds are cyclohexenes, even though that is the structural unit formed in the key step! In fact, only in yohimbine is the 6-membered ring formed by the Diels-Alder reaction preserved.

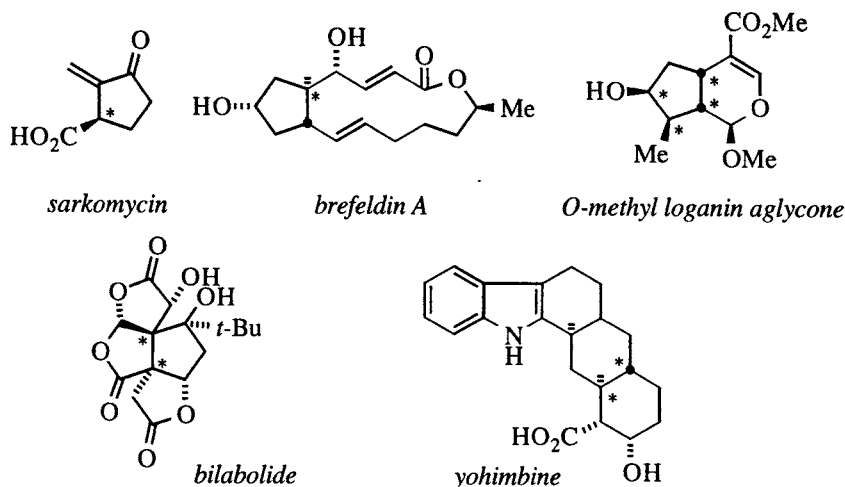
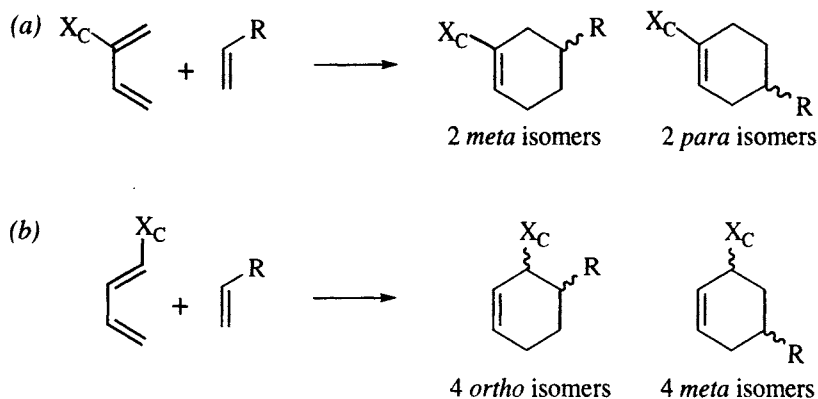


**Figure 6.15.** Natural products synthesized using asymmetric cycloadditions to chiral dienophiles as the key stereodifferentiating step: sarkomycin [167,195]; brefeldin A [168] (of the 3 stereocenters formed in the asymmetric acrylate/cyclopentadiene cycloaddition, the indicated stereocenter is the only one retained); *O*-methyl loganin aglycone [196]; bilabolide [197]; yohimbine [198].

#### 6.2.2.2 Diene auxiliaries

In comparison to the large amount of work on chiral dienophiles for the asymmetric Diels-Alder reaction, there have been very few reports of chiral auxiliaries for the diene component. This may be due, in part, to the lack of convenient methods for the synthesis of modified dienes, but it may also be due to the inherent complexity of the problem. A general analysis of the magnitude of the challenge is shown in Scheme 6.48 for the “simple” case of a monosubstituted diene and a monosubstituted dienophile. If the diene and dienophile are not  $C_2$  symmetric, two constitutional isomers may be produced as cycloadducts. If a substituent is present at the 2-position of the diene, only one stereocenter is formed in the cycloaddition (Scheme 6.48a), so that two stereoisomers are possible for each constitutional isomer (referred to as *meta* and *para* for simplicity). On the other hand, if the substituent is at  $C_1$  of the diene, two stereocenters are formed for each of the two regioisomeric products, for a total of 8 possible products from a single pair of reactants (Scheme 6.48b: 4 from each of the regioisomers, again labeled as *ortho* and *meta* for convenience). Of course, a great deal is known about the regioselectivity of the Diels-Alder reaction of unsymmetric dienes and dienophiles [152], and good regioselectivity is often possible. Nevertheless the primary and secondary molecular orbital considerations that govern regioselectivity constitute a limiting factor in auxiliary design. Regiochemical issues such as these undoubtedly



**Scheme 6.48.** Constitutional isomers (regioisomers) and stereoisomers possible from the Diels-Alder cycloaddition of a monosubstituted diene with a monosubstituted dienophile.

contribute to the paucity of examples of unsymmetrical dienes reported in the previous section, but they are more important here because unsymmetrical dienes are unavoidable if the diene is to be modified with a chiral auxiliary.

For a diene with the auxiliary at C<sub>2</sub>, C<sub>2</sub>–X<sub>c</sub> bond rotation will populate two rotational isomers unless the auxiliary is C<sub>2</sub>-symmetric, in which case the two rotamers are identical (Figure 6.16a) or unless there is a substituent either at C<sub>1</sub>, *cis* to the auxiliary, or at C<sub>3</sub>, in which case one of the conformers may be destabilized by repulsive van der Waals interactions (Figure 6.16b, R' ≠ H). When the auxiliary is at C<sub>1</sub>, a similar situation exists: a C<sub>2</sub>-symmetric auxiliary has only one conformational isomer possible (Figure 6.16c), but an otherwise unsubstituted diene will have two rotational isomers of unequal energy (Figure 6.16d). Thus, for a diene with the auxiliary at C<sub>2</sub>, a C<sub>2</sub>-symmetric auxiliary would seem to have an advantage [199]. When the auxiliary is at C<sub>1</sub>, the two conformers are unequally populated as long as there is no other substituent at C<sub>1</sub>. A similar analysis could be made for other substitution cases, but this analysis covers the examples which follow.

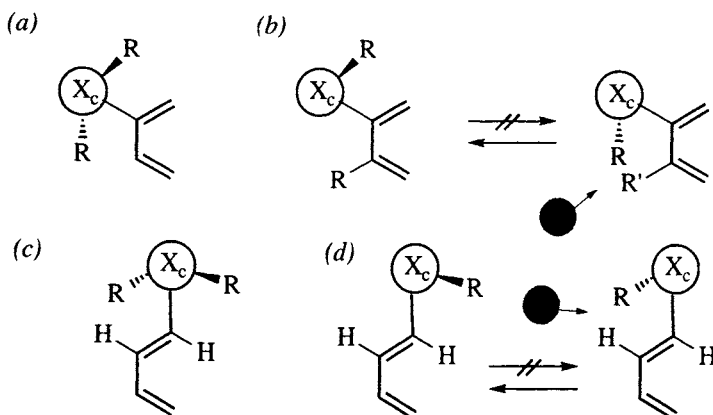
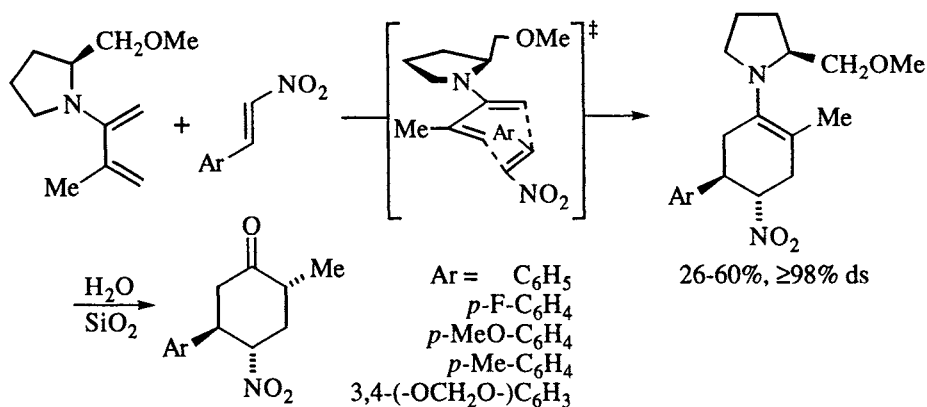


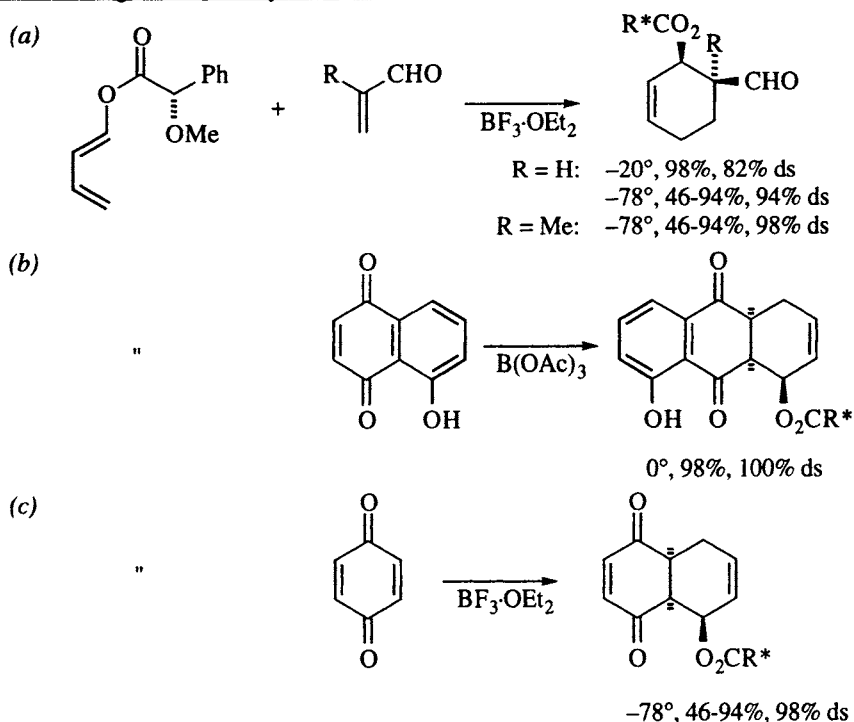
**Figure 6.16.** Generalized conformational considerations for chiral auxiliaries attached to butadiene: (a) C<sub>2</sub>-symmetric auxiliary at position 2; (b) C<sub>s</sub>-symmetric auxiliary at position 2; (c) C<sub>2</sub>-symmetric auxiliary at position 1; (d) C<sub>s</sub>-symmetric auxiliary at position 1.

Scheme 6.49 illustrates an asymmetric cycloaddition of an enamino diene developed in the Enders laboratory [200]. In this case the auxiliary, 2-methoxymethyl pyrrolidine, has  $C_s$  symmetry, and excellent selectivity is achieved with  $\beta$ -nitrostyrenes as dienophiles, although the yields are modest. The diastereoselectivity in the cycloaddition is  $\geq 98\%$  in each case, however hydrolysis of the enamine on workup affords a mixture of 2-methyl diastereomers with 75-95% ds. The proposed transition state for the cycloaddition is shown in the inset, although an alternative two step mechanism (Michael addition followed by aldol cyclization) has not been ruled out [200].

A more generally useful chiral auxiliary was introduced by Trost in 1980 [201]. This auxiliary, derived from mandelic acid, is available as either enantiomer. The original diastereoselectivity reported for addition to acrolein was 82% at  $-20^\circ$  (Scheme 6.50a), but Thornton later reported 94% ds at  $-78^\circ$  [202]. The other examples in Scheme 6.50 illustrate similarly high selectivities and yields, although the Thornton paper does not report specific yields for each example [202]. For the *S* auxiliary, addition to the  $C_1$  *Si* face of the diene is preferred (relative topicity *lk*). Figure 6.17 illustrates two conformational models that have been proposed to rationalize this preference. Trost suggested that  $\pi$ -stacking of the diene over the face of the phenyl group shields the  $C_1$  *Re* face, as shown in Figure 6.17a [201]. A weakness of this model is that reduction of the phenyl to a cyclohexyl group afforded an auxiliary that is equally selective [201,202]. This prompted Thornton to propose that the cycloaddition took place in a diene conformation in which the bond from the  $\alpha$ -carbon to the phenyl (or cyclohexyl) is perpendicular to the plane of the ester, as shown in Figure 6.17b [202]. Thornton asserts that the conformation in which the methoxy is nearest the carbonyl is preferred, but no explanation for this preference was offered. Nevertheless, crystal structures of three cycloadducts exhibit this conformation, which is similar to one proposed by Mosher to rationalize chemical anisotropies (*cf.*, Figure 2.4, ref. [203]).

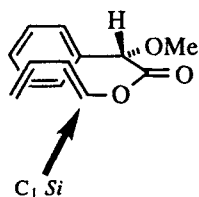


**Scheme 6.49.** Asymmetric Diels-Alder reaction of dieneamine [200].



**Scheme 6.50.** Asymmetric Diels-Alder reactions of *O*-methylmandelate esters: (a)  $R = H$  [201,202];  $R = Me$  [202]. (b) ref. [201]. (c) ref. [202].

(a) *Trost model*:



(b) *Thornton model*:

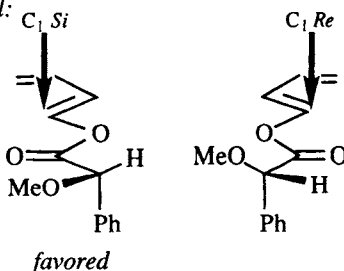


**Figure 6.17.** Conformational models to explain the relative topicity of the Trost auxiliary for asymmetric Diels-Alder reactions. (a) Trost model [201]. (b) Thornton model [202].

### 6.2.2.3 Chiral catalysts

Quite a number of ligand/metal combinations have been evaluated as chiral catalysts for the Diels-Alder reaction, with several being very successful. Much of the effort has been occupied in ligand synthesis and design, but the effort has largely been empirically driven (*i.e.*, trial and error). Figure 6.18 shows several complexes that have been tested as catalysts in the Diels-Alder reaction and which show both high diastereoselectivity and high enantioselectivity.<sup>22</sup> Among the metals,

<sup>22</sup> Cyclopentadiene addition to an acrylate gives two diastereomers (*endo* and *exo*), each of which has two enantiomers. In the presence of a chiral auxiliary, these four stereoisomers are all

the most commonly used are boron and titanium, but copper [204,205], magnesium [206], and lanthanides [207,208] have also found some use. In this section, detailed analysis is presented for only a few of these catalysts, chosen to illustrate current levels of understanding. Additional references and other Lewis acid catalysts can be found in recent reviews [152,157,209,210].

**Monodentate dienophiles.** The first chiral Lewis acid catalyst to show high selectivity (86% es in the cycloaddition of cyclopentadiene to 2-methylacrolein), is a dichloroaluminum alkoxide derived from menthol (Figure 6.18a, [211]). This catalyst, as well as several others (e.g., Figure 6.18b-d) have  $C_s$  symmetry, but most of the catalysts shown in Figure 6.18 are  $C_2$ -symmetric. This feature reduces the number of competing transition states, which is especially important when the ligand sphere is greater than 4-coordinate. Because of fewer possible coordination sites, the binding and face-selectivities of catalysts containing boron, aluminum, or other tetravalent metals are better understood than those of octahedral complexes, and these are examined first.

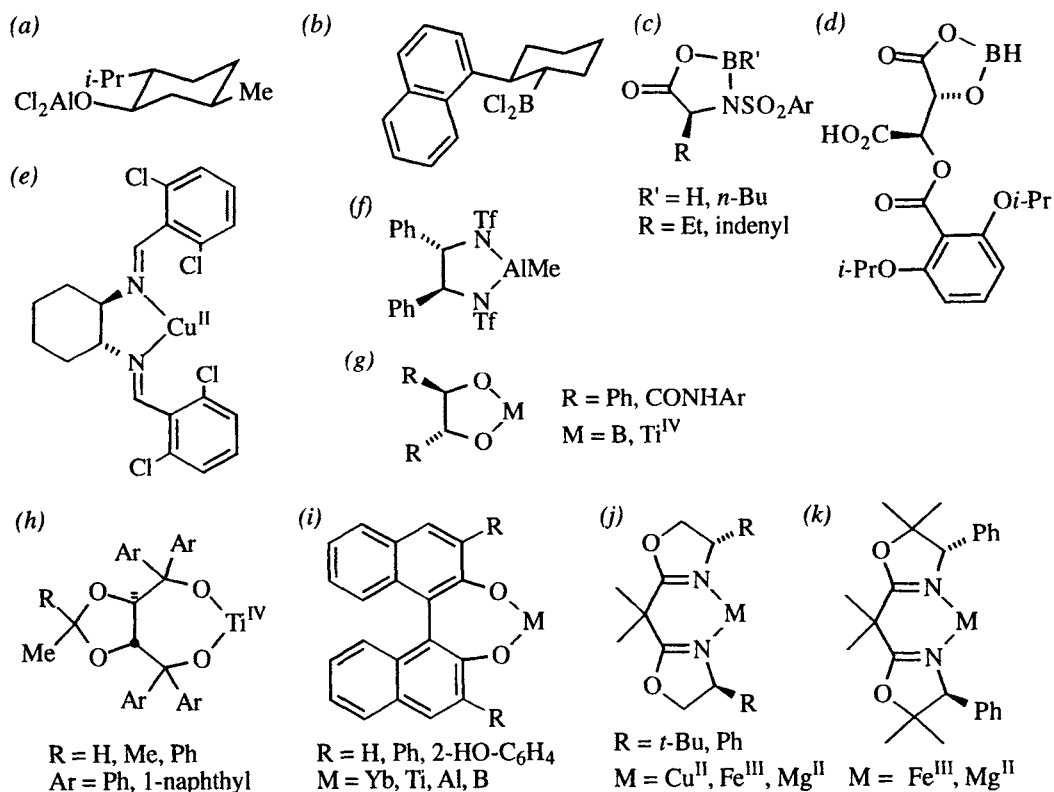
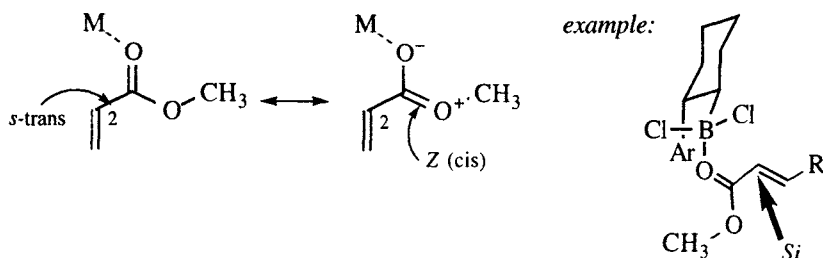


**Figure 6.18.** Selected catalysts for the asymmetric Diels-Alder reaction. (a) [211]. (b) [212,213]. (c)  $\text{R} = \text{Et}$  [214],  $\text{R} = \text{CH}_2\text{indenyl}$  [215-217]. (d) [218-220]. (e) [204]. (f) [221-223]. (g)  $\text{R} = \text{Ph}$  [224],  $\text{R} = \text{CONHAr}$  [225]. (h) [226-229]. (i)  $\text{R} = \text{H}$  [207,208,230],  $\text{R} = \text{Ph}$  [231,232],  $\text{R} = 2\text{-HO-C}_6\text{H}_4$  [233]. (j)  $\text{R} = \text{Ph}$  [205,234],  $\text{R} = t\text{-Bu}$  [205]. (k) [206]

diastereomers, so that selectivity for one of the four can be expressed as percent diastereoselectivity, % ds. But in the present case it is necessary to express selectivity in terms of both diastereoselectivity (*endo/exo*) and enantioselectivity (% es for the major diastereomer).

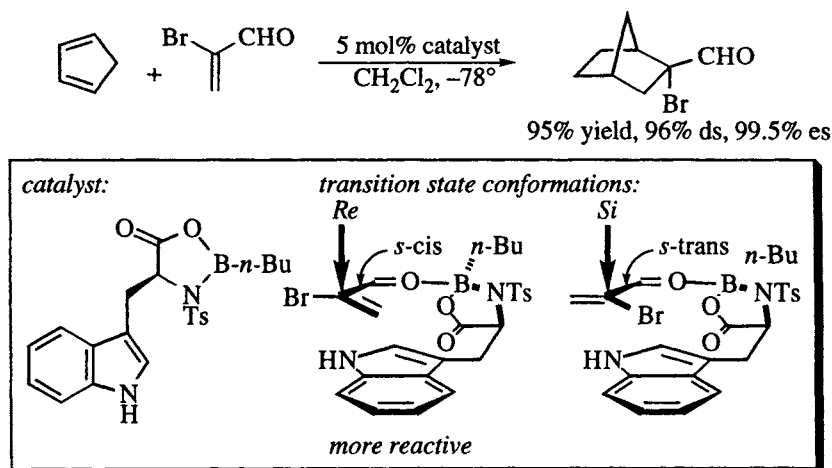


Figure 6.19 shows Hawkins's (2-aryl)cyclohexylboron dichloride catalyst (Figure 6.18b [212,213]) coordinated to methyl acrylate (*cf.* Figure 6.13). Note that monodentate coordination of the ester is thought to occur *trans* to the alkoxy group, which forces the enone into an *s-trans* conformation, similar to that seen previously (*cf.* Figure 6.13 and Scheme 6.45). The geometry shown in Figure 6.19 has been observed in the crystal of five related catalyst-crotonate complexes [213], and NMR studies show that this conformation persists in solution [212]. Comparison of these five structures indicates that, as the polarizability of the aryl group increases, a dipole-induced dipole attraction draws the polar ester group of the boron-bound crotonate towards the arene (the five complexes are, in increasing order of polarizability: Ar = phenyl, 3,5-dimethylphenyl, 3,5-dichlorophenyl, 3,5-dibromophenyl, and 1-naphthyl). Since this effect correlates with enantioselectivity, Hawkins concluded that the effect is operative in the transition state [213]. In this conformation, the rear ( $C_2$  *Re*) face of the dienophile is blocked by the aryl group, and approach of the diene toward the face of the crotonate that is not blocked by the aryl moiety is favored. The 2-(1-naphthyl)-cyclohexyl boron catalyst produces  $\geq 95\%$  enantioselectivities in the addition of cyclopentadiene to methyl acrylate, methyl crotonate, and dimethyl fumarate [212].



**Figure 6.19.** Methyl acrylate coordinated to Hawkins's 2-arylcyclohexyl boron catalyst [212,213].

Scheme 6.51 shows the reaction of 2-bromoacrolein and cyclopentadiene catalyzed by the indenyl oxazaborolidine shown in Figure 6.18c [215,216]. This reaction, which is both highly diastereoselective and enantioselective, is thought to react *via* the *s-cis* conformation shown in the inset of Scheme 6.51. This catalyst conformation is suggested by nuclear Overhauser effects in the NMR spectrum of the catalyst-dienophile complex, and by chemical shift changes upon complexation to boron trifluoride [216]. Also, a 1:1 complex of the catalyst and 2-bromoacrolein is orange-red at 210° K, a color that is attributed to charge-transfer complexation between the indene ring and the boron-bound aldehyde [216]. Similar catalysts with different substituents on the nitrogen [216] or the carbon of the oxazaborolidine [216,217] show significantly lower selectivities. For example the oxazaborolidine having a 2-naphthyl group (comparable in size, but not as good a  $\pi$ -donor) in place of the indene exhibits only 88% enantioselectivity. Phenyl, cyclohexyl, or isopropyl groups give only about 65% enantioselectivity with *opposite* topicity [216]. Oxazaborolidine auxiliaries having donor *atoms* in the side chain also show improved selectivities [217].

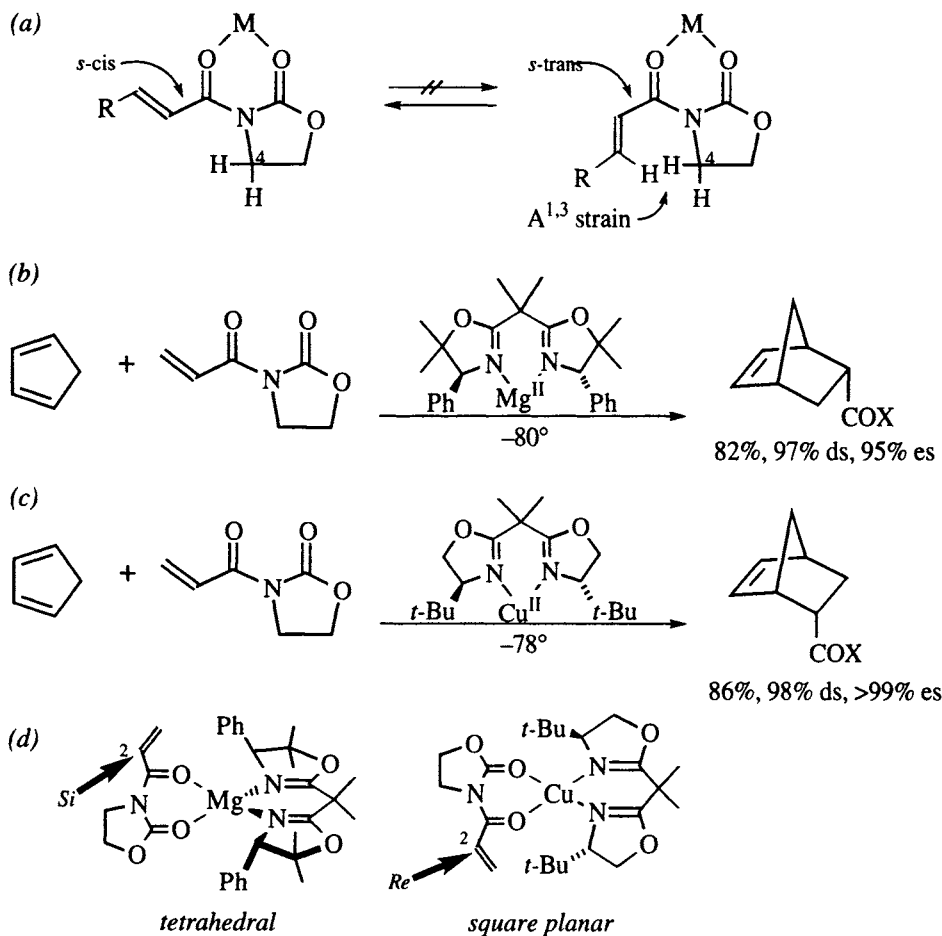


**Scheme 6.51.** Asymmetric cycloaddition of 2-bromoacrolein and cyclopentadiene using Corey's indenyl oxazaborolidine catalyst [215,216]

Note that the illustrated conformation has the acrolein oriented in an *s-cis* conformation. This is in contrast to the usual *s-trans* conformation of acroleins coordinated to a Lewis acid (Figure 6.13a), but it is supported by the fact that cyclopentadiene adds to the opposite face of acrolein itself [216]. It is likely that both *s-cis* and *s-trans* dienophile conformers are present, and that the *s-cis* conformer is more reactive. In other words, Curtin-Hammett kinetics [235] are operative. The rationale for this increased reactivity is as follows: the *s-trans* conformation of 2-bromoacrolein would place the bromine above the indene ring. Cycloaddition to the top (*Si*) face of the *s-trans* conformer would force the bromine into closer proximity to the indene as C<sub>2</sub> rehybridizes from sp<sup>2</sup> to sp<sup>3</sup>, a situation that is avoided in cycloaddition to the top (*Re*) face of the *s-cis* conformer.

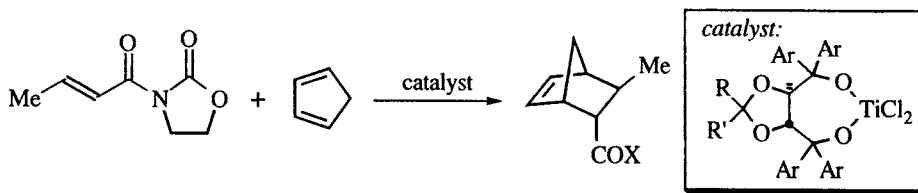
**Bidentate dienophiles.** When a dienophile such as *N*-acryloyloxazolidinone coordinates the metal in a bidentate fashion (*cf.* Figure 6.13b), A<sup>1,3</sup> strain between the enone β-carbon and the oxazolidinone C-4 methylene forces the enone into an *s-cis* conformation, as shown in Figure 6.20a. Interactions between the other ligands on the metal, the coordinated dienophile, and the approaching diene then determine the topicity of the cycloaddition. The exact nature of the interactions will depend on the coordination sphere of the metal.

For example, Figure 6.20b and c shows examples of similar C<sub>2</sub>-symmetric ligands (Figure 6.18j,k) coordinated to metals having different tetravalent geometries and which result in enantiomeric cycloadducts, but with excellent selectivity in both cases. The explanation for the topicity of the two catalysts is revealed by examination of the proposed arrangements of the catalyst/dienophile complexes, as shown in Scheme 6.20d. The tetrahedral magnesium [206] complex facilitates addition to the C<sub>2</sub> *Si* face because the rear phenyl is blocking the *Re* face [206]. In contrast, the square-planar copper complex facilitates C<sub>2</sub> *Re* addition because the *Si* face is blocked by the *tert*-butyl group [205]. It should be noted, however, that in these two examples, the geometry of the coordination complex appears to be inferred (at least partly) from the topicity of the cycloaddition (note the absence of any anionic ligands in these models).



**Figure 6.20.** (a) Acryloyloxazolidinone in bidentate coordination.  $A^{1,3}$  strain favors the *s*-cis conformation. (b) Cycloaddition of  $C_2$ -symmetric bisoxazoline-magnesium complex [206]. (c) Cycloaddition of  $C_2$ -symmetric bisoxazoline-copper complex [205]. (d) Rationale for the different topologies of the bisoxazoline complexes, even though both ligands have the same absolute configuration. The dienophile is drawn in the plane of the paper, and the favored approach is from the direction of the viewer.

Ligands having  $C_2$ -symmetry have also been used with metals that are undoubtedly octahedral, however the analysis of facial selectivity in octahedral complexes is complicated by several possible competing coordination modes of the dienophile. One class of ligand that has been well studied are the TADDOLs (TADDOL is an acronym for  $\alpha,\alpha',\alpha',\alpha'$ -tetraaryl-1,3-dioxolane-4,5-dimethanol). Both the Narasaka [236] and the Seebach [228] groups have evaluated a number of TADDOLs as ligands for titanium in the asymmetric Diels-Alder reaction. Table 6.6 lists selected data from two extensive reports, which illustrates not only the utility of the titanium TADDOLate complex as an asymmetric catalyst, but which also illustrates some subtle differences that are not readily explained. For example, Narasaka found that the tetraphenyl dimethyldioxolane ligand ( $R = R' = \text{Me}$ ;  $\text{Ar} = \text{Ph}$ ) promoted the reaction (88% yield) when used in stoichiometric quantities

**Table 6.6.** Asymmetric cycloadditions of crotyloxazolidinones and cyclopentadiene catalyzed by titanium TADDOLate complexes.

Entry	R/R'	Ar	Temp.	Eq. cat.	% yield	% ds	% es	Ref.
1	Me/Me	Ph	-15	1	88	93	77	[236]
2	Me/Me	Ph	-15	0.15	25	83	72	[228]
3	Me/Me	2-naphthyl	-15	0.15	96 <sup>a</sup>	90	94	[228]
4	Me/Ph	Ph	-15	2	93	90	96	[236]
5	Me/Ph	Ph	0	0.10	87	92	95	[236]

<sup>a</sup> This experiment done on a >4g (crotyloxazolidinone) scale.

(entry 1), but Seebach found that a catalytic amount was not as effective (25% yield) under similar conditions (entry 2). Note the difference in diastereo- and enantioselectivity for these two entries, as well. In contrast, replacing the phenyl group with a 2-naphthyl group affords an outstanding catalyst (entry 3), that gives excellent yields and selectivities on a multigram scale [228]. Entries 4 and 5 illustrate the tetraphenyl methyl-phenyl dioxolane catalyst (R = Me, R' = Ph; Ar = Ph), which affords outstanding yields and selectivities in either stoichiometric or catalytic modes [236]. Comparison of entry 2 with entry 5 is particularly puzzling: replacement of one the dioxolane substituents (a position remote from the catalytic site) results in an amazing improvement in catalyst efficiency and selectivity.<sup>23</sup>

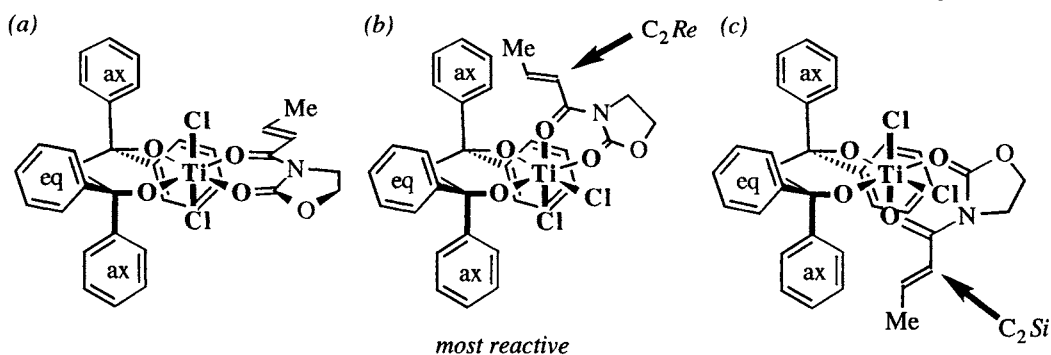


**Figure 6.21.** Titanium TADDOLate - crotyloxazolidinone complexes. The dioxolane ring of the chiral ligand (Figure 6.18h) is deleted for clarity, and the phenyl groups are labelled as axial (ax) or equatorial (eq). (a) Symmetrical complex found by NMR to be the predominant species in solution [237], and also characterized crystallographically [238]. (b) Complex judged to be most likely to be responsible for the asymmetric cycloaddition [228,237]. (c) This complex is probably less reactive, since approach of the dienophile is hindered by the axial phenyl [228].

<sup>23</sup> Although entries 2 and 5 are from different laboratories, Seebach's group has reported results similar to those of entry 5: 99% conversion, 88% ds, and 94% es using 15 mol% catalyst at -5° [228].

NMR studies have shown that at least three hexacoordinate catalyst oxazolidinone complexes exist in solution [237]. The most abundant has been assigned a structure that has the oxazolidinone oxygens trans to the TADDOL oxygens and the chlorines trans to each other, as shown in Figure 6.21a. This species has also been characterized crystallographically [238]. There are four other possible complexes, two of which are illustrated in Figure 6.21b and c.<sup>24</sup> It is not known whether these two complexes are the ones that are observed in the NMR [237], but these two are judged to be more reactive, since in these structures, the enone oxygen is trans to the weaker  $\pi$ -donor ligand (chlorine) and may therefore experience a higher degree of Lewis acid activation. NMR studies show that one of the axial phenyls undergoes restricted rotation when bidentate ligands are bound to the titanium TADDOLate [237]. When the oxazolidinone ligand is oriented as shown in Figure 6.21b, the dienophile and the axial phenyl are in close proximity and approach of the diene from the direction of the viewer (toward the C<sub>2</sub> *Re* face) is unhindered, and would result in cycloadduct with the observed absolute configuration [228]. The alternative geometry, shown in Scheme 6.21c, is judged to be less reactive, since the diene must approach either from the direction of the viewer (toward the C<sub>2</sub> *Si* face), where it may encounter the nearby axial phenyl, or from the rear, where it is blocked by the equatorial phenyl [228].<sup>25</sup>

This explanation is described as a “mnemonic rule” [228], which can only be taken as a first approximation of reality. The same rule can be used to rationalize the topicity of other asymmetric Diels-Alder reactions, such as those employing titanium BINOLate catalysts (Figure 6.18i, [230]), or iron bisoxazoline catalysts (Figure 6.18j,k [206,215]). Although the explanation seems reasonable, the picture is not complete, since it does not account for a number of observations, including the fact that the dioxolane substituents exert an extraordinary effect on catalyst efficiency (*cf.* Table 6.6, entries 2 and 5). Additionally, both titanium TADDOLate [228] and BINOLate [230] complexes show a nonlinear relationship between enantiomeric purity of the catalyst and that of the product, which suggests that some sort of dimerization phenomenon is involved.<sup>26</sup>

#### 6.2.2.4 Prostaglandins: A case study in the synthesis of enantiopure compounds

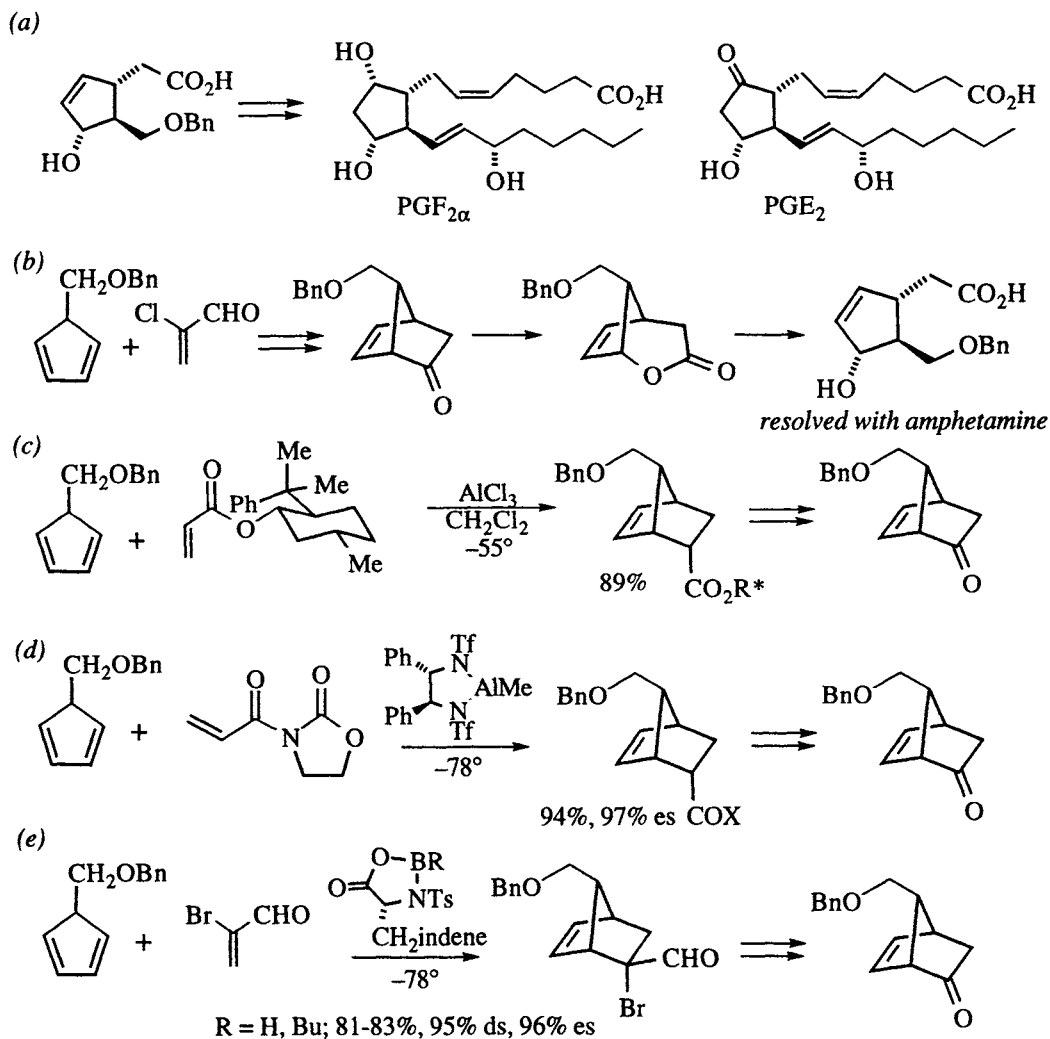
Efficiency in the synthesis of prostanoids has been an important aspect of organic chemistry for over two decades. Because the prostaglandins are chiral, synthesis of enantiopure drugs is highly desirable for clinical applications. The following examples of prostaglandin synthesis are taken from the work of Corey, much of which is summarized in Chapter 11 of his recent book [239]. The hydroxy acid shown in Scheme 6.52a has been used as a key intermediate in a number of

<sup>24</sup> The other two have the oxazolidinone transposed such that the enone oxygen is trans to a TADDOL oxygen.

<sup>25</sup> Jørgensen has proposed another rationale, based on the geometry observed in the crystal structure [238].

<sup>26</sup> One possibility is that heterochiral dimerization of the ligand or the titanium complex produces an inactive catalyst; this tends to sequester the minor enantiomer (*cf.* Scheme 4.6). Another is that the catalyst is a dinuclear species, which is more reactive when homochiral.

prostaglandin syntheses, two of which are shown. To control the *relative* configuration of the stereocenters in the cyclopentane ring, the lactone was synthesized by a Diels-Alder strategy employing a substituted cyclopentadiene, as shown in Scheme 6.52b. Baeyer-Villiger oxidation of the key bicycloheptenone and hydrolysis afforded a hydroxy acid that was initially (in the early 1970s) separated into its enantiomers by resolution [240]. Asymmetric synthesis was then applied to the problem. For example in 1975, 8-phenylmenthol (Figure 6.12b) was used as an acrylate auxiliary to provide an endo bicycloheptene carboxylate [165] that was oxidatively cleaved to the ketone, and carried on to the hydroxy acid as before (Scheme 6.52c). Then in 1989, the first of two chiral catalysts (Figure 6.18f) was



**Scheme 6.52.** Corey's synthetic approaches to prostaglandins (see also ref. [239], chapter 11): (a) Key hydroxy acid intermediate for the synthesis of PGF<sub>2α</sub> and PGE<sub>2</sub>. (b) Early synthesis that relied on resolution for obtaining enantiopure products [240]. (c) 8-Phenylmenthol as a chiral auxiliary [165]. (d) Acryloyl oxazolidinone as dienophile with a chiral catalyst [221,222]. (e) 2-Bromoacrolein as dienophile with a chiral catalyst [215].

applied to the problem: with an acryloyl oxazolidinone as the dienophile, a bicycloheptene carboximide similar to the ester obtained previously was obtained, as shown in Scheme 6.52 [221,222]. Development of the oxazaborolidine catalyst (Figure 6.18c) and 2-bromoacrolein as a dienophile provided a means for streamlining the preparation even further (Scheme 6.52e, [215]). Thus, the development of an efficient synthetic plan has been continually improved as progress in asymmetric synthesis has taken the route from classical chemical resolution, through auxiliary-based methods, to efficient chiral catalysts.

### 6.3 References

1. S. J. Rhoads; N. R. Raulins *Org. React.* **1975**, 22, 1-252.
2. F. E. Ziegler *Acc. Chem. Res.* **1977**, 10, 227-232.
3. K. Mori; H. Nomi; T. Chuman; M. Kohno; K. Kato; M. Noguchi *Tetrahedron* **1982**, 38, 3705-3711.
4. R. E. Ireland *Aldrichimica Acta* **1988**, 21, 59-69.
5. S. Blechert *Synthesis* **1989**, 71-82.
6. P. Wipf In *Comprehensive Organic Synthesis. Selectivity, Strategy, and Efficiency in Modern Organic Chemistry*; B. M. Trost, I. Fleming, Eds.; Pergamon: Oxford, 1991; Vol. 5, p 827-873.
7. R. K. Hill In *Comprehensive Organic Synthesis. Selectivity, Strategy, and Efficiency in Modern Organic Chemistry*; B. M. Trost, I. Fleming, Eds.; Pergamon: Oxford, 1991; Vol. 5, p 785-826.
8. S. Pereira; M. Srebnik *Aldrichimica Acta* **1993**, 26, 17-29.
9. E. J. Corey; B. E. Roberts; B. R. Dixon *J. Am. Chem. Soc.* **1995**, 117, 193-196.
10. S. G. Davies *Organotransition Metal Chemistry Applications to Organic Synthesis*; Pergamon: Oxford, 1982.
11. S. Otsuka; K. Tani *Synthesis* **1991**, 665-680.
12. A. J. Birch; I. D. Jenkins In *Transition Metal Organometallics in Organic Synthesis*; H. Alper, Ed.; Academic: New York, 1976; Vol. 1, p 1-82.
13. H. M. Colquhoun; J. Holton; D. J. Thompson; M. V. Twigg In *New Pathways for Organic Synthesis. Practical Applications of Transition Metals*; Plenum: New York, 1984, p 173-193.
14. H. Kumobayashi; S. Akutagawa; S. Otsuka *J. Am. Chem. Soc.* **1978**, 100, 3949-3950.
15. K. Tani; T. Yamagata; S. Otsuka; S. Akutagawa; H. Kumobayashi; T. Taketomi; H. Takaya; A. Miyashita; R. Noyori In *Asymmetric Reactions and Processes in Organic Chemistry. ACS Symposium Series 185*; E. L. Eliel, S. Otsuka, Eds.; American Chemical Society: Washington, 1982, p 187-193.
16. S. Akutagawa; K. Tani In *Catalytic Asymmetric Synthesis*; I. Ojima, Ed.; VCH: New York, 1993, p 41-61.
17. R. A. Sheldon In *Chirotechnology. Industrial Synthesis of Optically Active Compounds*; Marcel Dekker: New York, 1993, p 304.
18. V. Prelog; G. Helmchen *Angew. Chem. Int. Ed. Engl.* **1982**, 21, 567-583.
19. K. Tani; T. Yamagata; S. Akutagawa; H. Kumobayashi; T. Taketomi; H. Takaya; A. Miyashita; R. Noyori; S. Otsuka *J. Am. Chem. Soc.* **1984**, 106, 5208-5217.
20. T. Ohta; H. Takaya; R. Noyori *Inorg. Chem.* **1988**, 27, 566-569.
21. K. Mashima; K. Kusano; T. Ohta; R. Noyori; H. Takaya *J. Chem. Soc., Chem. Commun.* **1989**, 1208-1210.
22. K. Tani *Pure Appl. Chem.* **1985**, 57, 1845-1854.
23. M. Kitamura; K. Manabe; R. Noyori; H. Takaya *Tetrahedron Lett.* **1987**, 28, 4719-4720.

24. K. Tani; T. Yamagata; S. Otsuka; H. Kumobayashi; S. Akutagawa *Organic Syntheses* **1993**, Coll. Vol. VIII, 183-188.
25. H. Takaya; S. Akutagawa; R. Noyori *Organic Syntheses* **1993**, Coll. Vol. VIII, 57-63.
26. P. Schorigen *Chem. Ber.* **1925**, 58, 2028-2036.
27. P. Schorigen *Chem. Ber.* **1924**, 57, 1634-1637.
28. W. Schlenk; E. Bergmann *Liebigs Ann. Chem.* **1928**, 464, 35-42.
29. G. Wittig; L. Löhmann *Liebigs Ann. Chem.* **1942**, 550, 260-268.
30. G. Wittig; L. Löhmann *Liebigs Ann. Chem.* **1947**, 557, 205-220.
31. C. R. Hauser; S. W. Kantor *J. Am. Chem. Soc.* **1951**, 73, 1437-1441.
32. W. C. Still; A. Mitra *J. Am. Chem. Soc.* **1978**, 100, 1927-1928.
33. P. T. Lansbury; V. A. Pattison; J. D. Sidler; J. B. Bieber *J. Am. Chem. Soc.* **1966**, 88, 78-84.
34. K. Tomooka; T. Igarashi; T. Nakai *Tetrahedron Lett.* **1993**, 34, 8139-8142.
35. R. B. Woodward; R. Hoffmann *The Conservation of Orbital Symmetry*; Academic: New York, 1970.
36. G. Wittig; H. Döser; I. Lorenz *Liebigs Ann. Chem.* **1949**, 562, 192-205.
37. U. Schöllkopf; K. Feldenberger *Liebigs Ann. Chem.* **1966**, 698, 80-85.
38. Y. Makisumi; S. Notzumoto *Tetrahedron Lett.* **1966**, 6393-6397.
39. J. E. Baldwin; J. DeBernardis; J. E. Patrick *Tetrahedron Lett.* **1970**, 353-356.
40. V. Rautenstrauch *J. Chem. Soc., Chem. Commun.* **1970**, 4-6.
41. J. E. Baldwin; J. E. Patrick *J. Am. Chem. Soc.* **1971**, 93, 3556-3558.
42. R. Hoffmann *Angew. Chem. Int. Ed. Engl.* **1979**, 18, 563-640.
43. R. K. Hill In *Asymmetric Synthesis*; J. D. Morrison, Ed.; Academic: Orlando, 1984; Vol. 3, p 503-572.
44. T. Nakai; K. Mikami *Chem. Rev.* **1986**, 86, 885-902.
45. K. Mikami; T. Nakai *Synthesis* **1991**, 594-604.
46. J. A. Marshall In *Comprehensive Organic Synthesis. Selectivity, Strategy, and Efficiency in Modern Organic Chemistry*; B. M. Trost, I. Fleming, Eds.; Pergamon: Oxford, 1991; Vol. 3, p 975-1014.
47. R. Brückner In *Comprehensive Organic Synthesis. Selectivity, Strategy, and Efficiency in Modern Organic Chemistry*; B. M. Trost, I. Fleming, Eds.; Pergamon: Oxford, 1991; Vol. 6, p 873-908.
48. K. Mikami; K. Azuma; T. Nakai *Tetrahedron* **1984**, 40, 2303-2308.
49. K. Mikami; T. Maeda; T. Nakai *Tetrahedron Lett.* **1986**, 27, 4189-4190.
50. M. Koreeda; J. I. Luengo *J. Am. Chem. Soc.* **1985**, 107, 5572-5573.
51. J. I. Luengo; M. Koreeda *J. Org. Chem.* **1989**, 54, 5415-5417.
52. L. Castedo; J. R. Granja; A. Mouriño *Tetrahedron Lett.* **1985**, 26, 4959-4960.
53. M. Koreeda; D. J. Ricca *J. Org. Chem.* **1986**, 51, 4090-4092.
54. W. C. Still; C. Sreekumar *J. Am. Chem. Soc.* **1980**, 102, 1201-1202.
55. Y.-D. Wu; K. N. Houk; J. A. Marshall *J. Org. Chem.* **1990**, 55, 1421-1423.
56. E. J. Verner; T. Cohen *J. Am. Chem. Soc.* **1992**, 114, 375-377.
57. R. Hoffmann; R. Brückner *Angew. Chem. Int. Ed. Engl.* **1992**, 31, 647-649.
58. K. Tomooka; T. Igarashi; M. Watanabe; T. Nakai *Tetrahedron Lett.* **1992**, 33, 5795--5798.
59. H. Eichenauer; E. Friedrich; W. Lutz; D. Enders *Angew. Chem. Int. Ed. Engl.* **1978**, 17, 206-208.
60. D. Seebach; J. Golinski *Helv. Chim. Acta* **1981**, 64, 1413-1423.
61. K. Mikami; Y. Kimura; N. Kishi; T. Nakai *J. Org. Chem.* **1983**, 48, 279-281.
62. E. Nakai; T. Nakai *Tetrahedron Lett.* **1988**, 29, 5409-5412.
63. M. Uchikawa; T. Katsuki; M. Yamaguchi *Tetrahedron Lett.* **1986**, 27, 4581-4582.
64. H. B. Meckelburger; C. S. Wilcox In *Comprehensive Organic Synthesis. Selectivity, Strategy, and Efficiency in Modern Organic Chemistry*; B. M. Trost, I. Fleming, Eds.; Pergamon: Oxford, 1991; Vol. 2, p 99-131.



65. S. D. Burke; W. F. Fobare; G. J. Pacofsky *J. Org. Chem.* **1983**, *48*, 5221-5228.
66. J. Kallmerten; T. J. Gould *Tetrahedron Lett.* **1983**, *24*, 5177-5180.
67. J. K. Whitesell; A. M. Helbing *J. Org. Chem.* **1980**, *45*, 4135-4139.
68. R. E. Ireland; S. Thaisrivongs; N. Vanier; C. S. Wilcox *J. Org. Chem.* **1980**, *45*, 48-61.
69. K. Mikami; O. Takahashi; T. Kasuga; T. Nakai *Chem. Lett.* **1985**, 1729-1732.
70. J. A. Marshall; X. Wang *J. Org. Chem.* **1992**, *57*, 2747-2750.
71. T. Nakai; K. Mikami; S. Taya; Y. Kimura; T. Mimura *Tetrahedron Lett.* **1981**, *22*, 69-72.
72. J. A. Marshall; W. Y. Gung *Tetrahedron Lett.* **1988**, *29*, 1657-1660.
73. P. C.-M. Chan; J. M. Chong *J. Org. Chem.* **1988**, *53*, 5584-5586.
74. J. A. Marshall; G. S. Welmaker; B. W. Gung *J. Am. Chem. Soc.* **1991**, *113*, 647-656.
75. J. M. Chong; E. K. Mar *Tetrahedron Lett.* **1991**, *32*, 5683-5686.
76. D. S. Matteson; P. B. Tripathy; A. Sarkur; K. N. Sadhu *J. Am. Chem. Soc.* **1989**, *111*, 4399-4402.
77. A. F. Thomas; R. Dubini *Helv. Chim. Acta* **1974**, *57*, 2084-2087.
78. D. J.-S. Tsai; M. M. Midland *J. Org. Chem.* **1984**, *49*, 1842-1843.
79. N. Sayo; K. Azuma; K. Mikami; T. Nakai *Tetrahedron Lett.* **1984**, *25*, 565-568.
80. J. A. Marshall; T. M. Jensen *J. Org. Chem.* **1984**, *49*, 1707-1712.
81. J. A. Marshall; X. Wang *J. Org. Chem.* **1990**, *55*, 2995-2996.
82. J. A. Marshall; X. Wang *J. Org. Chem.* **1991**, *56*, 4913-4918.
83. J. A. Marshall; E. D. Robinson; A. Zapata *J. Org. Chem.* **1989**, *54*, 5854-5855.
84. K. Mikami; O. Takahashi; T. Tabei; T. Nakai *Tetrahedron Lett.* **1986**, *27*, 4511-4514.
85. M. M. Midland; Y. C. Kwon *Tetrahedron Lett.* **1985**, *26*, 5013-5016.
86. O. Takahashi; K. Mikami; T. Nakai *Chem. Lett.* **1987**, 69-72.
87. J. A. Marshall; J. Lebreton *Tetrahedron Lett.* **1987**, *28*, 3323-3326.
88. J. A. Marshall; J. Lebreton *J. Am. Chem. Soc.* **1988**, *110*, 2925-2931.
89. J. A. Marshall; J. Lebreton *J. Org. Chem.* **1988**, *53*, 4108-4112.
90. M. Uchikawa; T. Hanemoto; T. Katsuki; M. Yamaguchi *Tetrahedron Lett.* **1986**, *27*, 4577-4580.
91. P. Helquist In *Comprehensive Organic Synthesis. Selectivity, Strategy, and Efficiency in Modern Organic Chemistry*; B. M. Trost, I. Fleming, Eds.; Pergamon: Oxford, 1991; Vol. 4, p 951-997.
92. H. M. L. Davies In *Comprehensive Organic Synthesis. Selectivity, Strategy, and Efficiency in Modern Organic Chemistry*; B. M. Trost, I. Fleming, Eds.; Pergamon: Oxford, 1991; Vol. 4, p 1031-1067.
93. H. E. Simmons, Jr.; T. L. Cairns; S. A. Vladuchick; C. M. Hoiness *Org. React.* **1973**, *20*, 1-131.
94. M. P. Doyle; R. L. Dorow; W. E. Buhro; J. H. Griffin; W. H. Tamblin; M. L. Trudell *Organometallics* **1984**, *3*, 44-52.
95. M. P. Doyle; R. L. Dorow; W. H. Tamblin; W. E. Buhro *Tetrahedron Lett.* **1982**, *23*, 2261-2264.
96. M. P. Doyle; V. Bagheri; T. J. Wandless; N. K. Harn; D. A. Brinker; C. T. Eagle; K. L. Loh *J. Am. Chem. Soc.* **1990**, *112*, 1906-1912.
97. H. M. L. Davies; T. J. Clark; L. A. Church *Tetrahedron Lett.* **1989**, *30*, 5057-5060.
98. H. Abdallah; R. Grée; R. Carrié *Tetrahedron Lett.* **1982**, *23*, 503-506.
99. I. Arai; A. Mori; H. Yamamoto *J. Am. Chem. Soc.* **1985**, *107*, 8254-8256.
100. A. Mori; I. Arai; H. Yamamoto; H. Nakai; Y. Arai *Tetrahedron* **1986**, *42*, 6447-6458.
101. E. A. Mash; K. A. Nelson *J. Am. Chem. Soc.* **1985**, *107*, 8256-8258.
102. E. A. Mash; K. A. Nelson *Tetrahedron* **1987**, *43*, 679-692.
103. E. A. Mash; D. S. Torok *J. Org. Chem.* **1989**, *54*, 250-253.
104. E. A. Mash; S. B. Hemperly; K. A. Nelson; P. C. Heidt; S. V. Deussen *J. Org. Chem.* **1990**, *55*, 2045-2055.
105. P. W. Ambler; S. G. Davies *Tetrahedron Lett.* **1988**, *29*, 6979-6982.

106. A. B. Charette; B. Côté; J.-F. Marcoux *J. Am. Chem. Soc.* **1991**, *113*, 8166-8167.
107. A. B. Charette; J.-F. Marcoux *Tetrahedron Lett.* **1993**, *34*, 7157-7160.
108. A. B. Charette; B. Côté *J. Org. Chem.* **1993**, *58*, 933-936.
109. T. Sugimura; T. Futugawa; A. Tai *Tetrahedron Lett.* **1988**, *29*, 5775-5778.
110. T. Sugimura; T. Futugawa; M. Yoshikawa; A. Tai *Tetrahedron Lett.* **1989**, *30*, 3807-3810.
111. T. Sugimura; M. Yoshikawa; T. Futugawa; A. Tai *Tetrahedron* **1990**, *46*, 5955-5966.
112. M. P. Doyle *Rec. Trav. Chim. Pays-Bas* **1991**, *110*, 305-316.
113. M. P. Doyle; W. R. Winchester; J. A. A. Hoorn; V. Lynch; S. H. Simonsen; R. Ghosh *J. Am. Chem. Soc.* **1993**, *115*, 9968-9978.
114. P. A. Krieger; J. A. Landgrebe *J. Org. Chem.* **1978**, *43*, 4447-4452.
115. M. P. Doyle; M. N. Protopopova; B. D. Brandes; H. M. L. Davies; N. J. S. Hruby; J. K. Whitesell *Synlett* **1993**, 151-153.
116. H. M. L. Davies; N. J. S. Huby; W. R. Cantrell, Jr.; J. L. Olive *J. Am. Chem. Soc.* **1993**, *115*, 9468-9479.
117. H. M. L. Davies *Tetrahedron Lett.* **1991**, *32*, 6509-6512.
118. H. M. L. Davies; N. J. S. Huby *Tetrahedron Lett.* **1992**, *33*, 6935-6938.
119. H. M. L. Davies *Tetrahedron* **1993**, *49*, 5203-5223.
120. A. B. Charette; H. Juteau *J. Am. Chem. Soc.* **1994**, *116*, 2651-2652.
121. A. B. Charette *Chem. Eng. News* **1995**, Feb 6, p. 2.
122. A. B. Charette; S. Prescott; C. Brochu *J. Org. Chem.* **1995**, *60*, 1081-1083.
123. H. Takayashi; M. Yoshioka; M. Ohno; S. Kobayashi *Tetrahedron Lett.* **1992**, *33*, 2575-2578.
124. Y. Ukaji; M. Nishimura; T. Fujisawa *Chem. Lett.* **1992**, 61-64.
125. H. Nozaki; S. Moriuti; H. Takaya; R. Noyori *Tetrahedron Lett.* **1966**, 5239-5242.
126. T. Aratani; Y. Yoneyoshi; T. Nagase *Tetrahedron Lett.* **1977**, 2599-2602.
127. T. Aratani; Y. Yoneyoshi; T. Nagase *Tetrahedron Lett.* **1982**, *23*, 685-688.
128. T. Aratani *Pure Appl. Chem.* **1985**, *57*, 1839-1844.
129. H. Fritsch; U. Leutenegger; A. Pfaltz *Helv. Chim. Acta* **1988**, *71*, 1553-1565.
130. U. Leutenegger; G. Umbricht; C. Fahrni; P. von Matt; A. Pfaltz *Tetrahedron* **1992**, *48*, 2143-2156.
131. R. E. Lowenthal; A. Abiko; S. Masamune *Tetrahedron Lett.* **1990**, *31*, 6005-6008.
132. R. E. Lowenthal; S. Masamune *Tetrahedron Lett.* **1991**, *32*, 7373-7376.
133. D. A. Evans; K. A. Woerpel; M. M. Hinman; M. M. Faul *J. Am. Chem. Soc.* **1991**, *113*, 726-728.
134. K. Ito; T. Katsuki *Tetrahedron Lett.* **1993**, *34*, 2662-2664.
135. H. Nishiyama; Y. Itoh; H. Matsumoto; S.-B. Park; K. Itoh *J. Am. Chem. Soc.* **1994**, *116*, 2223-2224.
136. W. Klyne; V. Prelog *Experientia* **1960**, *16*, 521-523.
137. M. P. Doyle; B. D. Brandes; A. P. Kazala; R. J. Pieters; M. B. Jartsfer; L. M. Watkins; C. T. Eagle *Tetrahedron Lett.* **1990**, *31*, 6613-6616.
138. M. N. Protopopova; M. P. Doyle; P. Müller; D. Ene *J. Am. Chem. Soc.* **1992**, *114*, 2755-2757.
139. H. M. L. Davies; D. K. Hutcheson *Tetrahedron Lett.* **1993**, *34*, 7243-7246.
140. M. P. Doyle; R. J. Pieters; S. F. Martin; R. E. Austin; C. J. Oalman; P. Müller *J. Am. Chem. Soc.* **1991**, *113*, 1423-1424.
141. S. F. Martin; C. J. Oalman; S. Liras *Tetrahedron Lett.* **1992**, *33*, 6727-6730.
142. S. F. Martin; M. R. Spaller; S. Liras; B. Hartmann *J. Am. Chem. Soc.* **1994**, *116*, 4493-4494.
143. G. Quinkert; U. Schwartz; H. Stark; W.-D. Weber; H. Baier; F. Adam; G. Dürner *Angew. Chem. Int. Ed. Engl.* **1980**, *19*, 1029-1030.
144. G. Quinkert; U. Schwartz; H. Stark; W.-D. Weber; F. Adam; A. Baier; G. Frank; G. Dürner *Liebigs Ann. Chem.* **1982**, 1999-2040.
145. D. Romo; J. L. Romine; W. Midura; A. I. Meyers *Tetrahedron* **1990**, *46*, 4951-4994.

146. D. Romo; A. I. Meyers *J. Org. Chem.* **1992**, *57*, 6265-6270.
147. E. J. Corey; M. J. Chaykovsky *J. Am. Chem. Soc.* **1965**, *87*, 1353-1364.
148. C. R. Johnson *Aldrichimica Acta* **1985**, *18*, 3-11.
149. R. M. Williams; G. J. Fegley *J. Am. Chem. Soc.* **1991**, *113*, 8796-8806.
150. Wasserman *Diels-Alder Reactions*; Elsevier: New York, 1965.
151. D. F. Taber *Intramolecular Diels-Alder and Alder Ene Reactions*; Springer: Berlin, 1984.
152. W. Oppolzer In *Comprehensive Organic Synthesis. Selectivity, Strategy, and Efficiency in Modern Organic Chemistry*; B. M. Trost, I. Fleming, Eds.; Pergamon: Oxford, 1991; Vol. 5, p 315-399.
153. W. R. Roush In *Comprehensive Organic Synthesis. Selectivity, Strategy, and Efficiency in Modern Organic Chemistry*; B. M. Trost, I. Fleming, Eds.; Pergamon: Oxford, 1991; Vol. 5, p 513-550.
154. J. March In *Advanced Organic Chemistry, 4th ed.*; Wiley-Interscience: New York, 1992, p 839-852.
155. W. Oppolzer *Angew. Chem. Int. Ed. Engl.* **1984**, *23*, 876-889.
156. G. Helmchen; R. Karge; J. Weetman In *Modern Synthetic Methods*; R. Scheffold, Ed.; Springer: Berlin, 1986; Vol. 4, p 262-306.
157. M. Taschner In *Organic Synthesis. Theory and Applications*; T. Hudlicky, Ed.; JAI: Greenwich, CT, 1989; Vol. 1, p 1-101.
158. D. L. Boger; S. M. Weinreb *Hetero Diels-Alder Methodology in Organic Synthesis*; Academic: New York, 1987.
159. S. M. Weinreb In *Comprehensive Organic Synthesis. Selectivity, Strategy, and Efficiency in Modern Organic Chemistry*; B. M. Trost, I. Fleming, Eds.; Pergamon: Oxford, 1991; Vol. 5, p 401-449.
160. D. L. Boger In *Comprehensive Organic Synthesis. Selectivity, Strategy, and Efficiency in Modern Organic Chemistry*; B. M. Trost, I. Fleming, Eds.; Pergamon: Oxford, 1991; Vol. 5, p 451-512.
161. H. Waldmann *Synthesis* **1994**, 535-551.
162. H. B. Kagan; O. Riant *Chem. Rev.* **1992**, *92*, 1007-1019.
163. K. B. Wiberg; K. E. Laidig *J. Am. Chem. Soc.* **1987**, *109*, 5935-5943.
164. J. Sauer; J. Kredel *Tetrahedron Lett.* **1966**, 6359-6364.
165. E. J. Corey; H. E. Ensley *J. Am. Chem. Soc.* **1975**, *97*, 6908-6909.
166. W. Oppolzer; M. Kurth; D. Reichlin; F. Moffatt *Tetrahedron Lett.* **1981**, *22*, 2545-2548.
167. R. K. Boeckman, Jr.; P. C. Naegley; S. D. Arthur *J. Org. Chem.* **1980**, *45*, 752-754.
168. C. LeDrain; A. E. Greene *J. Am. Chem. Soc.* **1982**, *104*, 5473-5483.
169. E. J. Corey; X.-M. Cheng; K. A. Crimprich *Tetrahedron Lett.* **1991**, *32*, 6839-6842.
170. W. Oppolzer; C. Chapuis; G. M. Dao; D. Reichlin; T. Godel *Tetrahedron Lett.* **1982**, *23*, 4781-4784.
171. W. Oppolzer; C. Chapuis *Tetrahedron Lett.* **1984**, *25*, 5383-5386.
172. W. Oppolzer In *Selectivity, a Goal for Synthetic Efficiency: Proceedings of the 14th Workshop Conference Hoechst*; W. Bartmann, B. M. Trost, Eds.; Verlag Chemie: Weinheim, 1984; Vol. 14, p 137-167.
173. W. Oppolzer; C. Chapuis; G. Bernardinelli *Tetrahedron Lett.* **1984**, *25*, 5885-5888.
174. T. Poll; A. Sobczak; H. Hartmann; G. Helmchen *Tetrahedron Lett.* **1985**, *26*, 3095-3098.
175. T. Poll; A. F. A. Hady; R. Karge; G. Linz; J. Weetman; G. Helmchen *Tetrahedron Lett.* **1989**, *30*, 5595-5598.
176. J.-L. Gras; H. Pellissier *Tetrahedron Lett.* **1991**, *32*, 7043-7046.
177. W. Oppolzer; C. Chapuis; G. Bernardinelli *Helv. Chim. Acta* **1984**, *67*, 1397-1401.
178. D. A. Evans; K. T. Chapman; J. Bisaha *J. Am. Chem. Soc.* **1988**, *110*, 1238-1256.
179. R. J. Loncharich; T. R. Schwarz; K. N. Houk *J. Am. Chem. Soc.* **1987**, *109*, 14-23.
180. S. Castellino; W. J. Dwight *J. Am. Chem. Soc.* **1993**, *115*, 2986-2987.
181. T. Poll; J. O. Metter; G. Helmchen *Angew. Chem. Int. Ed. Engl.* **1985**, *24*, 112-114.

182. E. Ciganek *Org. React.* **1984**, 32, 1-374.
183. P. Deslongchamps *Pure Appl. Chem.* **1992**, 64, 31-47.
184. W. Oppolzer; D. Dupuis *Tetrahedron Lett.* **1985**, 26, 5437-5440.
185. W. R. Roush; H. R. Gillis; A. I. Ko *J. Am. Chem. Soc.* **1982**, 104, 2269-2283.
186. H. M. Walborsky; L. Barash; T. C. Davis *J. Org. Chem.* **1961**, 26, 4778-4779.
187. H. M. Walborsky; L. Barash; T. C. Davis *Tetrahedron* **1963**, 19, 2333-2351.
188. K. Furuta; K. Iwanaga; H. Yamamoto *Tetrahedron Lett.* **1986**, 27, 4507-4510.
189. Y. N. Ito; A. K. Beck; A. Bohác; C. Ganter; R. E. Gawley; F. N. M. Kühnle; J. A. Piquer; J. Tuleja; Y. M. Wang; D. Seebach *Helv. Chim. Acta* **1994**, 77, 2071-2110.
190. G. Helmchen; R. Schmierer *Angew. Chem. Int. Ed. Engl.* **1981**, 20, 205-207.
191. K. Tomioka; N. Hamada; T. Suenaga; K. Koga *J. Chem. Soc., Perkin Trans. 1* **1990**, 426-428.
192. K. Maruoka; S. Saito; H. Yamamoto *J. Am. Chem. Soc.* **1992**, 114, 1089-1090.
193. S. W. Baldwin; P. Greenspan; C. Alaimo; A. T. McPhail *Tetrahedron Lett.* **1991**, 32, 5877-5880.
194. K. Maruoka; M. Akakura; S. Saito; T. Ooi; H. Yamamoto *J. Am. Chem. Soc.* **1994**, 116, 6153-6158.
195. G. Linz; J. Weetman; A. F. Abdel-Hady; G. Helmchen *Tetrahedron Lett.* **1989**, 30, 5599-5602.
196. M. Vandewalle; J. V. d. Eyken; W. Oppolzer; C. Vullioud *Tetrahedron* **1986**, 42, 4035-4043.
197. E. J. Corey; W. Su *Tetrahedron Lett.* **1988**, 29, 3423-3426.
198. J. Aubé; S. Ghosh; M. Tanol *J. Am. Chem. Soc.* **1994**, 116, 9009-9018.
199. D. Enders; O. Meyer; G. Raabe; J. Runsink *Synthesis* **1994**, 66-72.
200. D. Enders; O. Meyer; G. Raabe *Synthesis* **1992**, 1242-1244.
201. B. M. Trost; D. O'Krongly; J. L. Belletire *J. Am. Chem. Soc.* **1980**, 102, 7595-7596.
202. C. Siegel; E. R. Thornton *Tetrahedron Lett.* **1988**, 29, 5225-5228.
203. J. A. Dale; H. S. Mosher *J. Am. Chem. Soc.* **1973**, 95, 512-519.
204. D. A. Evans; T. Lectka; S. J. Miller *Tetrahedron Lett.* **1993**, 34, 7027-7030.
205. D. A. Evans; S. J. Miller; T. Lectka *J. Am. Chem. Soc.* **1993**, 115, 6460-6461.
206. E. J. Corey; K. Ishihara *Tetrahedron Lett.* **1992**, 33, 6807-6810.
207. S. Kobayashi; I. Hachiya; H. Ishitani; M. Araki *Tetrahedron Lett.* **1993**, 34, 4535-4538.
208. S. Kobayashi; H. Ishitani *J. Am. Chem. Soc.* **1994**, 116, 4083-4084.
209. K. Tomioka *Synthesis* **1990**, 541-549.
210. K. Narasaka *Synthesis* **1991**, 1-11.
211. S. Hashimoto; N. Komeshima; K. Koga *J. Chem. Soc., Chem. Commun.* **1979**, 437-438.
212. J. M. Hawkins; S. Loren *J. Am. Chem. Soc.* **1991**, 113, 7794-7795.
213. J. M. Hawkins; S. Loren; M. Nambu *J. Am. Chem. Soc.* **1994**, 116, 1657-1660.
214. M. Takasu; H. Yamamoto *Synlett* **1990**, 194-196.
215. E. J. Corey; T.-P. Loh *J. Am. Chem. Soc.* **1991**, 113, 8966-8967.
216. E. J. Corey; T.-P. Loh; T. D. Roper; M. D. Azimioara; M. C. Noe *J. Am. Chem. Soc.* **1992**, 114, 8290-8292.
217. J.-P. G. Seerden; H. W. Scheeren *Tetrahedron Lett.* **1993**, 34, 2669-2672.
218. K. Furuta; S. Shimizu; Y. Miwa; H. Yamamoto *J. Org. Chem.* **1989**, 54, 1481-1483.
219. K. Furuta; A. Kanamatsu; H. Yamamoto; S. Takaoka *Tetrahedron Lett.* **1989**, 30, 7231-7232.
220. K. Ishihara; Q. Gao; H. Yamamoto *J. Am. Chem. Soc.* **1993**, 115, 10412-10413.
221. E. J. Corey; R. Imwinkelreid; S. Pikul; Y. B. Xiang *J. Am. Chem. Soc.* **1989**, 111, 5493-5495.
222. E. J. Corey; N. Imai; S. Pikul *Tetrahedron Lett.* **1991**, 32, 7517-7520.
223. E. J. Corey; S. Sarshar; J. Bordner *J. Am. Chem. Soc.* **1992**, 114, 7938-7939.
224. P. N. Devine; T. Oh *J. Org. Chem.* **1992**, 57, 396-399.
225. K. Maruoka; M. Sakurai; J. Fujiwara; H. Yamamoto *Tetrahedron Lett.* **1986**, 27, 4895-4898.
226. K. Narasaka; M. Inoue; N. Okada *Chem. Lett.* **1986**, 1109-1112.

227. D. Seebach; A. K. Beck; R. Imwinkelried; S. Roggo; A. Wonnacott *Helv. Chim. Acta* **1987**, *70*, 954-974.
228. D. Seebach; R. Dahinden; R. E. Marti; A. K. Beck; D. A. Plattner; F. N. M. Kühnle *J. Org. Chem.* **1995**, *60*, 1788-1799.
229. T. A. Engler; M. A. Letavic; K. O. Lynch, Jr.; F. Takusagawa *J. Org. Chem.* **1994**, *59*, 1179-1183.
230. K. Mikami; Y. Motoyama; M. Terada *J. Am. Chem. Soc.* **1994**, *116*, 2812-2820.
231. T. R. Kelly; A. Whiting; N. S. Chandrakumar *J. Am. Chem. Soc.* **1986**, *108*, 3510-3512.
232. C. Chapuis; J. Jurczak *Helv. Chim. Acta* **1987**, *70*, 436-440.
233. K. Ishihara; H. Yamamoto *J. Am. Chem. Soc.* **1994**, *116*, 1561-1562.
234. E. J. Corey; N. Imai; H.-Y. Zhang *J. Am. Chem. Soc.* **1991**, *113*, 728-729.
235. J. I. Seeman *Chem. Rev.* **1983**, *83*, 83-134.
236. K. Narasaka; N. Iwasawa; M. Inoue; T. Yamada; M. Nakashima; J. Sugimori *J. Am. Chem. Soc.* **1989**, *111*, 5340-5345.
237. C. Haase; C. R. Sarko; M. DiMare *J. Org. Chem.* **1995**, *60*, 1777-1787.
238. K. V. Gothelf; R. G. Hazell; K. A. Jørgensen *J. Am. Chem. Soc.* **1995**, *117*, 4435-4436.
239. E. J. Corey; X.-M. Cheng *The Logic of Chemical Synthesis*; Wiley: New York, 1989.
240. E. J. Corey; S. M. Albonico; U. Koelliker; T. K. Schaaf; R. K. Varma *J. Am. Chem. Soc.* **1971**, *93*, 1491-1493.